A Deep Dive into the Distribution Function:

Understanding Phase Space Dynamics Using Continuum Vlasov-Maxwell Simulations

James Juno

Acknowledgements:
The Gkeyll team: **Ammar Hakim,** Greg Hammett, **Jason TenBarge**, Petr Cagas, Noah Mandell, Manaure Francisquez, Tess Bernard, Valentin Skoutnev, and Liang Wang

Greg Howes, Marc Swisdak, and William Dorland

The Scales of the Luminous Universe

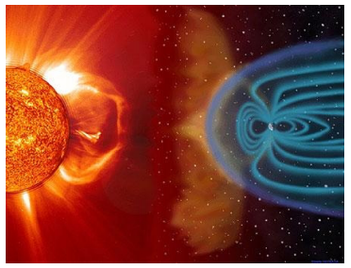

ℓ

ρ_e ρ_i
d_e d_i

λ_{mfp}
L

λ_D

10^{-10} 10^{-6} 10^{-2} 1 au

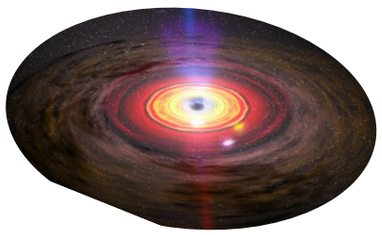

ℓ

ρ_e ρ_i
d_e d_i

λ_{mfp}
L

λ_D

10^{-14} 10^{-11} 0.1 pc

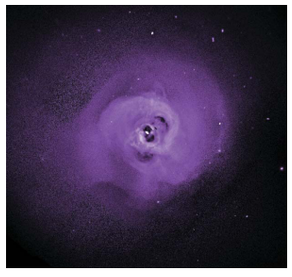

ℓ

ρ_e ρ_i
d_e d_i

λ_{mfp}
L

λ_D

10^{-18} 10^{-14} $1\ 10^2$ kpc

The Vlasov-Maxwell System

$$\frac{\partial f}{\partial t} + \nabla_{\mathbf{z}} \cdot (\boldsymbol{\alpha} f) = 0$$

where $\nabla_{\mathbf{z}} = (\nabla_{\mathbf{x}}, \nabla_{\mathbf{v}})$ and $\alpha = (\mathbf{v}, \frac{q_s}{m_s}(\mathbf{E} + \mathbf{v} \times \mathbf{B}))$

$$\frac{\partial \mathbf{B}}{\partial t} + \nabla \times \mathbf{E} = 0$$

$$\epsilon_0 \mu_0 \frac{\partial \mathbf{E}}{\partial t} - \nabla \times \mathbf{B} = -\mu_0 \mathbf{J}$$

$$\nabla \cdot \mathbf{B} = 0$$

$$\nabla \cdot \mathbf{E} = \rho_c / \epsilon_0$$

$$\rho_c = \sum_s q_s \int_{-\infty}^{\infty} f_s(t, \mathbf{x}, \mathbf{v}) d\mathbf{v} \qquad \mathbf{J} = \sum_s q_s \int_{-\infty}^{\infty} \mathbf{v} f_s(t, \mathbf{x}, \mathbf{v}) d\mathbf{v}$$

This equation system is high-dimensional **(up to 6 dimensions plus time)**

A deep dive into phase space

- We know the distribution function contains a wealth of data
- Obtaining a clean enough representation of the distribution function, and accessing this data is hard
- But well worth the effort since, for example, many energization mechanisms are most easily identified by the phase space structure they create

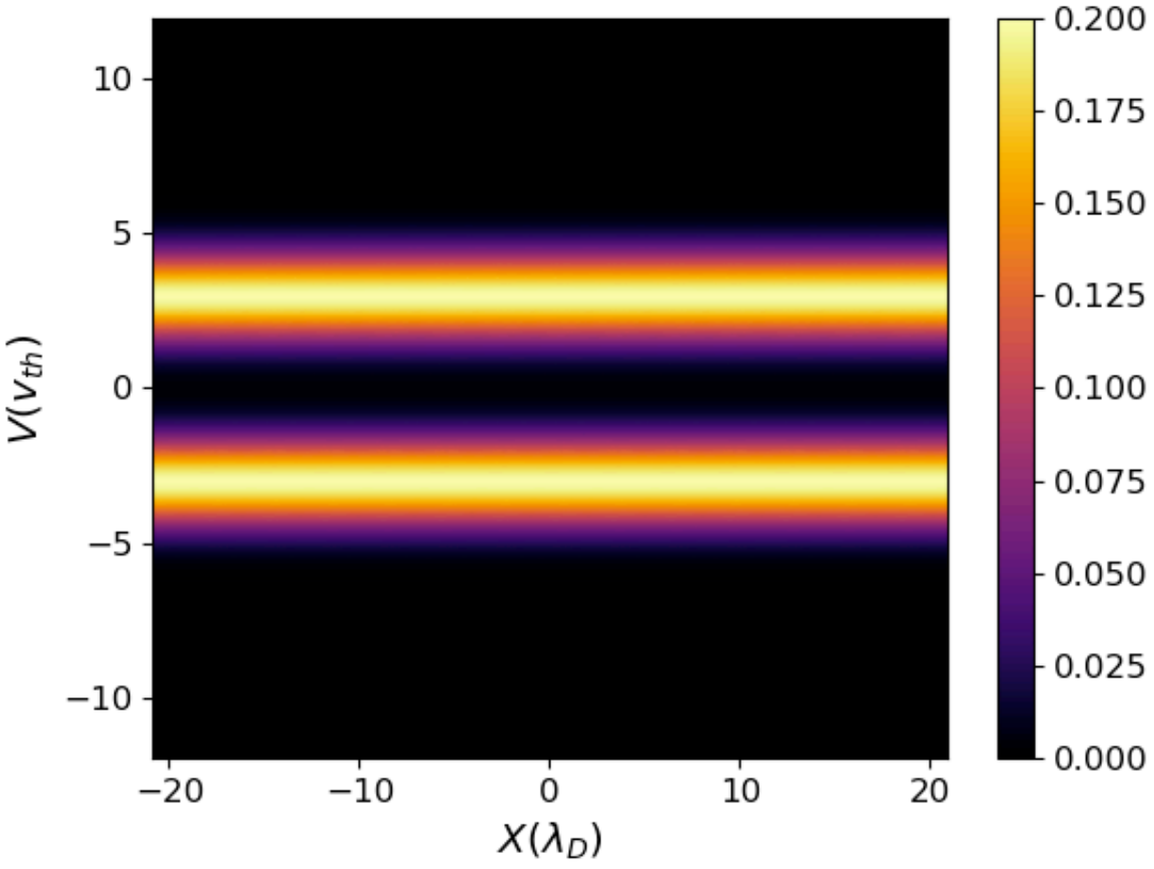

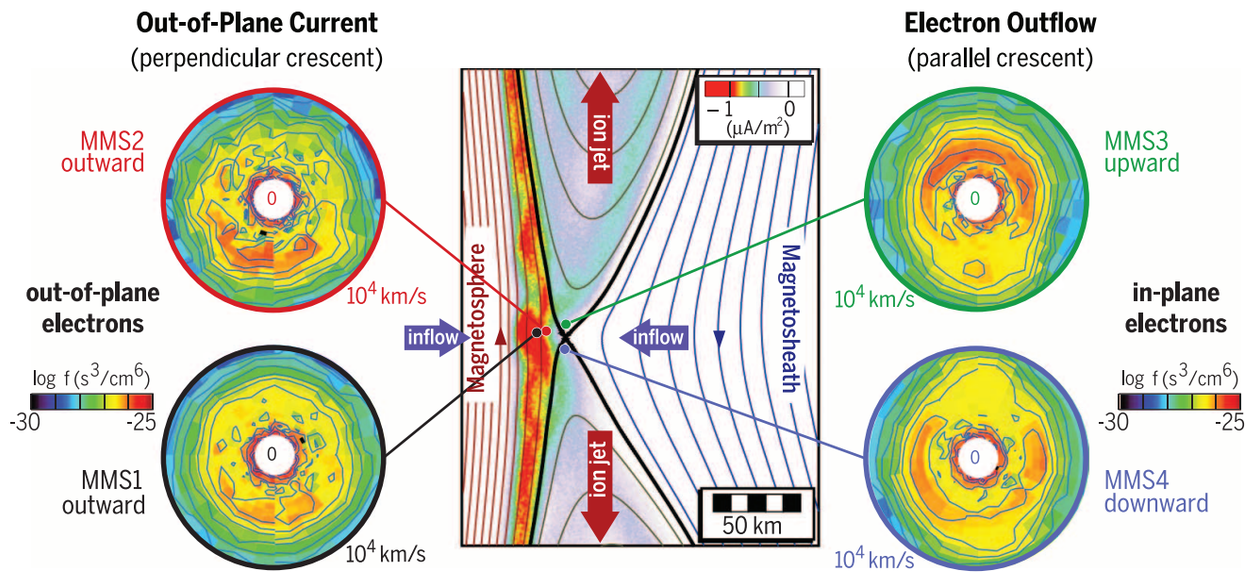

MMS electron data from Burch et al (2016).

The Gkeyll (and Hyde) Framework

"It is one thing to mortify curiosity, another to conquer it."

- The Gkeyll framework is flexible suite of solvers for plasma physics being developed at the Princeton Plasma Physics Lab, UMD, Virginia Tech, General Atomics, and MIT

- Multiple Vlasov-Maxwell publications already:

  - Physics

    - P. Cagas, A. Hakim, J. Juno, B. Srinivasan. Continuum kinetic and multi-fluid simulation of a classical sheath, Phys. Plasmas (2017).

    - I. Pusztai, J. M. TenBarge, A. N. Csapo, J. Juno, A. Hakim, L. Yi, T. Fulop. Low Mach-number collisionless electrostatic shocks and associated ion acceleration, PPCF (2018)

    - **V. Skoutnev, A. Hakim, J. Juno, J. M. TenBarge. Temperature Dependent Saturation of Weibel Type Instabilities in Counter-Streaming Plasmas, ApJL (2019)**

    - A. Sundstrom, J. Juno, J. M. TenBarge, and I. Pusztai. Effect of a weak ion collisionality on the dynamics of kinetic electrostatic shocks, JPP (2019)

    - J. Ng, A. Hakim, J. Juno, A. Bhattacharjee. Drift Instabilities in Thin Current Sheets Using a Two-Fluid Model With Pressure Tensor Effects, JGR (2019)

  - Algorithms

    - **J. Juno, A. Hakim, J. TenBarge, E. Shi, W. Dorland. Discontinuous Galerkin Algorithms for fully kinetic plasmas, JCP (2018).**

    - A. Hakim, M. Francisquez, J. Juno, G. Hammett. Conservative Discontinuous Galerkin Discretization of Fokker-Planck Operators. Submitted to JPP (2019)

https://github.com/ammarhakim/gkyl.git

The Discontinuous Galerkin Finite Element Method

- We choose to use the discontinuous Galerkin framework as our spatial discretization because it combines aspects of
  - Finite elements: high order accuracy and ability to handle complicated geometries
  - Finite volume: locality of data and stability enforcing limiters

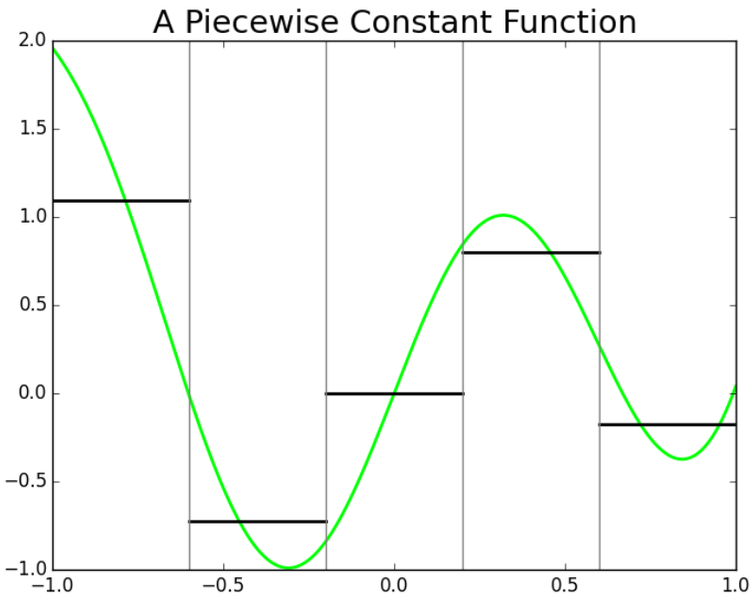

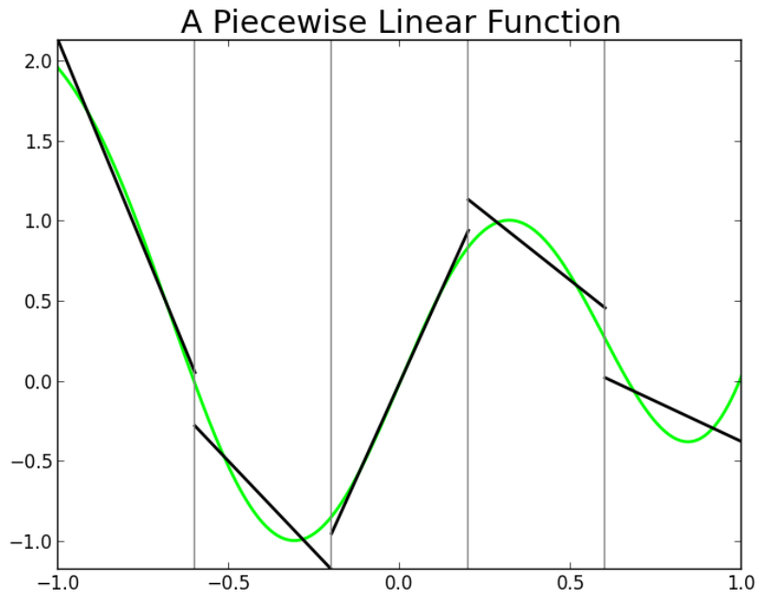

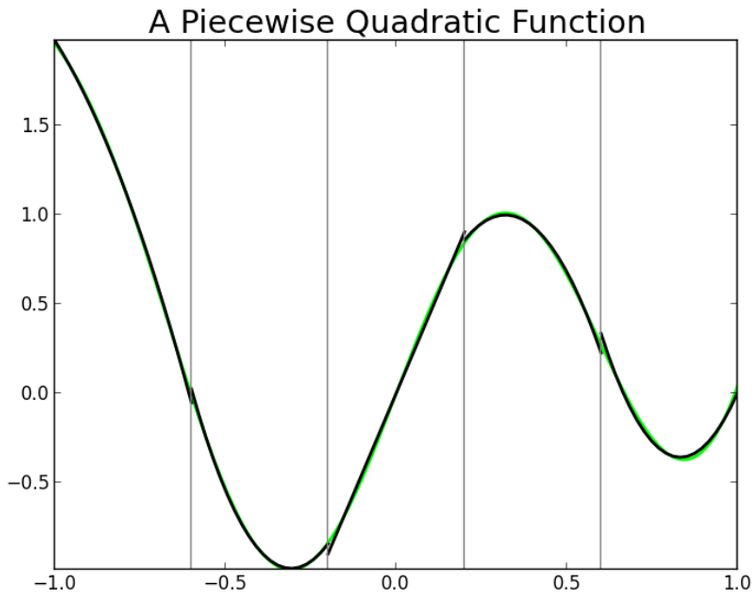

The Discrete Vlasov Equation

- What does the discontinuous Galerkin discretization of the Vlasov equation look like?

  - Consider a phase space mesh $\mathcal{T}$ with cells $K_j \in \mathcal{T}, j = 1, \ldots, N$.
  - Then the problem formulation is, find $f_h \in \mathcal{V}_h^p$, such that for all $K_j \in \mathcal{T}$,

$$\int_{K_j} w \frac{\partial f_h}{\partial t}\, d\mathbf{z} + \oint_{\partial K_j} w^- \mathbf{n} \cdot \hat{\mathbf{F}}\, dS - \int_{K_j} \nabla_{\mathbf{z}} w \cdot \boldsymbol{\alpha}_h f_h\, d\mathbf{z} = 0$$

$$f_h(\mathbf{z}, t) = \sum_n^{N_p} F_n(t) w_n(\mathbf{z}) \qquad \mathcal{V}_h^p = \{v : v|_{K_j} \in \mathbf{P}^p, \forall K_j \in \mathcal{T}\},$$

Upwind fluxes are used for the streaming term and a relaxed global Lax-Friedrichs flux is used for the acceleration

$$\mathbf{n} \cdot \hat{\mathbf{F}} = \frac{1}{2} \mathbf{n} \cdot \left(\boldsymbol{\alpha}_{\boldsymbol{h}}^+ (f_h^+ + f_h^-) - \boldsymbol{\tau}(f^+ - f^-) \right)$$

$$\text{where } \tau = \max_{\mathcal{T}} \left(\frac{q}{m} \mathbf{E}_h + \frac{q}{m} \mathbf{v} \times \mathbf{B}_h \right)$$

note that the phase space flux is continuous at corresponding surface interfaces

The Discrete Maxwell Equations

$$\int_{\Omega_j} \phi \frac{\partial \mathbf{B}_h}{\partial t} d\mathbf{x} + \oint_{\partial\Omega_j} d\mathbf{s} \times (\phi^- \hat{\mathbf{E}}_h) - \int_{\Omega_j} \nabla\phi \times \mathbf{E}_h d\mathbf{x} = 0$$

$$\epsilon_0\mu_0 \int_{\Omega_j} \phi \frac{\partial \mathbf{E}_h}{\partial t} d\mathbf{x} - \oint_{\partial\Omega_j} d\mathbf{s} \times (\phi^- \hat{\mathbf{B}}_h) + \int_{\Omega_j} \nabla\phi \times \mathbf{B}_h d\mathbf{x} = -\mu_0 \int_{\Omega_j} \phi \mathbf{J}_h d\mathbf{x}$$

with central fluxes

$$\hat{\mathbf{E}}_h = [\![\mathbf{E}]\!] \qquad \hat{\mathbf{B}}_h = [\![\mathbf{B}]\!]$$

$$[\![g]\!] \equiv (g^+ + g^-)/2$$

or upwind fluxes

$$\hat{E}_2 = [\![E_2]\!] - c\{B_3\} \qquad \hat{E}_3 = [\![E_3]\!] + c\{B_2\}$$

$$\hat{B}_2 = [\![B_2]\!] + \{E_3\}/c \qquad \hat{B}_3 = [\![B_3]\!] + \{E_2\}/c$$

$$\{g\} \equiv (g^+ - g^-)/2$$

Note that upwind fluxes are defined with respect to a local coordinate system where subscripts 2 and 3 define the two directions tangential to the surface

Proving conservation relations

- The continuous Vlasov-Maxwell system has a number of conserved quantities
  - Density
  - Momentum
  - Energy
  - etc.

- What conserved quantities does our spatial discretization retain?

$$\int_{K_j} w \frac{\partial f_h}{\partial t}\, d\mathbf{z} + \oint_{\partial K_j} w^- \mathbf{n} \cdot \hat{\mathbf{F}}\, dS - \int_{K_j} \nabla_{\mathbf{z}} w \cdot \boldsymbol{\alpha}_h f_h\, d\mathbf{z} = 0$$

- Can choose the test function carefully, as long as test function is in the solution space

$$\sum_j \int_{K_j} \frac{\partial f_h}{\partial t}\, d\mathbf{z} + \sum_j \oint_{\partial K_j} \mathbf{n} \cdot \hat{\mathbf{F}}\, dS = 0$$

$$\sum_s \sum_j \int_{K_j} \frac{1}{2} m_s |\mathbf{v}|^2 \frac{\partial f_{h_s}}{\partial t}\, d\mathbf{z} + \sum_s \sum_j \oint_{\partial K_j} \frac{1}{2} m_s |\mathbf{v}|^2 \mathbf{n} \cdot \hat{\mathbf{F}}\, dS - \underbrace{\sum_s \sum_j \int_{K_j} \nabla_{\mathbf{z}} \left(\frac{1}{2} m_s |\mathbf{v}|^2 \right) \cdot \boldsymbol{\alpha}_{h_s} f_{h_s}\, d\mathbf{z}}_{\sum_j \int_{\Omega_j} \mathbf{J}_h \cdot \mathbf{E}_h\, d^3\mathbf{x}} = 0$$

Conservation Relations

- The discrete system conserves total density
- The discrete phase space flow is incompressible $\nabla_{\mathbf{z}} \cdot \boldsymbol{\alpha}_h = 0$
- Electromagnetic energy is conserved when using central fluxes, and bounded when using upwind fluxes

$$\sum_j \frac{d}{dt} \int_{\Omega_j} \left(\frac{\epsilon_0}{2} |\mathbf{E}_h|^2 + \frac{1}{2\mu_0} |\mathbf{B}_h|^2 \right) \, d^3\mathbf{x} \leq - \sum_j \int_{\Omega_j} \mathbf{J}_h \cdot \mathbf{E}_h \, d^3\mathbf{x}$$

- The total energy is conserved when central fluxes are used for Maxwell's equations

$$\frac{d}{dt} \sum_j \sum_s \int_{K_j} \frac{1}{2} m |\mathbf{v}|^2 f_h \, d\mathbf{z} + \frac{d}{dt} \sum_j \int_{\Omega_j} \left(\frac{\epsilon_0}{2} |\mathbf{E}_h|^2 + \frac{1}{2\mu_0} |\mathbf{B}_h|^2 \right) \, d^3\mathbf{x} = 0$$

A critical point: the importance of accurate integration

- A subtlety to the discretization of the Vlasov-Maxwell system is our conservations relations are *implicit* and require that certain integrals are computed exactly

$$\frac{d}{dt}\sum_j\sum_s\int_{K_j}\frac{1}{2}m|\mathbf{v}|^2 f_h\,d\mathbf{z} + \frac{d}{dt}\sum_j\int_{\Omega_j}\left(\frac{\epsilon_0}{2}|\mathbf{E}_h|^2 + \frac{1}{2\mu_0}|\mathbf{B}_h|^2\right)\,d^3\mathbf{x} = 0$$

- This is different than standard fluid algorithms, where errors in the integration (aliasing errors) are often tolerated:

$$\frac{\partial\rho}{\partial t} + \nabla\cdot(\rho\mathbf{u}) = 0$$

$$\frac{\partial\rho\mathbf{u}}{\partial t} + \nabla\cdot(\rho\mathbf{u}\mathbf{u}) = -\nabla p + \mathbf{F}$$

$$\mathbf{u} = \sum_k u_k(t)\phi(\mathbf{x}) \quad \rightarrow \quad \mathbf{u} = \frac{\rho\mathbf{u}}{\rho} = \frac{\sum_j M_j(t)\phi(\mathbf{x})}{\sum_i \rho_i(t)\phi(\mathbf{x})}$$

- Exactly integrating the terms in the Vlasov equation with numerical quadrature is a nontrivial cost

$$\int_{K_j} w\frac{\partial f_h}{\partial t}\,d\mathbf{z} + \oint_{\partial K_j} w^-\mathbf{n}\cdot\hat{\mathbf{F}}\,dS - \int_{K_j}\nabla_{\mathbf{z}}w\cdot\boldsymbol{\alpha}_h f_h\,d\mathbf{z} = 0 \quad \rightarrow \quad \mathcal{O}(N_q N_p)$$

Orthonormal bases to the rescue

- The fundamental operations in our algorithm can be thought of as tensor-tensor products, for example the volume term for the Lorentz acceleration:

$$\int_{K_j} \nabla_{\mathbf{z}} w_l \cdot \boldsymbol{\alpha}_h f_h \, d\mathbf{z} = \sum_{m,n} \underbrace{\left(\int_{K_j} w_m w_n \nabla_{\mathbf{z}} w_l \, d\mathbf{z} \right)}_{\mathcal{C}_{lmn}} \cdot \boldsymbol{\alpha}_m f_n$$

- Naively, this tensor has between $N_c N_p^2$ and N_p^3 components, and that's not any better than direct quadrature..

- But we could choose our basis expansion to be a *modal, orthonormal* expansion

- Then these tensors would be sparse and we could do sparse tensor products!

  - Note that for a tensor product basis, this would correspond to a basis of Legendre polynomials

Making the update efficient using Maxima

```
void VlasovVol1x2vTensorP1(const double *w, const double *dxv, const double *EM, const double *f, double *out)
{
// w[NDIM]: Cell-center coordinates. dxv[NDIM]: Cell spacing. EM/f: Input EM-field/distribution function. out: Incremented output
  double dv0dx0 = dxv[1]/dxv[0];
  double w0dx0 = w[1]/dxv[0];
  const double dv10 = 2/dxv[1];
  const double *E0 = &EM[0];
  const double dv1 = dxv[1], wv1 = w[1];
  const double dv11 = 2/dxv[2];
  const double *E1 = &EM[2];
  const double dv2 = dxv[2], wv2 = w[2];
  const double *B2 = &EM[10];

  double alpha0[8];
  double alpha1[8];
  double alpha2[8];
  // vx
  alpha0[0] = 5.656854249492382*w0dx0;
  alpha0[2] = 1.632993161855453*dv0dx0;
  // q/m*(Ex + vy*Bz)
  alpha1[0] = 2.0*dv10*(B2[0]*wv2 + E0[0]);
  alpha1[1] = 2.0*dv10*(B2[1]*wv2 + E0[1]);
  alpha1[3] = 0.5773502691896258*B2[0]*dv10*dv2;
  alpha1[5] = 0.5773502691896258*B2[1]*dv10*dv2;
  // q/m*(Ey - vx*Bz)
  alpha2[0] = dv11*(2.0*E1[0] - 2.0*B2[0]*wv1);
  alpha2[1] = dv11*(2.0*E1[1] - 2.0*B2[1]*wv1);
  alpha2[2] = -0.5773502691896258*B2[0]*dv1*dv11;
  alpha2[4] = -0.5773502691896258*B2[1]*dv1*dv11;

  out[1] += 0.6123724356957944*(alpha0[2]*f[2] + alpha0[0]*f[0]);
  out[2] += 0.6123724356957944*(alpha1[5]*f[5] + alpha1[3]*f[3] + alpha1[1]*f[1] + alpha1[0]*f[0]);
  out[3] += 0.6123724356957944*(alpha2[4]*f[4] + alpha2[2]*f[2] + alpha2[1]*f[1] + alpha2[0]*f[0]);
  out[4] += 0.6123724356957944*(alpha1[3]*f[5] + f[3]*alpha1[5] + alpha0[0]*f[2] + f[0]*alpha0[2] + alpha1[0]*f[1] + f[0]*alpha1[1]);
  out[5] += 0.6123724356957944*(alpha0[2]*f[6] + alpha2[2]*f[4] + f[2]*alpha2[4] + alpha0[0]*f[3] + alpha2[0]*f[1] + f[0]*alpha2[1]);
  out[6] += 0.6123724356957944*(alpha1[1]*f[5] + f[1]*alpha1[5] + alpha2[1]*f[4] + f[1]*alpha2[4] + alpha1[0]*f[3] + f[0]*alpha1[3] + alpha2
[0]*f[2] + f[0]*alpha2[2]);
  out[7] += 0.6123724356957944*(alpha0[0]*f[6] + alpha1[0]*f[5] + f[0]*alpha1[5] + alpha2[0]*f[4] + f[0]*alpha2[4] + (alpha0[2] + alpha1[1])
*f[3] + f[1]*alpha1[3] + alpha2[1]*f[2] + f[1]*alpha2[2]);
}
```

$$\text{out}_l = \sum_{m,n} \mathcal{C}_{lmn} \cdot \boldsymbol{\alpha}_m f_n$$

- For reference, this update is ~250 multiplications with a nodal basis (now ~70)

Scaling of the update

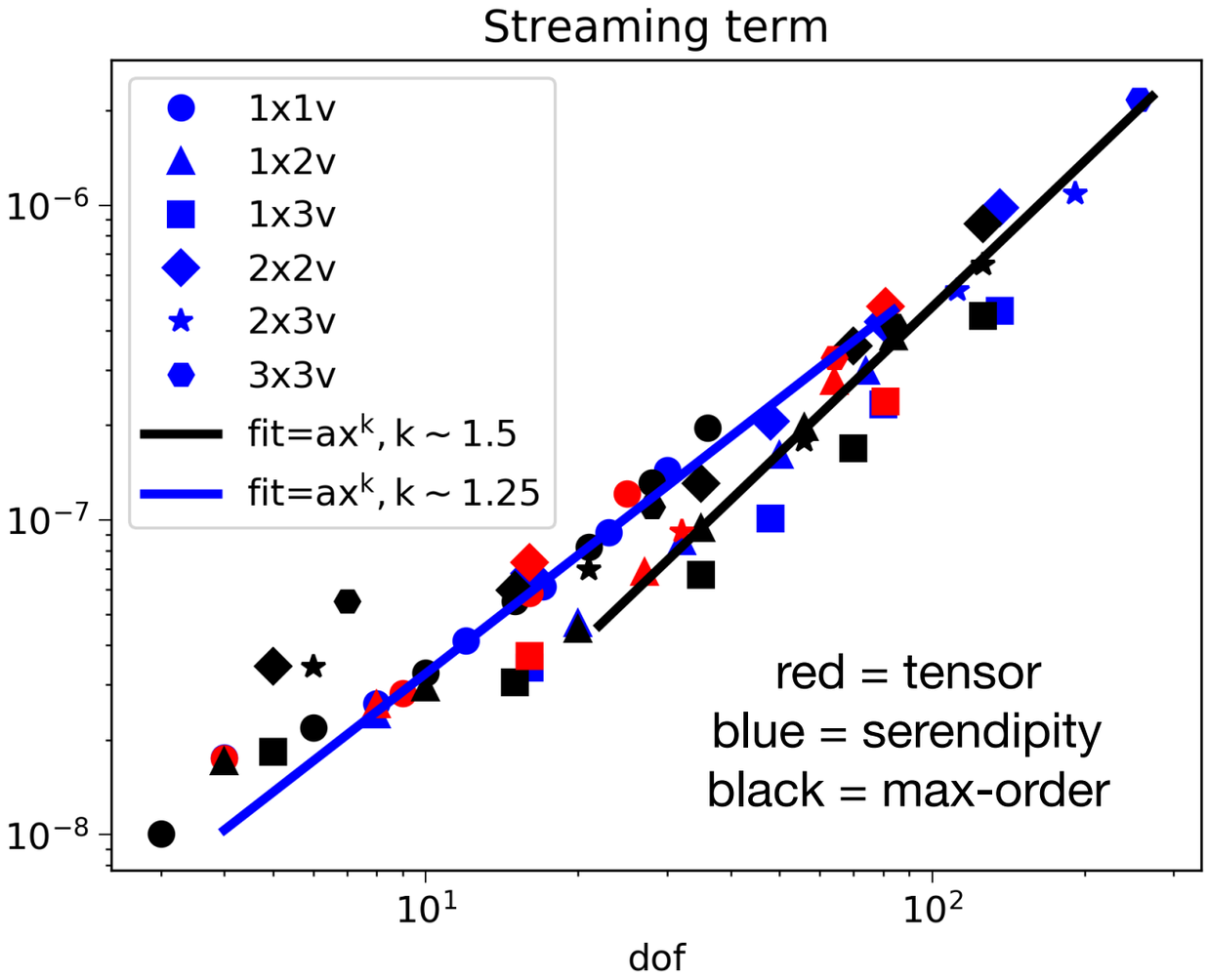

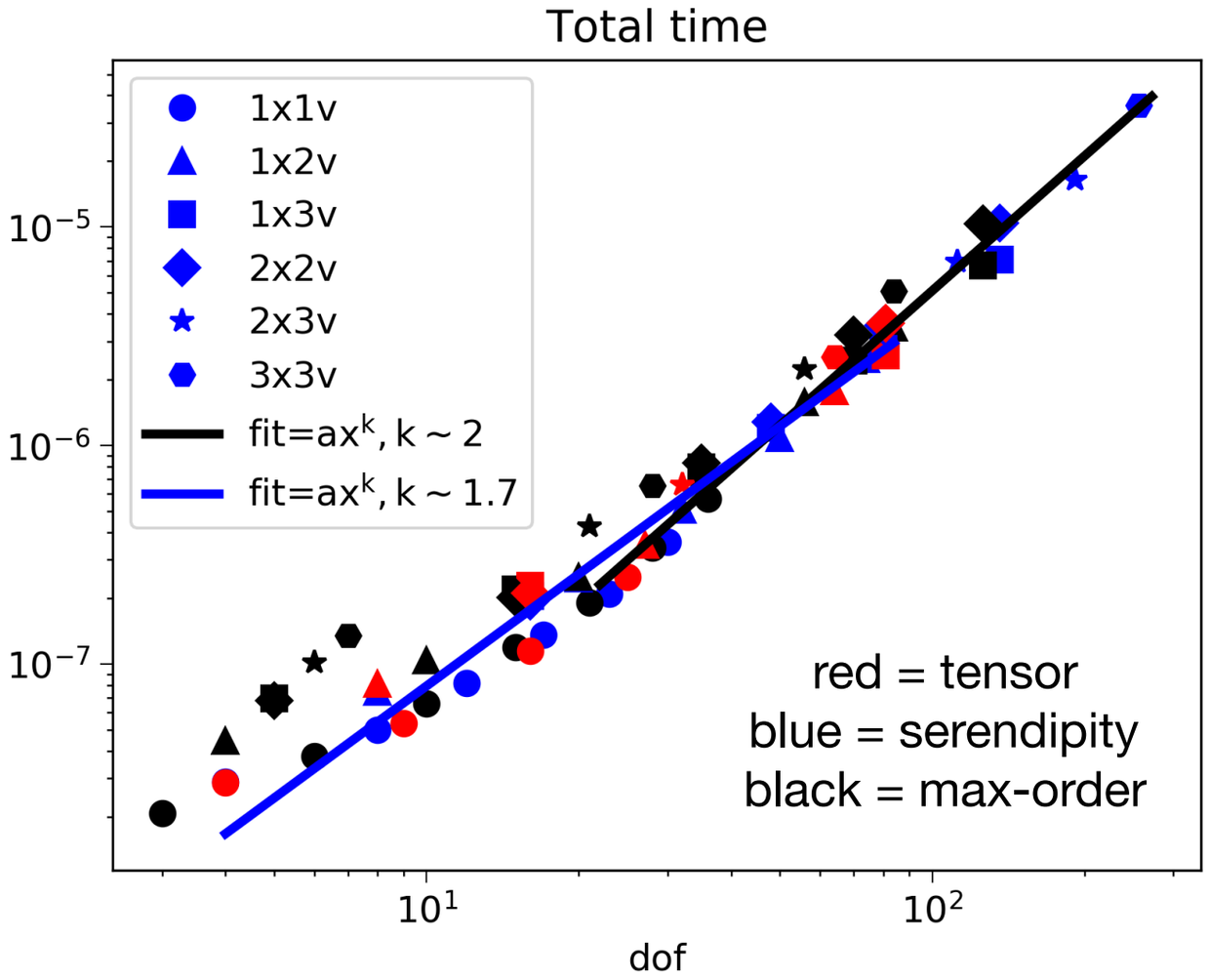

- Key takeaways
  - This is the scaling of the **full** update, not the update per dimension
  - The cost saving is thus ~ $\frac{dN_q}{N_p}$ ~ 20 in 2X3V

Let’s do some physics!

How to understand plasma energization?

$$\frac{\partial f_s}{\partial t} + \mathbf{v} \cdot \nabla_{\mathbf{x}} f_s + \frac{q_s}{m_s} (\mathbf{E} + \mathbf{v} \times \mathbf{B}) \cdot \nabla_{\mathbf{v}} f_s = 0$$

$$\frac{\partial \mathcal{E}_s}{\partial t} + \nabla_{\mathbf{x}} \cdot \left(\mathcal{E}_s \mathbf{u}_s + \mathbf{u}_s \cdot \overleftrightarrow{\mathbf{P}}_s + \mathbf{q}_s \right) = n_s q_s \mathbf{u}_s \cdot \mathbf{E}$$

$$C(\mathbf{x}, \mathbf{v}, t) = -q_s \frac{|\mathbf{v}|^2}{2} \mathbf{E}(\mathbf{x}, t) \cdot \nabla_{\mathbf{v}} f_s(\mathbf{x}, \mathbf{v}, t)$$

$$C(\mathbf{x}, \mathbf{v}, t, \tau) = -\frac{1}{\tau} \int_t^{t+\tau} q_s \frac{|\mathbf{v}|^2}{2} \mathbf{E}(\mathbf{x}, t') \cdot \nabla_{\mathbf{v}} f_s(\mathbf{x}, \mathbf{v}, t') \, dt'$$

Field-Particle Correlation [Howes, Klein, & Li JPP 2017]

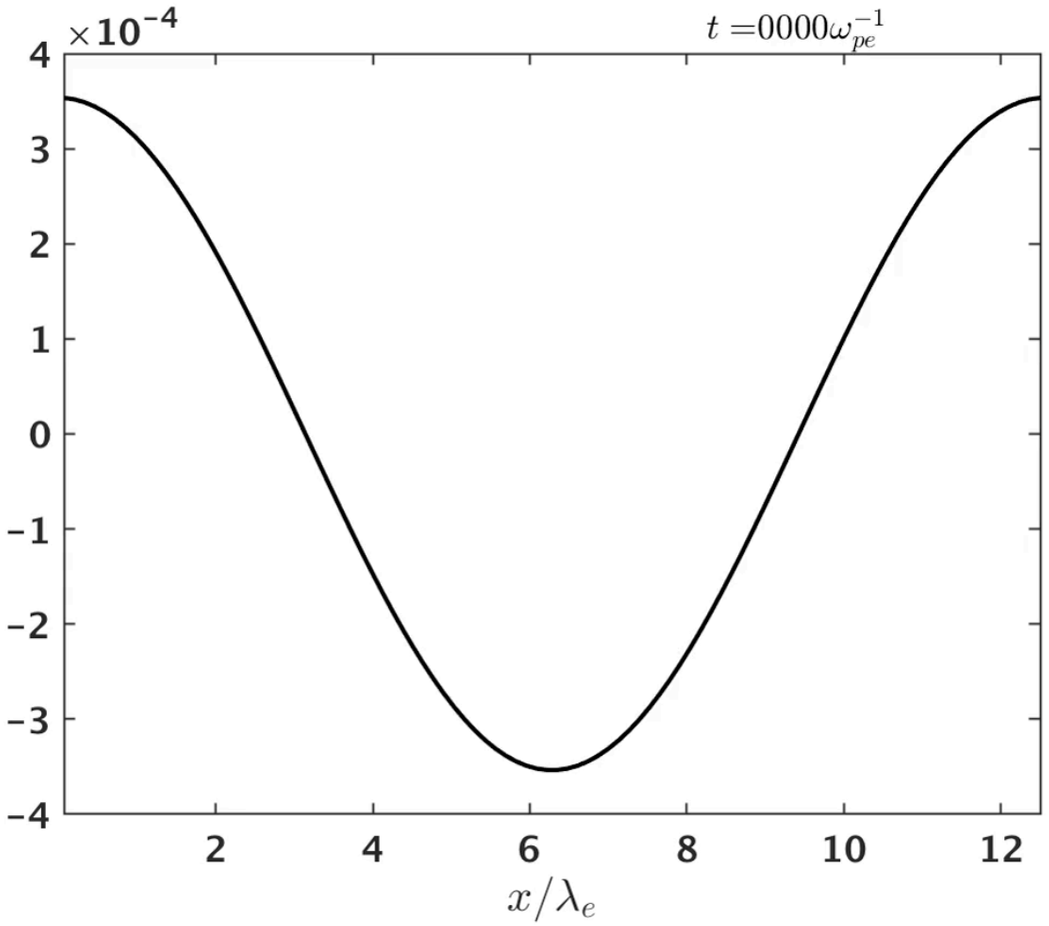

$$\delta n/n_0 = 0.005$$

$$(n_x, n_v) = (32, 64), p = 2$$

$$L_x = 4\pi\lambda_D$$

$$-10v_{te} \leq v \leq 10v_{te}$$

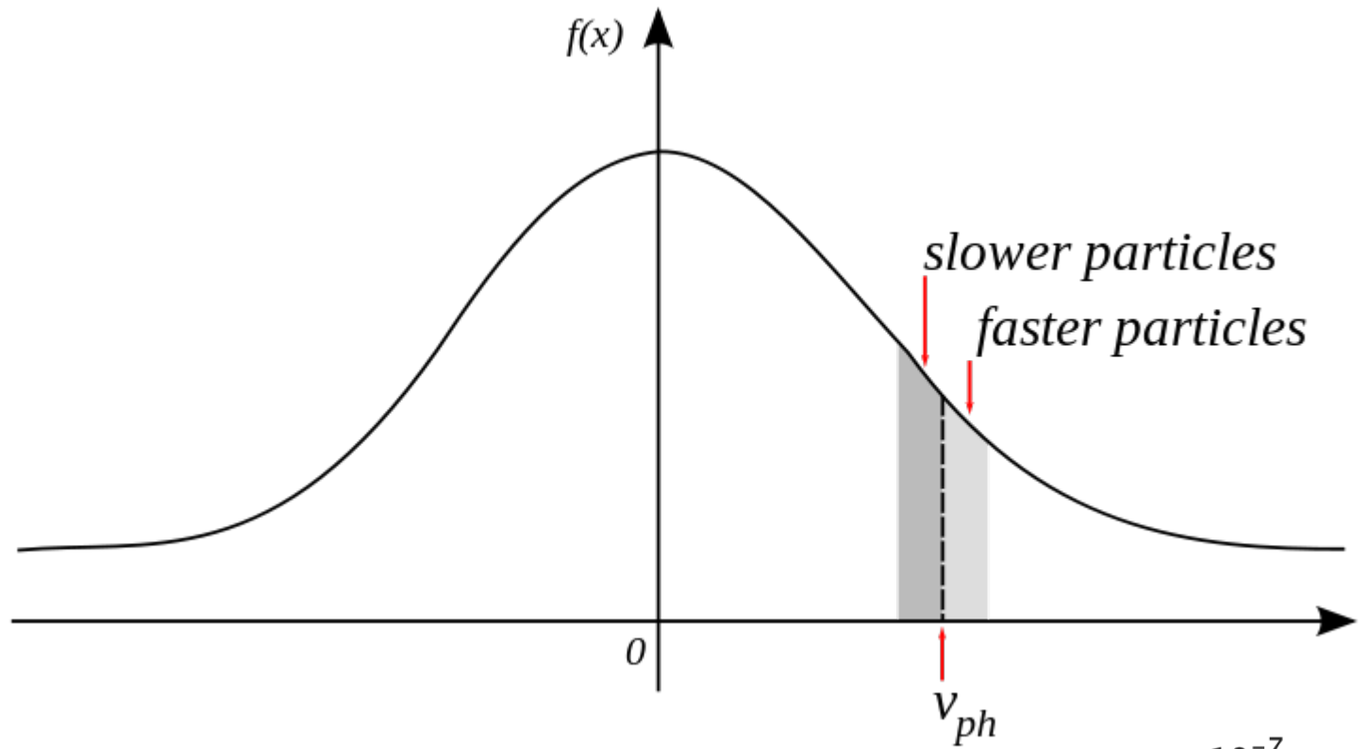

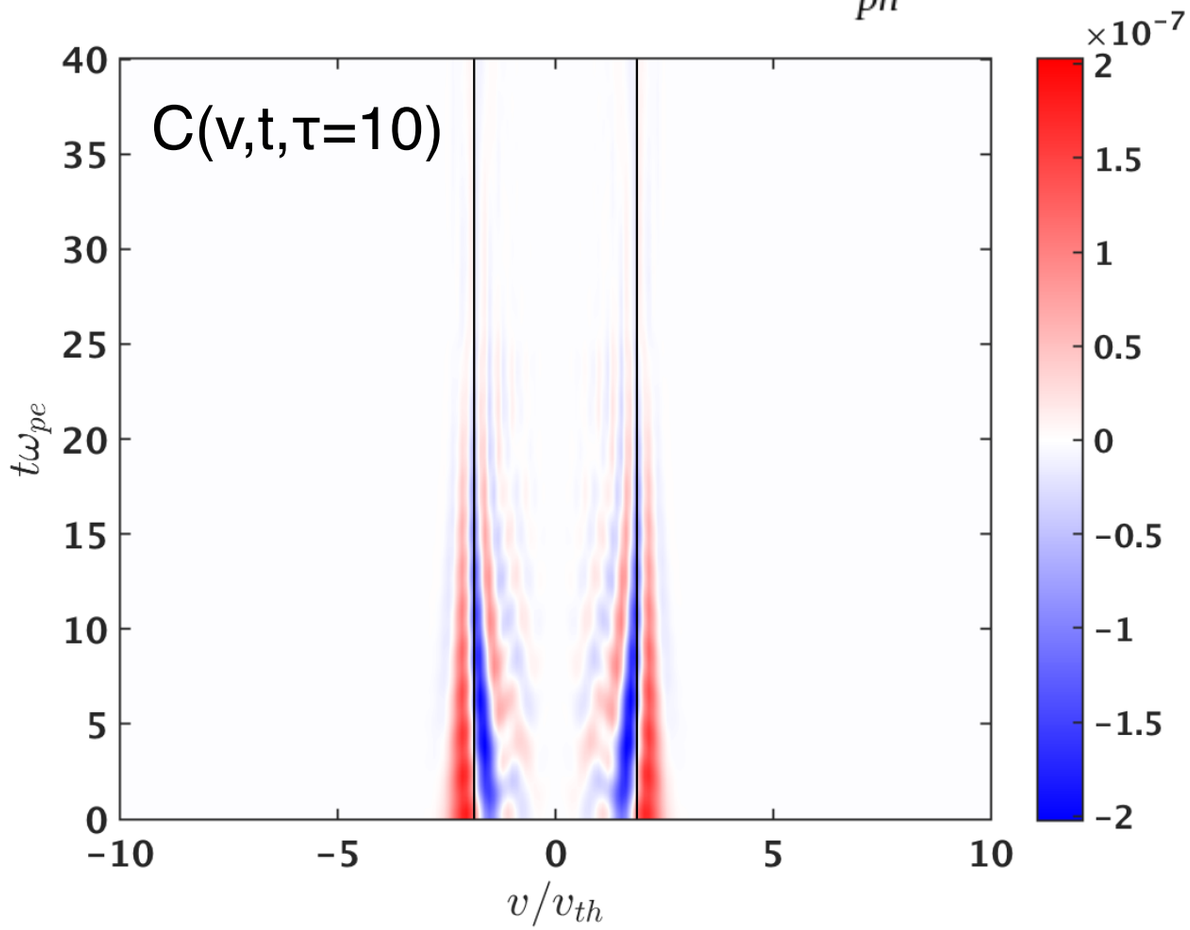

FPCs in spacecraft [Chen et al Nature Comm (2019)]

Single point spacecraft electron data from Earth's magnetosheath

$\langle f(v_{\parallel}, v_{\perp}) \rangle$

$\langle C_{\tau=0}(f, E) \rangle$

$\langle C_{\tau=0}(\delta f, E_{f>1Hz}) \rangle$

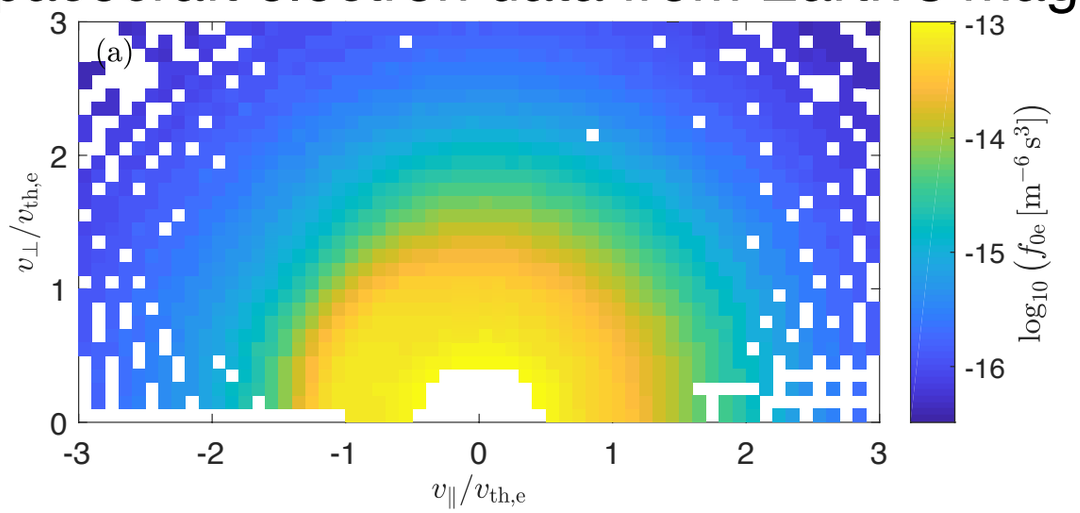

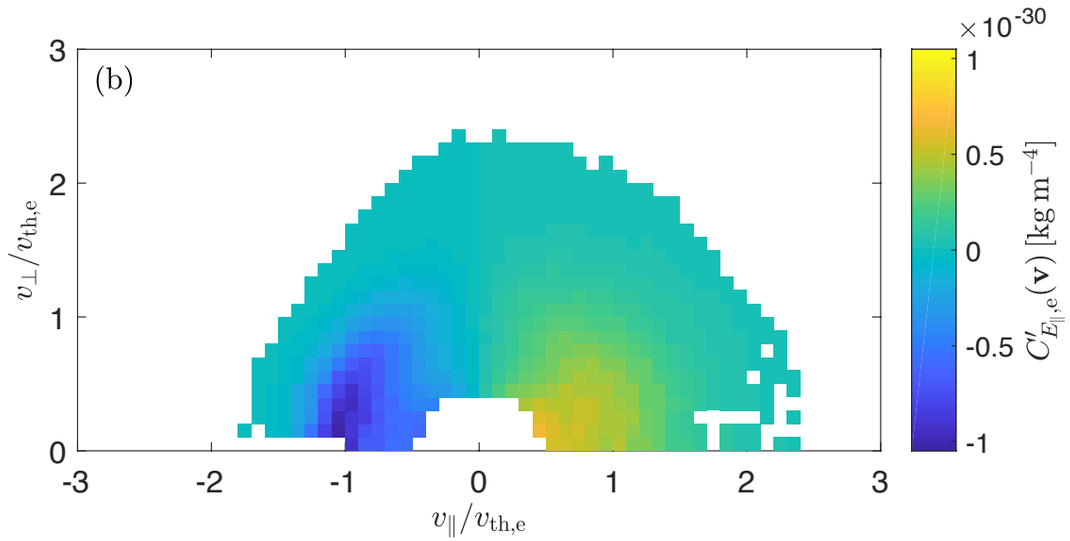

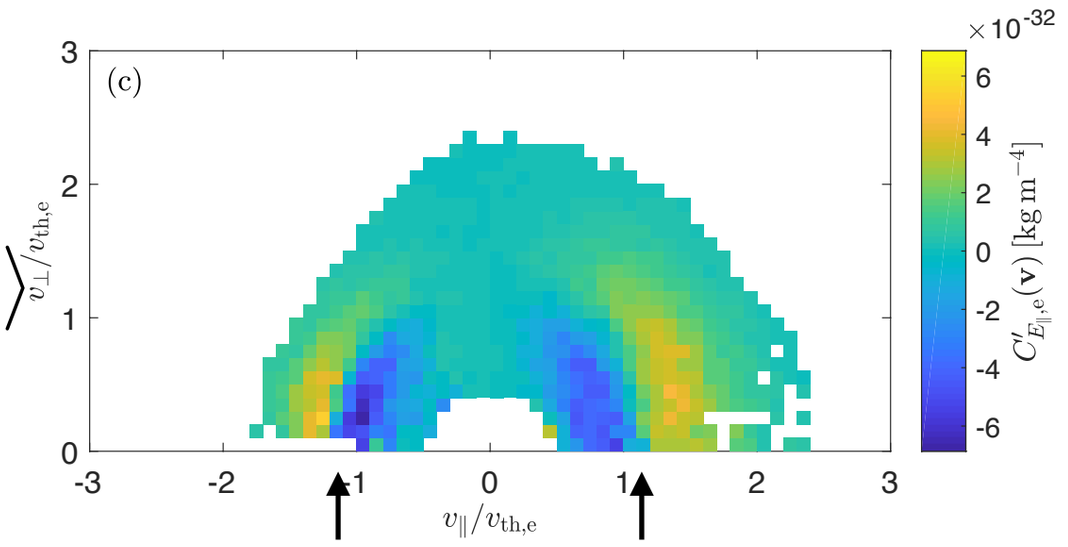

Other applications? (Figure adapted from Chen et al. 2018 PRL)

(a) Consecutive distribution functions in 30 second intervals (b) Sample distribution functions from the main ramp of the shock

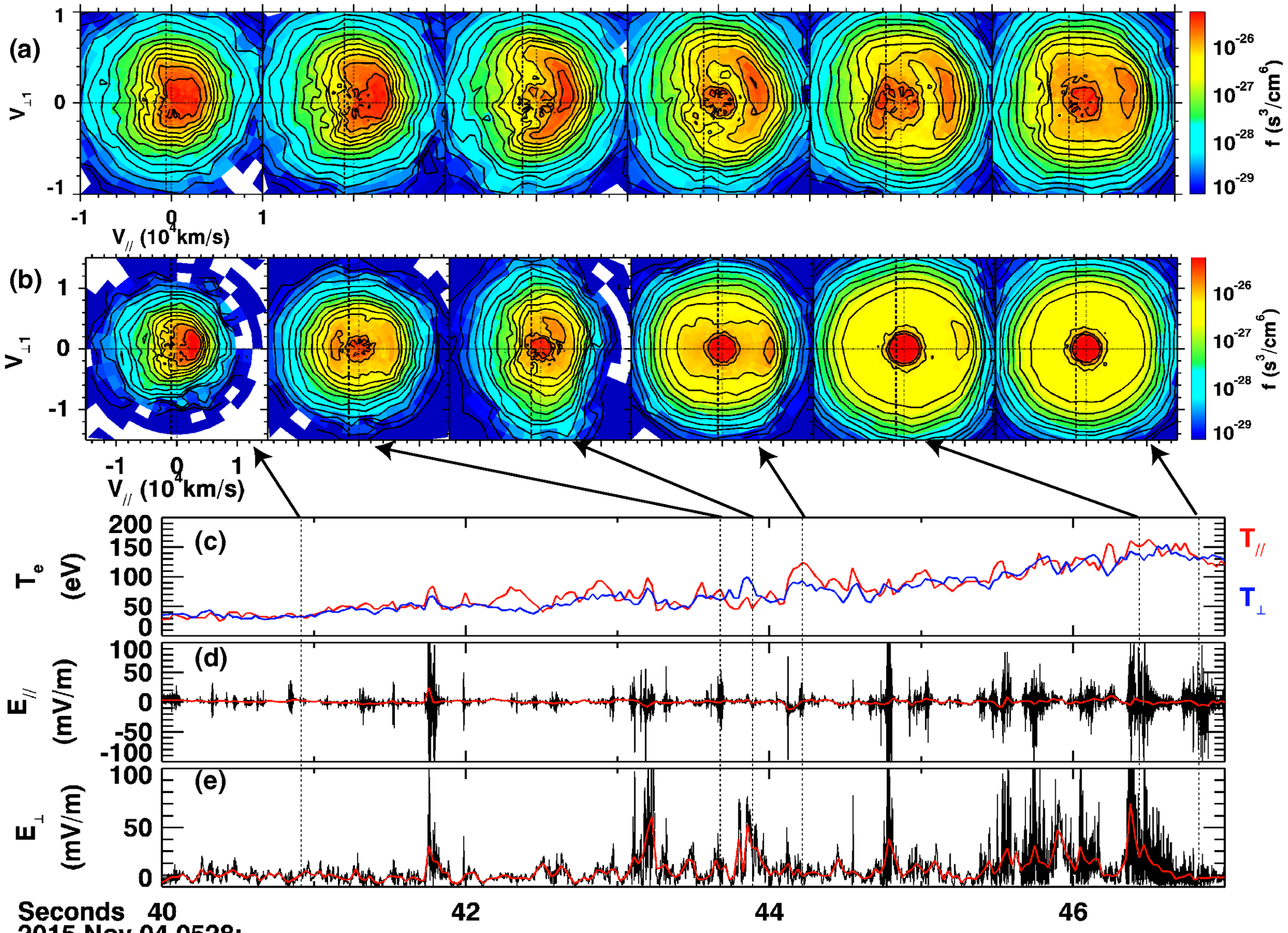

Building the Field Particle Correlation Rosetta Stone

$$\mathbf{B}(t=0) = B_0\hat{\mathbf{z}}, \quad \mathbf{E}(t=0) = -\mathbf{u}\times\mathbf{B} = U_x B_0 \hat{\mathbf{y}}$$

$$U_x = -3v_A, \quad \rightarrow \quad r \sim 2.5, \quad U_{shock} = \frac{U_x}{r-1} \sim 2v_A$$

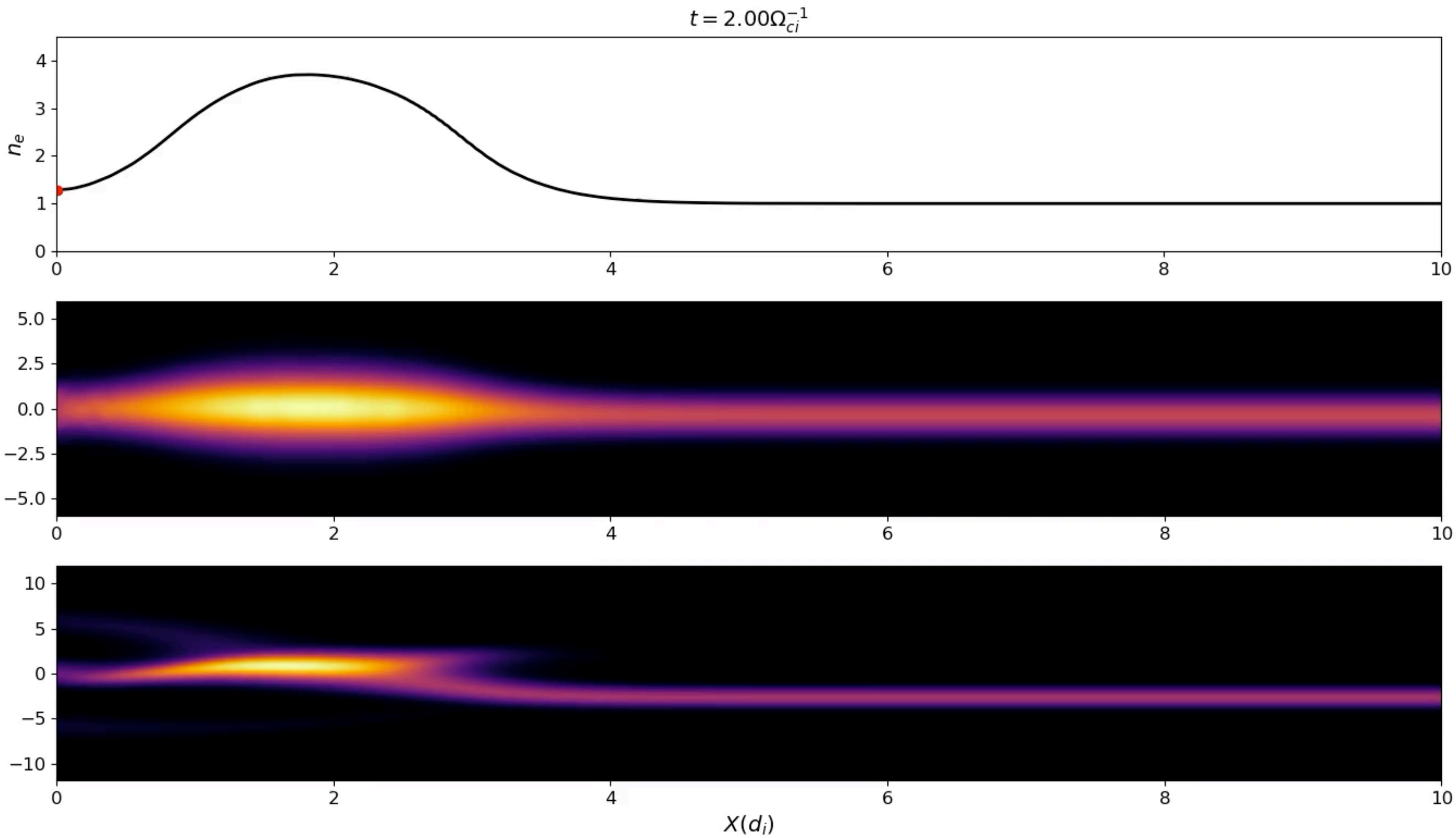

Field-Particle Correlation at fixed time

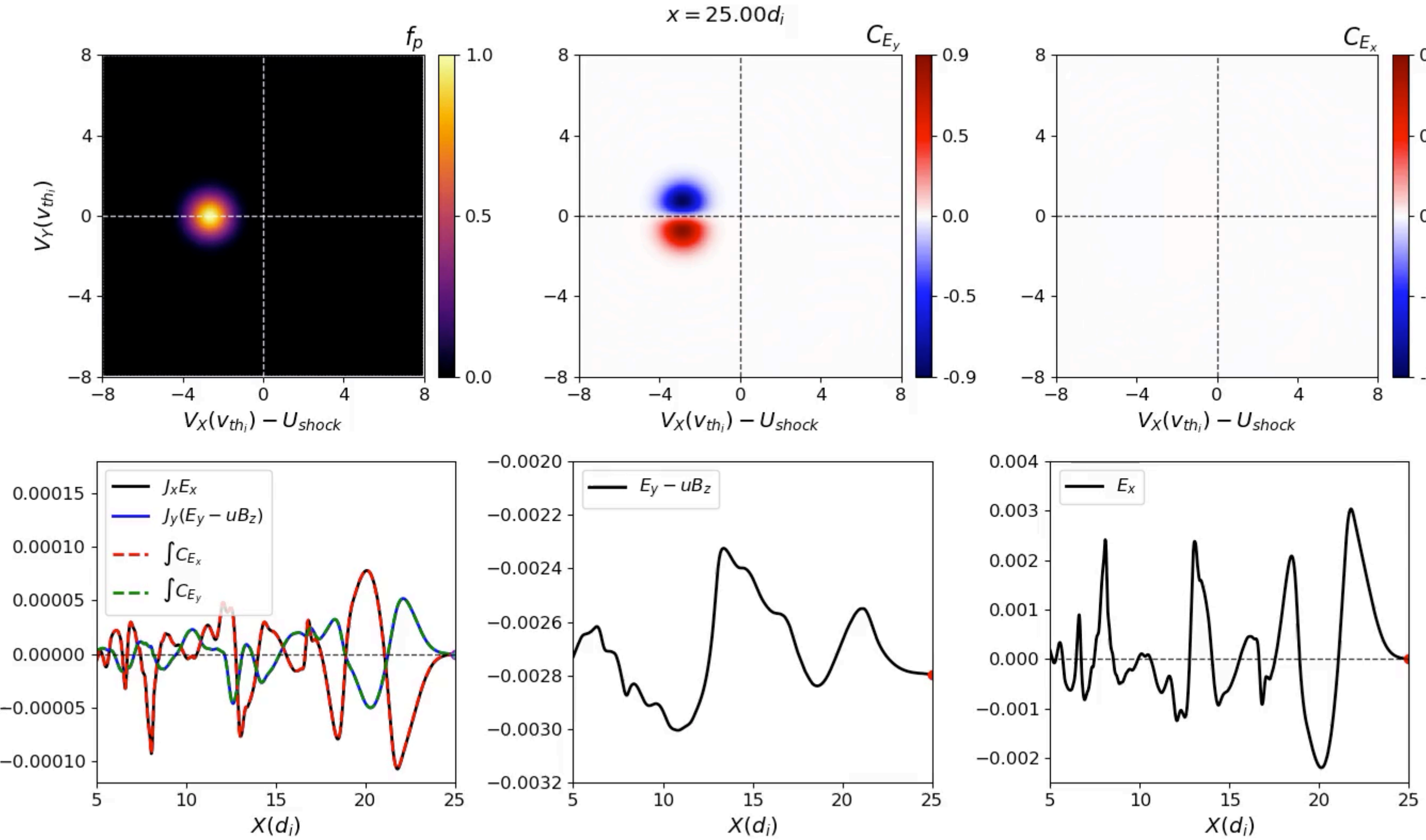

Highlighting the energization signature

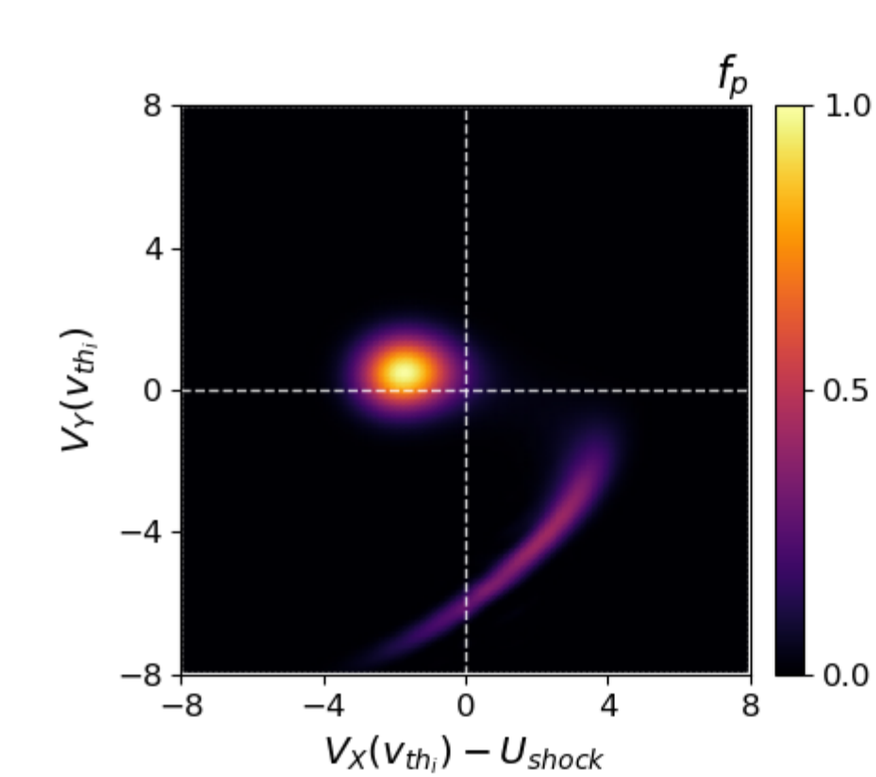

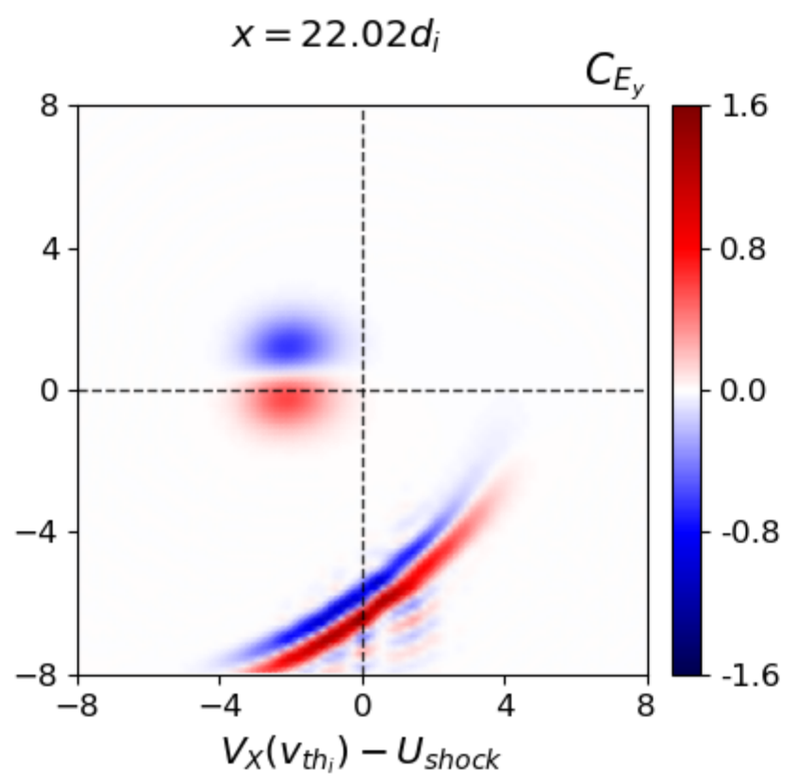

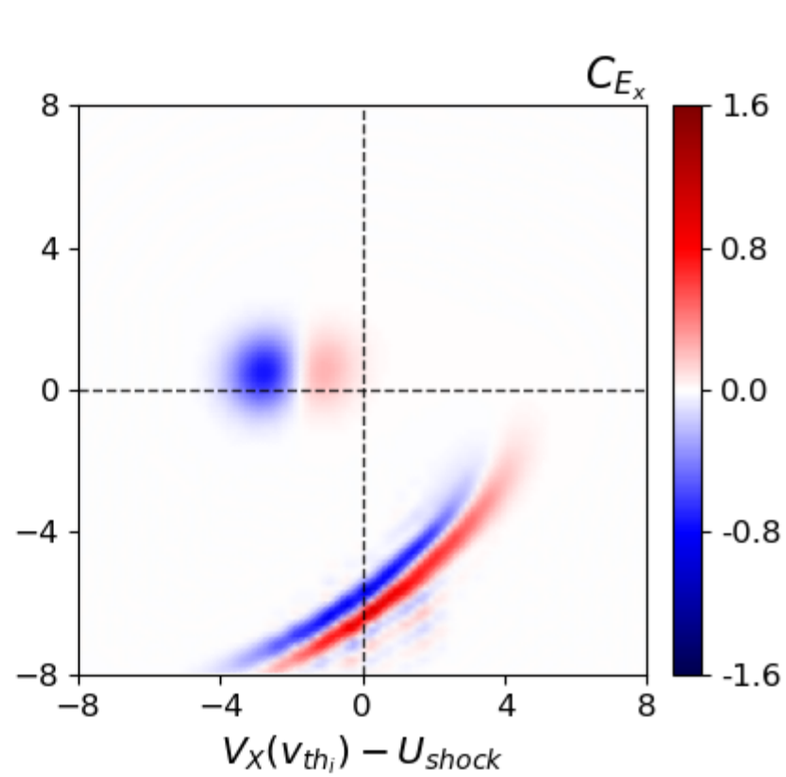

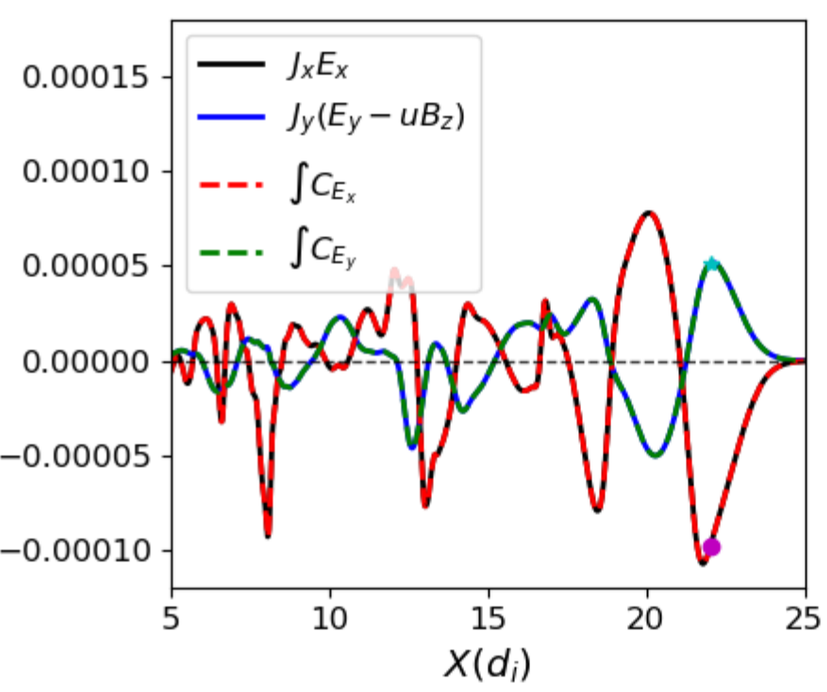

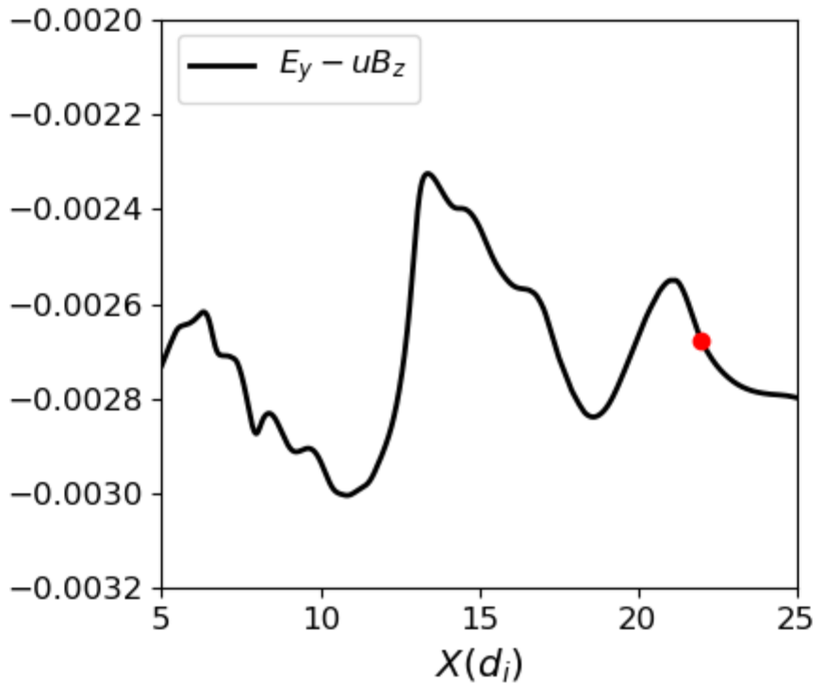

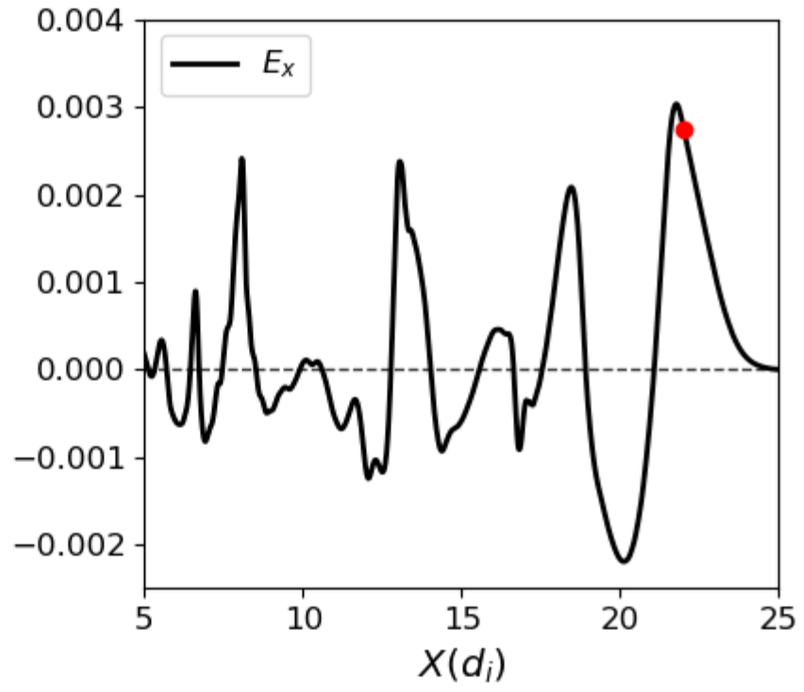

Intuition from single particle motion

- Protons E x B drifting into a magnetic field gradient can sample both the upstream and downstream, leading to net energization - **shock drift acceleration**
  - Video courtesy of NASA Scientific Visualization (Tom Bergman): https://svs.gsfc.nasa.gov/4513

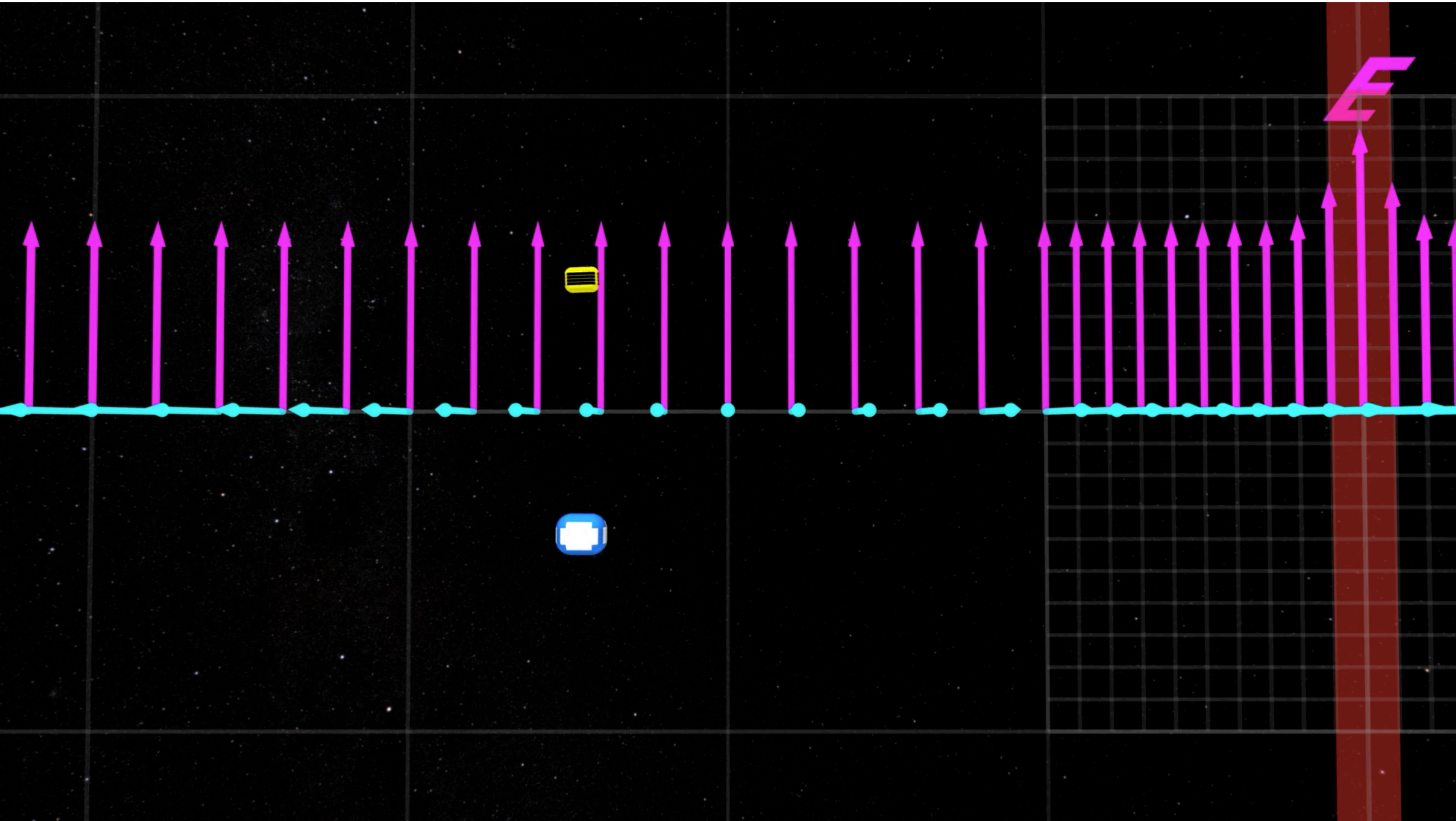

The universe is magnetized..

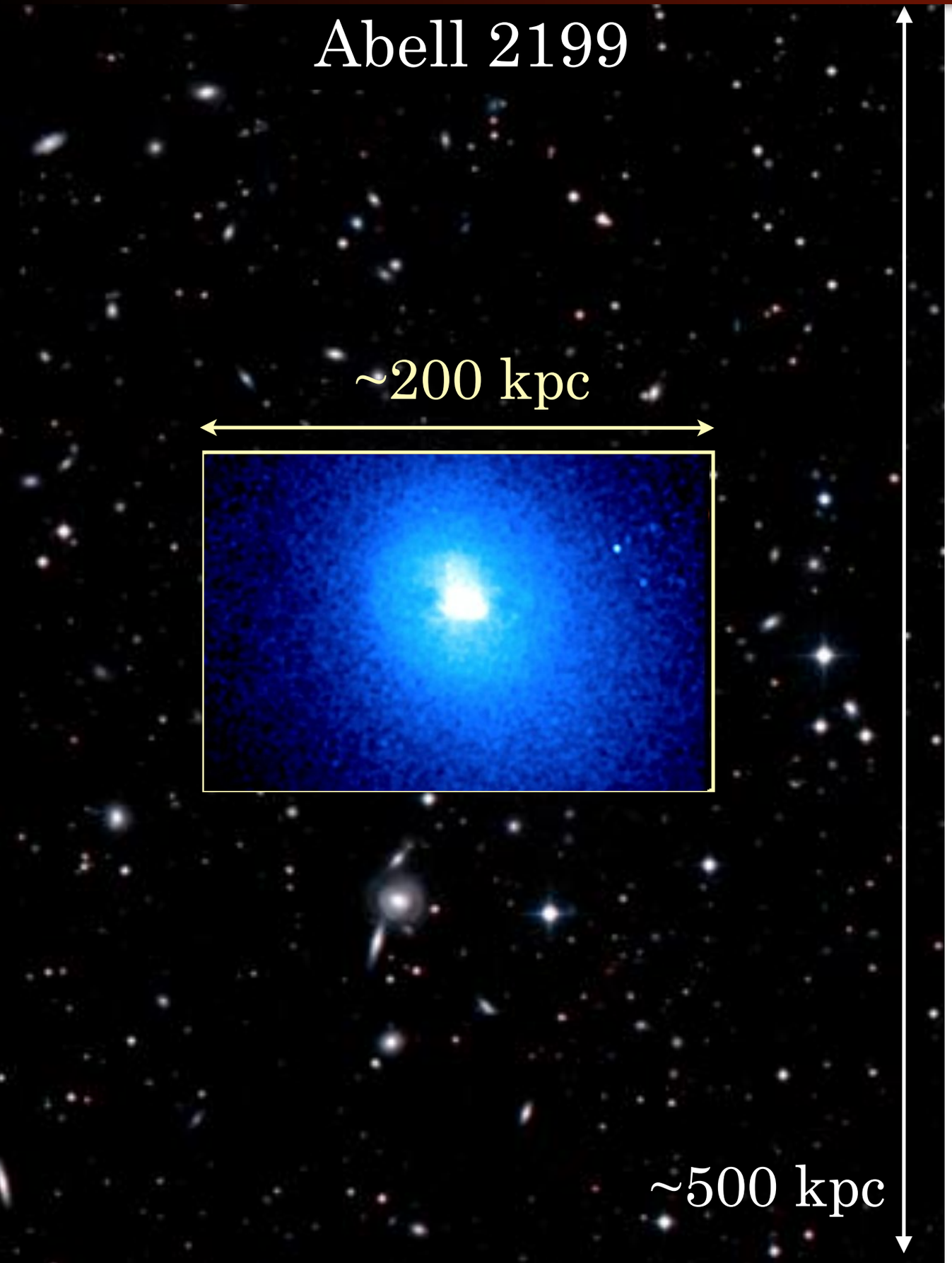

Galaxy Clusters

$$M \sim 10^{14-15}\ \mathrm{M}_\odot$$
$$\text{in } \sim 1\ \mathrm{Mpc}$$

14% thermal plasma

$$T \sim 1\text{–}10\ \mathrm{keV}$$
$$n \sim 10^{-4}\text{–}10^{-1}\ \mathrm{cm}^{-3}$$

The universe is magnetized..

ion Larmor orbit
if B ~ 10^{-18} G

200 kpc

ion Larmor orbit
now, with B ~ μG

But how did it get magnetized?

$$\rho_i \sim \left(\frac{T}{1\ \mathrm{keV}}\right)^{1/2} \left(\frac{B}{10^{-18}\ \mathrm{G}}\right)^{-1} \ \mathrm{kpc}$$

$$\Omega_i \sim \left(\frac{B}{10^{-18}\ \mathrm{G}}\right) \ \mathrm{Myr}^{-1}$$

why? | how?

likely dynamo!

but dynamo requires a seed field..

$$\rho_i \sim \left(\frac{T}{1\ \mathrm{keV}}\right)^{1/2} \left(\frac{B}{10^{-6}\ \mathrm{G}}\right)^{-1} \ \mathrm{npc}$$

$$\Omega_i \sim \left(\frac{B}{10^{-6}\ \mathrm{G}}\right) \ \mathrm{min}^{-1}$$

(ion Larmor orbit ~ size of Jupiter)

$(\beta \equiv 8\pi nT/B^2 \sim 10^{2-4})$

One seed field candidate: filamentation instability

- In 2D, two-stream and filamentation can compete with each other
- In addition, oblique modes can be present
- When drifts non-relativistic, many of these modes all have similar growth rates, the ultimate nonlinear evolution will involve a competition between these instabilities
- Need to consider non-relativistic limit to be relevant for reionization epoch

$$T \sim 10^4 - 10^6\, K,$$

$$v_{shock} \sim 10^2 - 10^4\, km/s$$

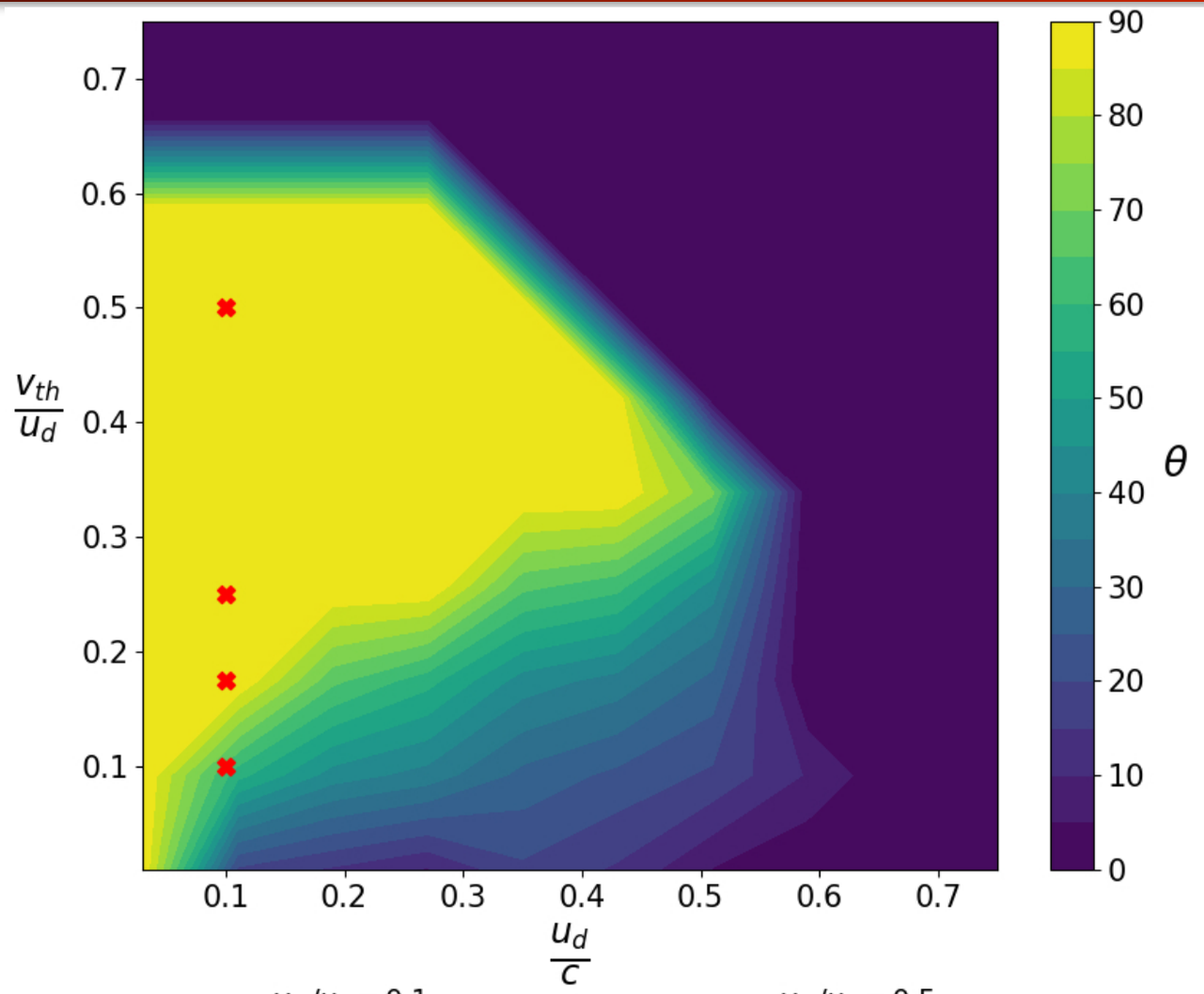

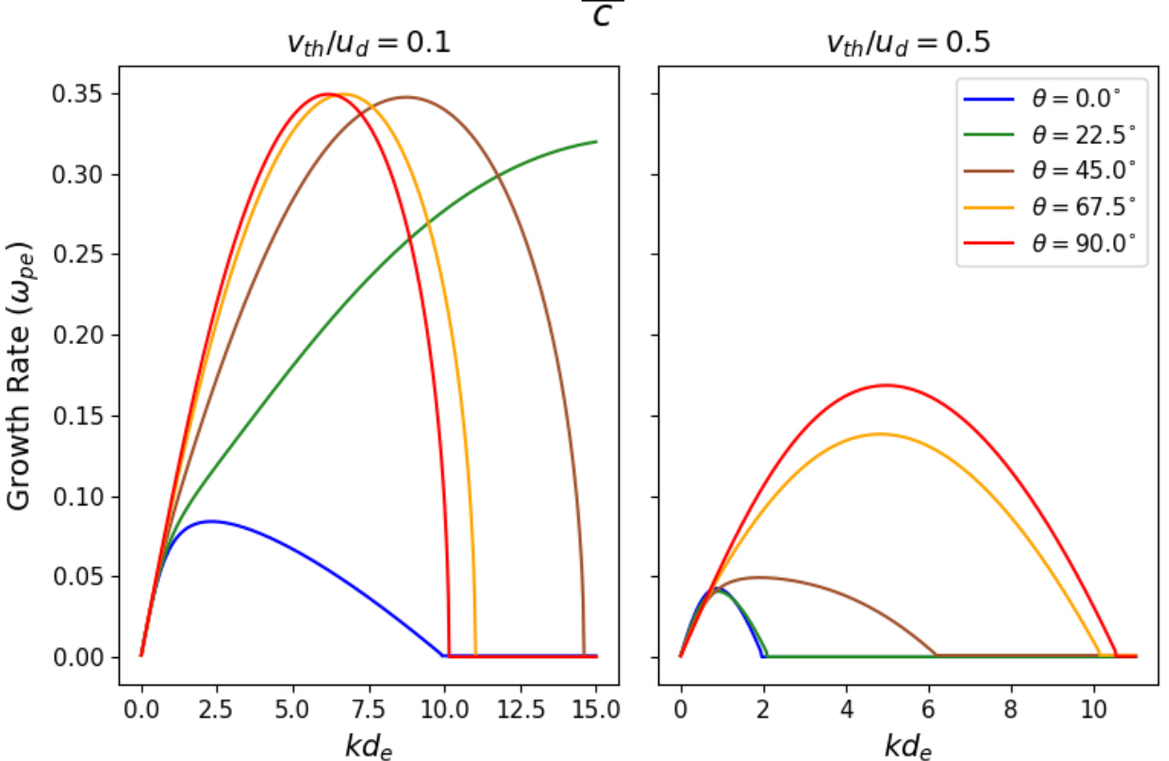

Geometry and Initial Condition

$$f_{0,e}(v_x,\, v_y) = \frac{1}{2\pi v_{\mathrm{th}}^2} e^{-\frac{v_x^2}{2v_{\mathrm{th}}^2}} \left[e^{-\frac{(v_y-u_d)^2}{2v_{\mathrm{th}}^2}} + e^{-\frac{(v_y+u_d)^2}{2v_{\mathrm{th}}^2}} \right]$$

$$B_z(t=0) = \sum_{n_x,n_y=0}^{16,16} \tilde{B}_{n_x,n_y} \sin\left(\frac{2\pi n_x x}{L_x} + \frac{2\pi n_y y}{L_y} + \tilde{\phi}_{n_x,n_y} \right)$$

$E_x(t=0)$ and $E_y(t=0)$ are initialized similarly

$$\langle \epsilon_0 E_x^2/2 \rangle = \langle \epsilon_0 E_y^2/2 \rangle = \langle B_z^2/2\mu_0 \rangle \simeq 10^{-7} E_K$$

The “hot” case

$$v_{th_e}/u_d = 0.5$$

$$\Delta x \sim \pi\lambda_D, \quad \Delta v \sim v_{th_e}/4, \quad p = 2$$

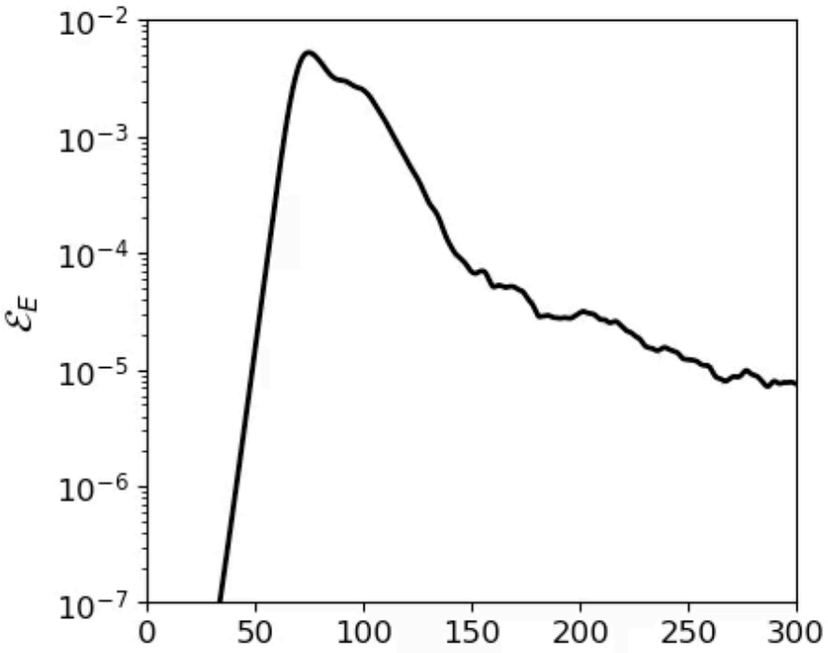

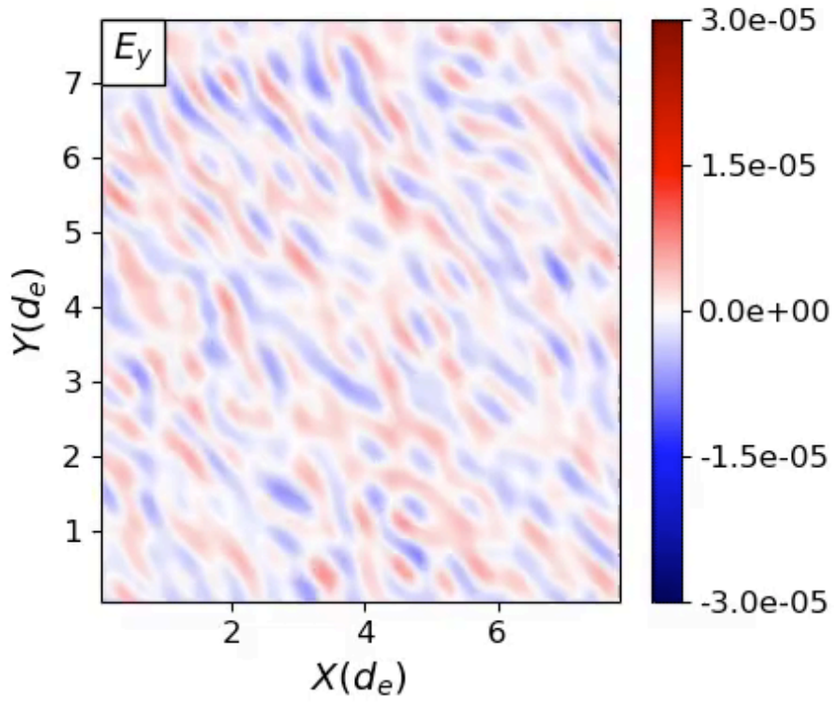

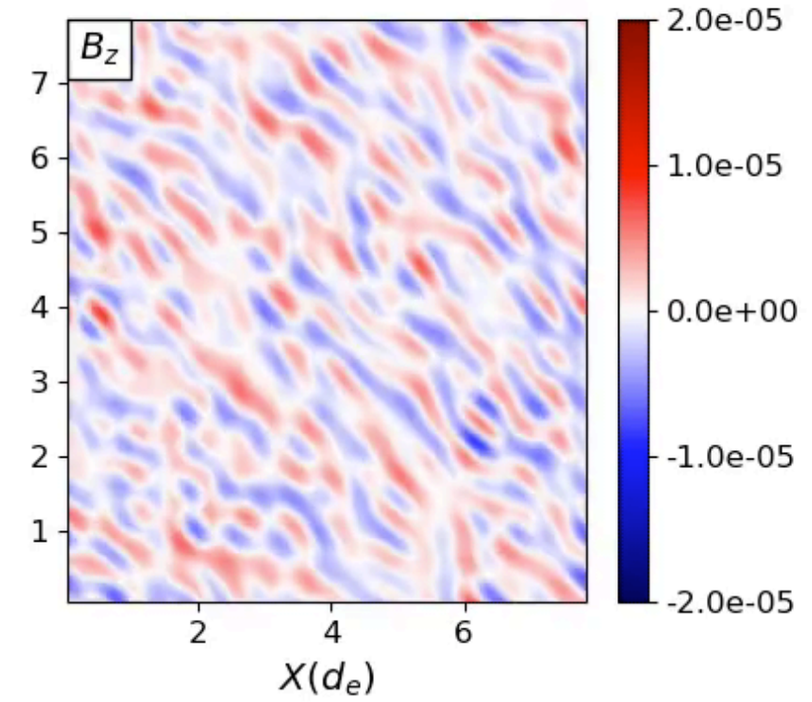

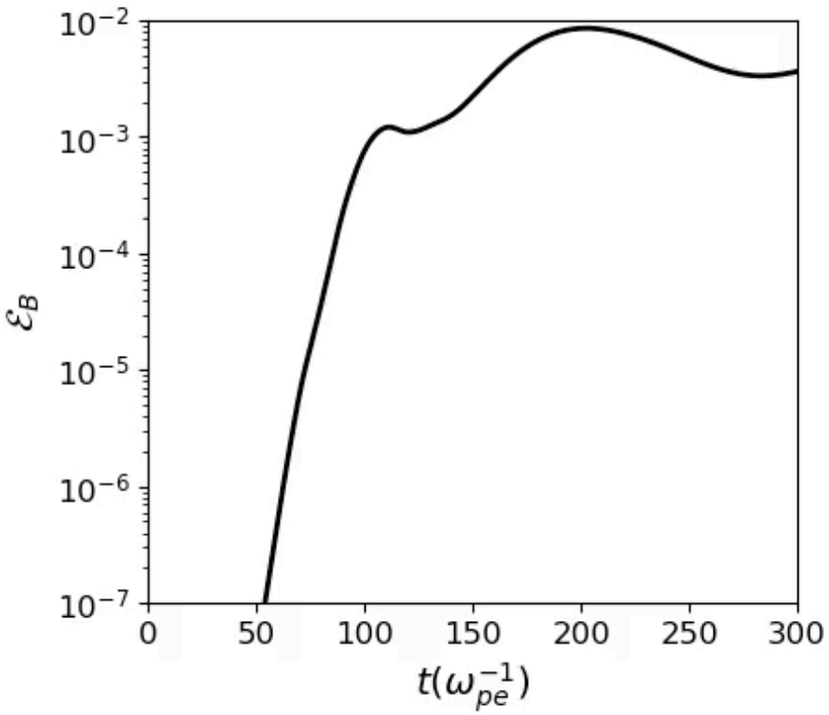

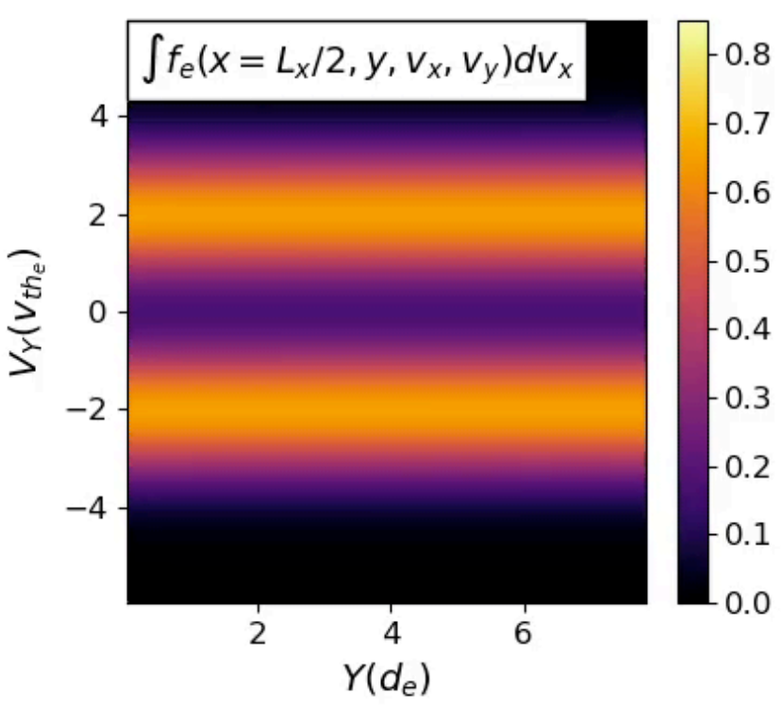

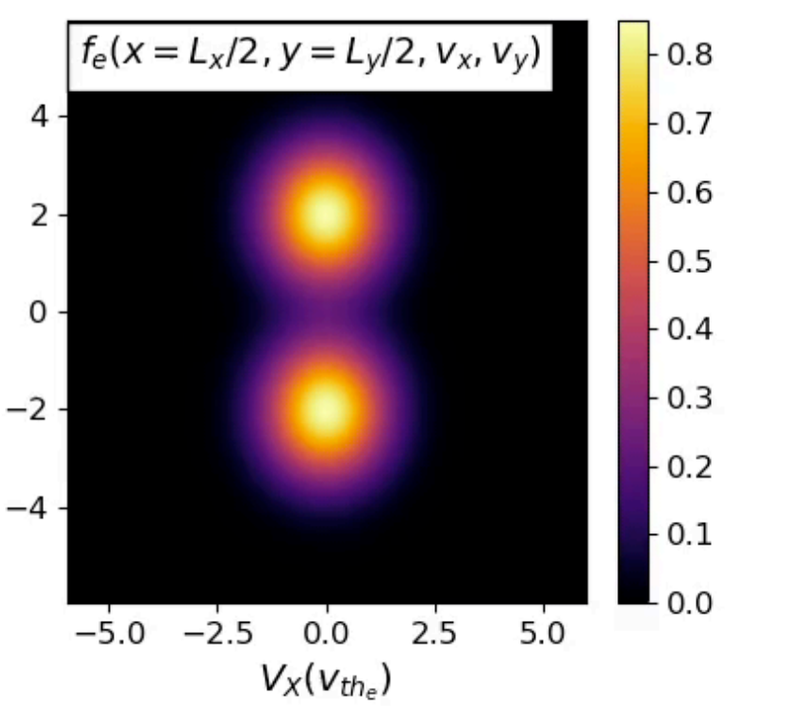

The “cold” case

$$v_{th_e}/u_d = 0.1$$

$$\Delta x \sim 2\pi\lambda_D, \quad \Delta v \sim v_{th_e}, \quad p = 2$$

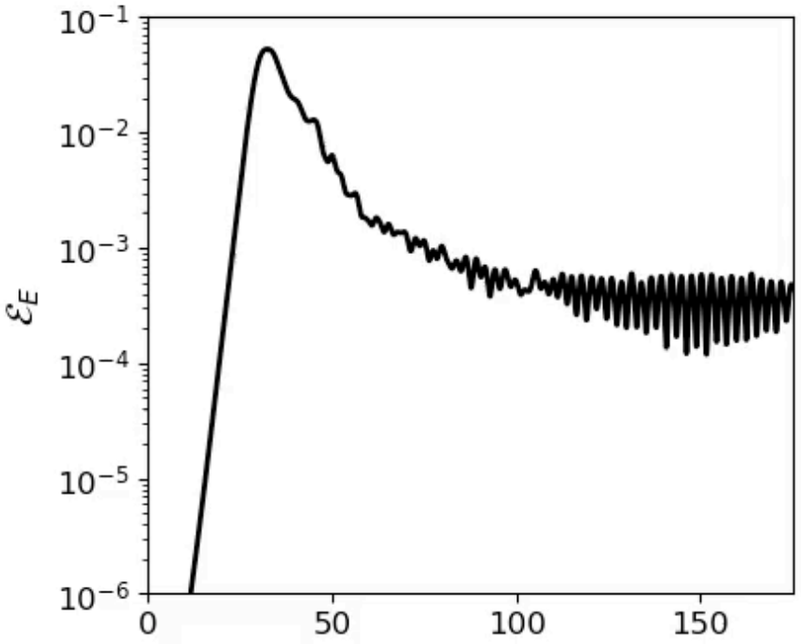

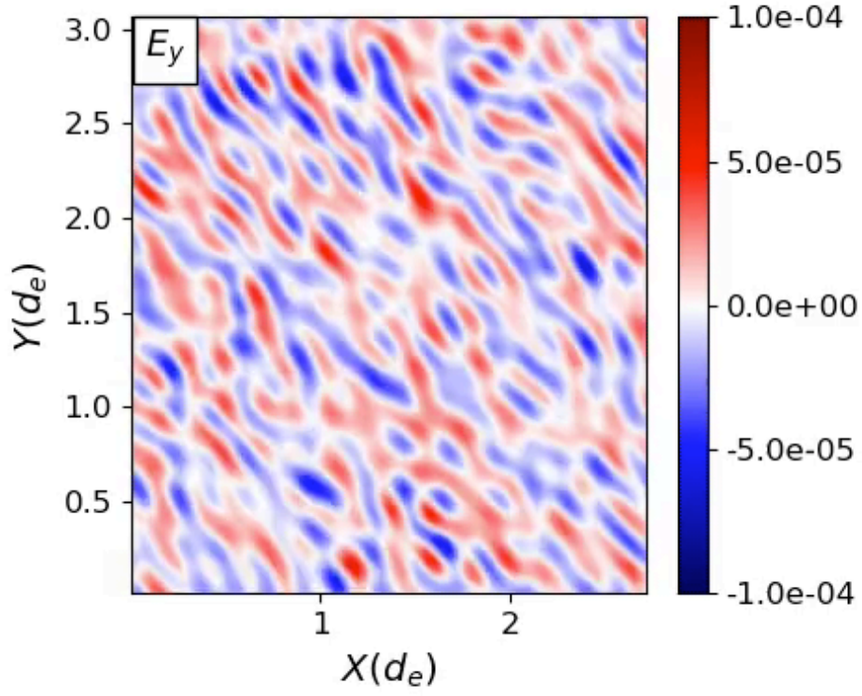

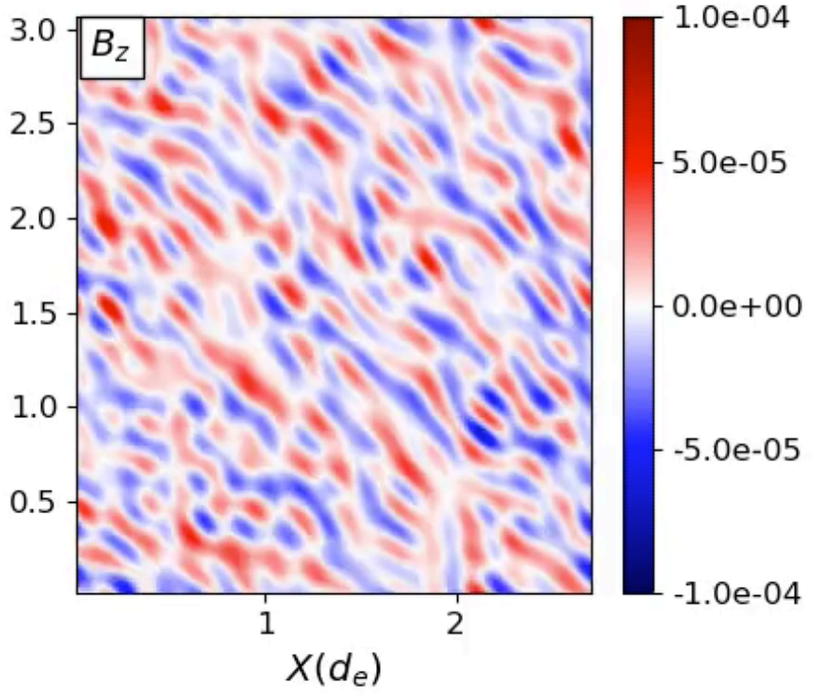

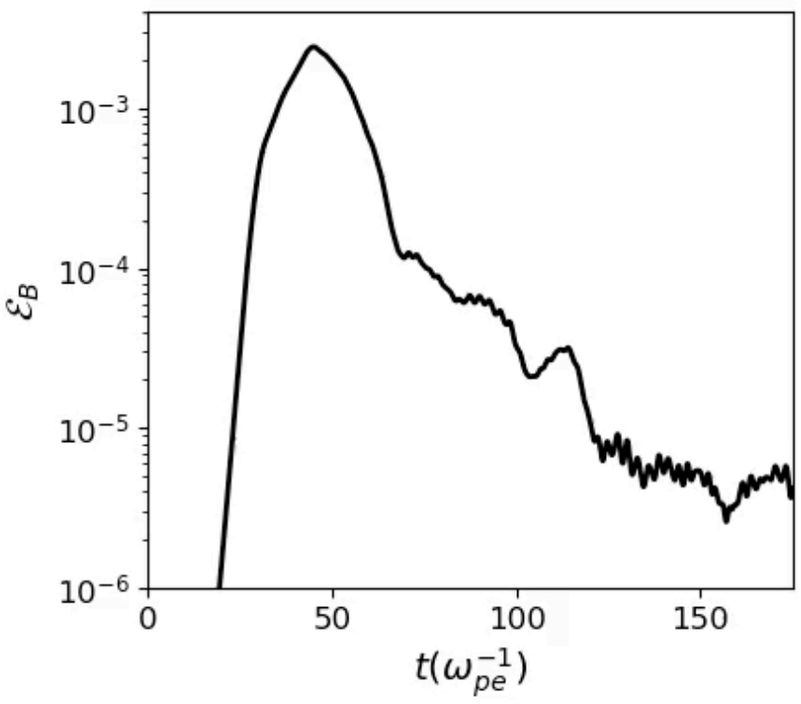

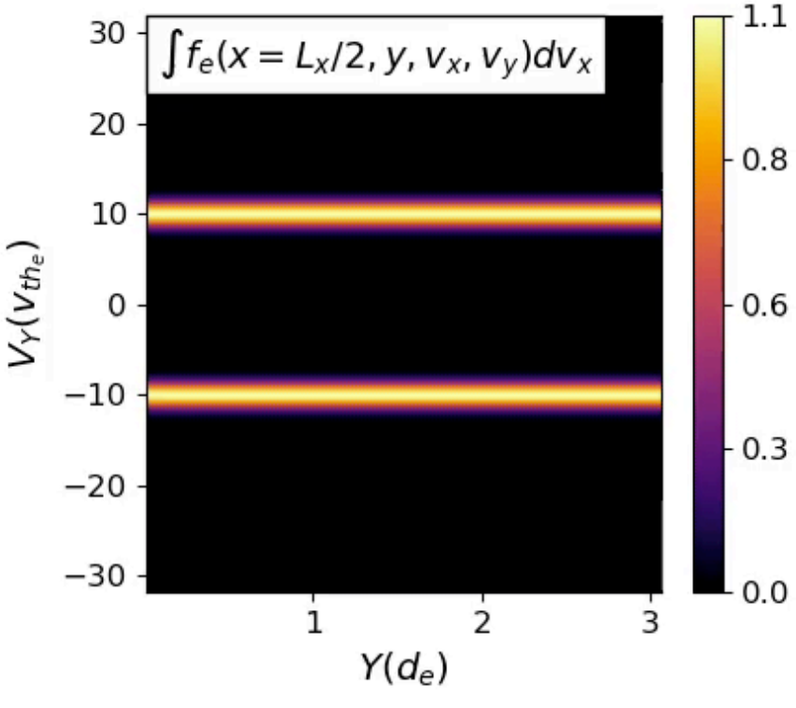

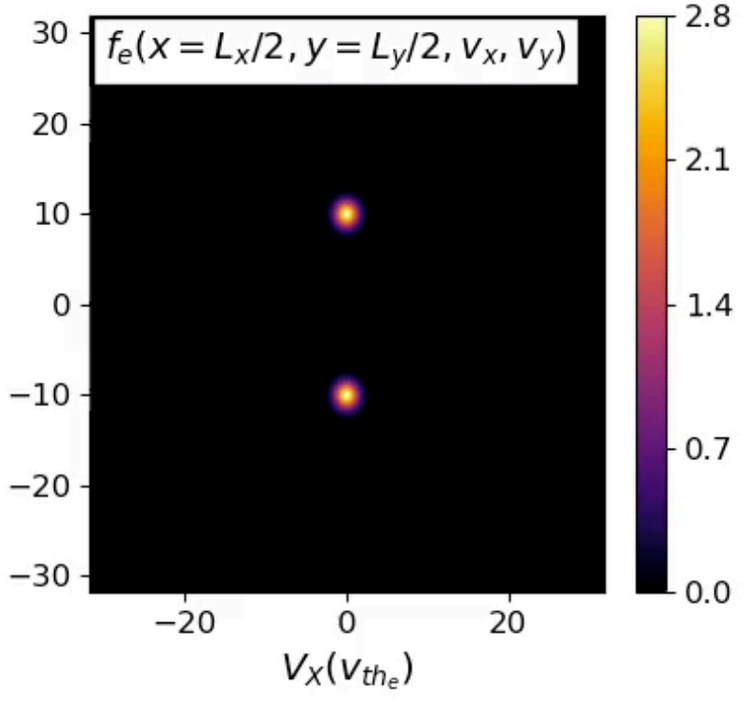

The energy exchange

- In the “hot” case, the energy exchange is dominantly in one velocity dimension, resulting in a net temperature anisotropy

- In the “cold” case, the energy exchange is more isotropic, leading to the collapse of the magnetic field

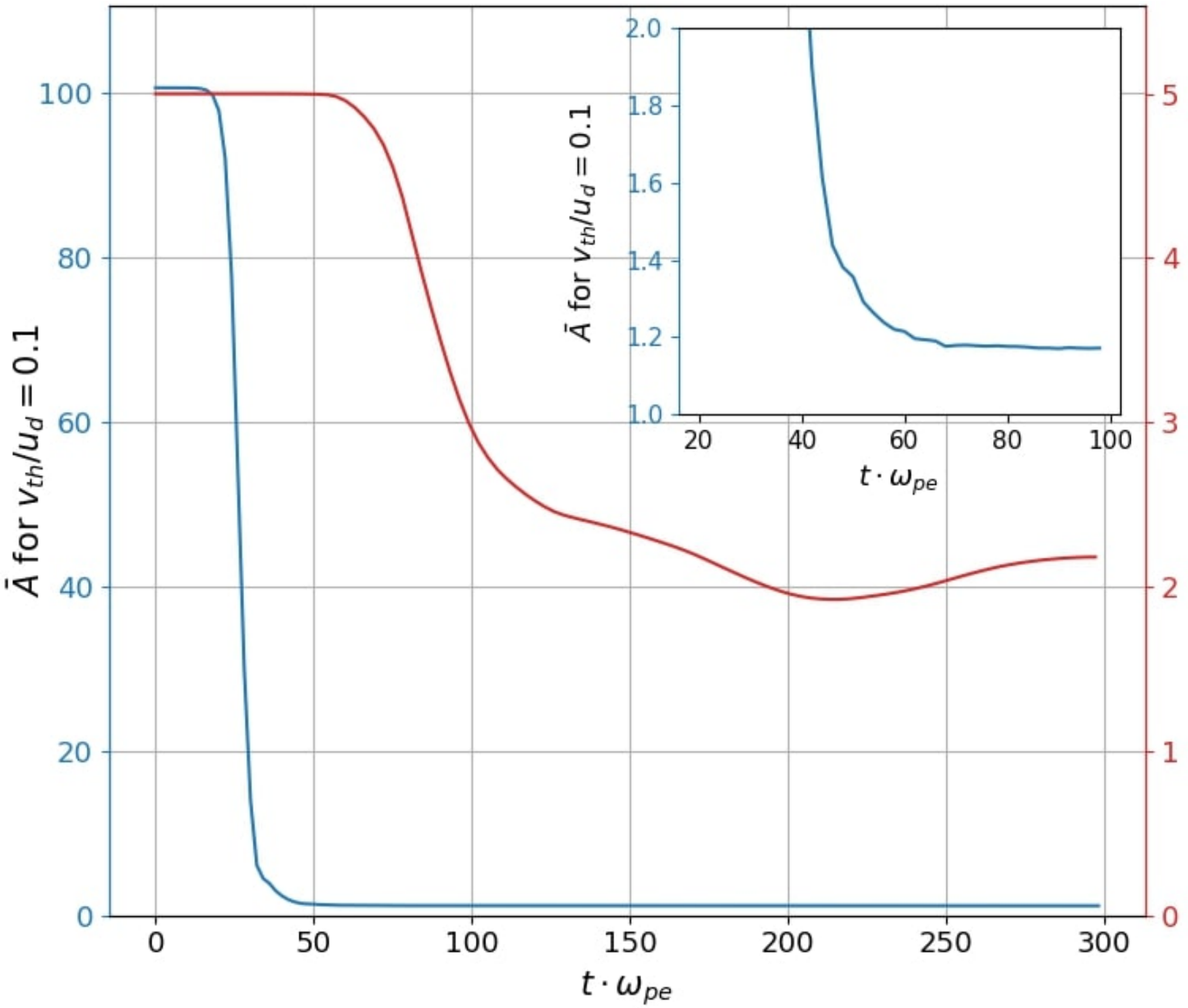

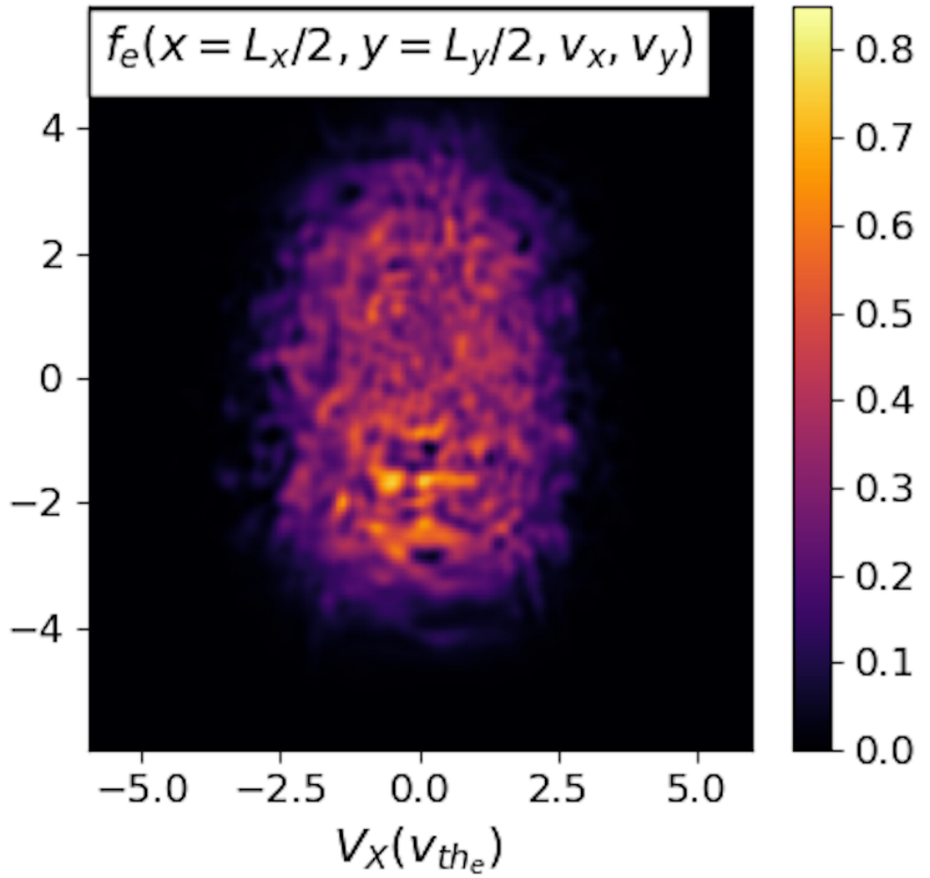

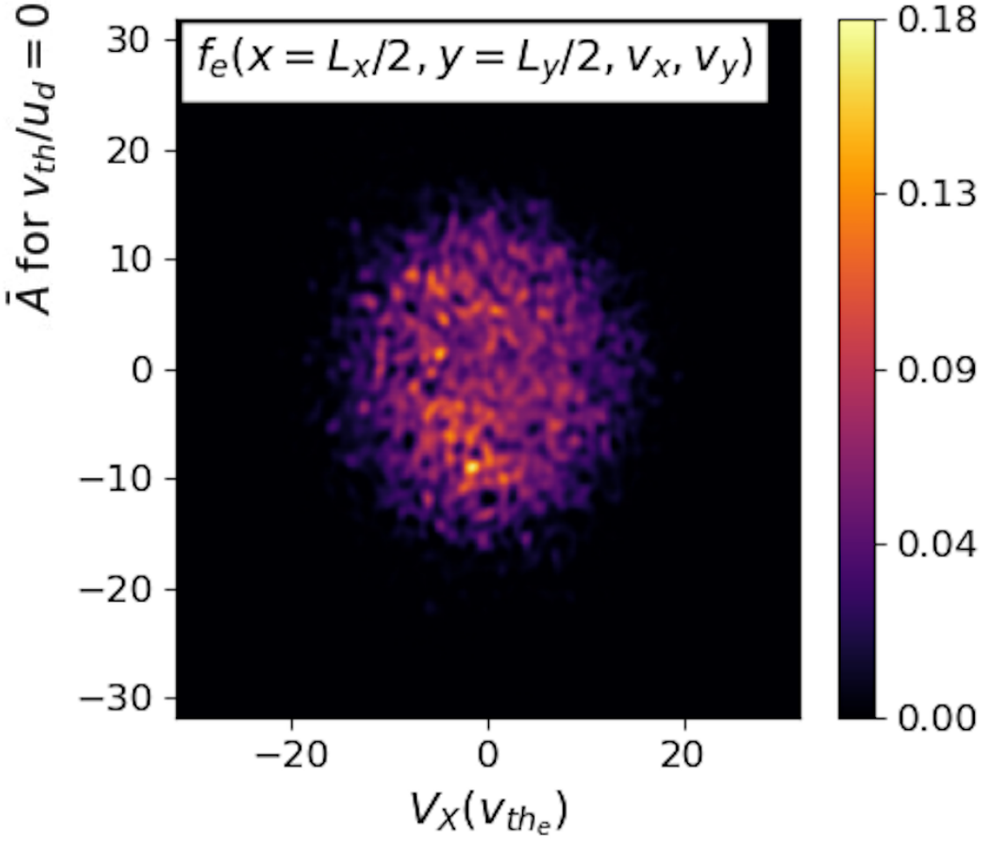

Evolution of the electromagnetic energy

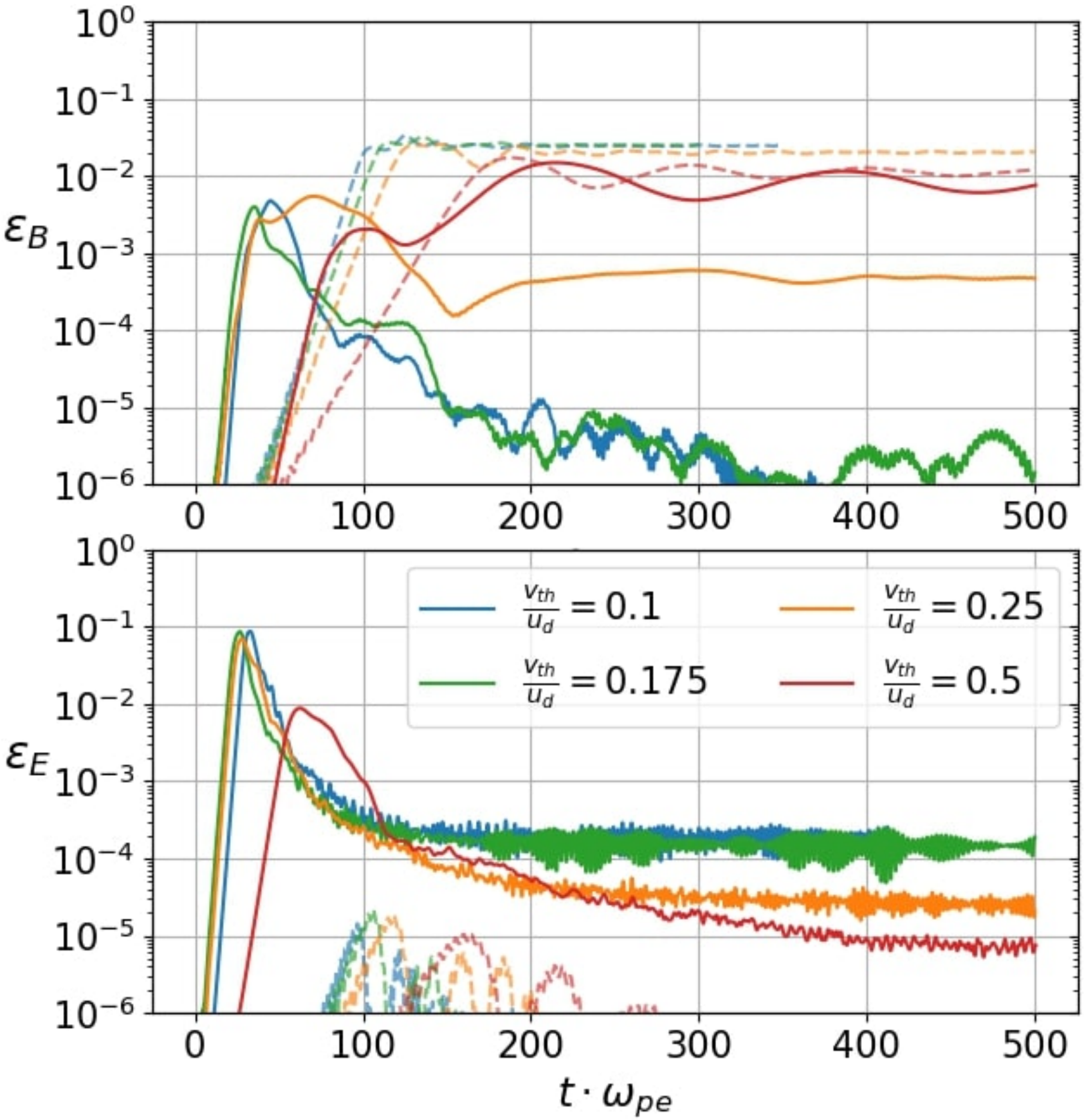

Transition occurs at

$v_{th_e}/u_d < 0.2$

Comparing to the Particle in Cell Method

Thermal fluctuations in the magnetic field

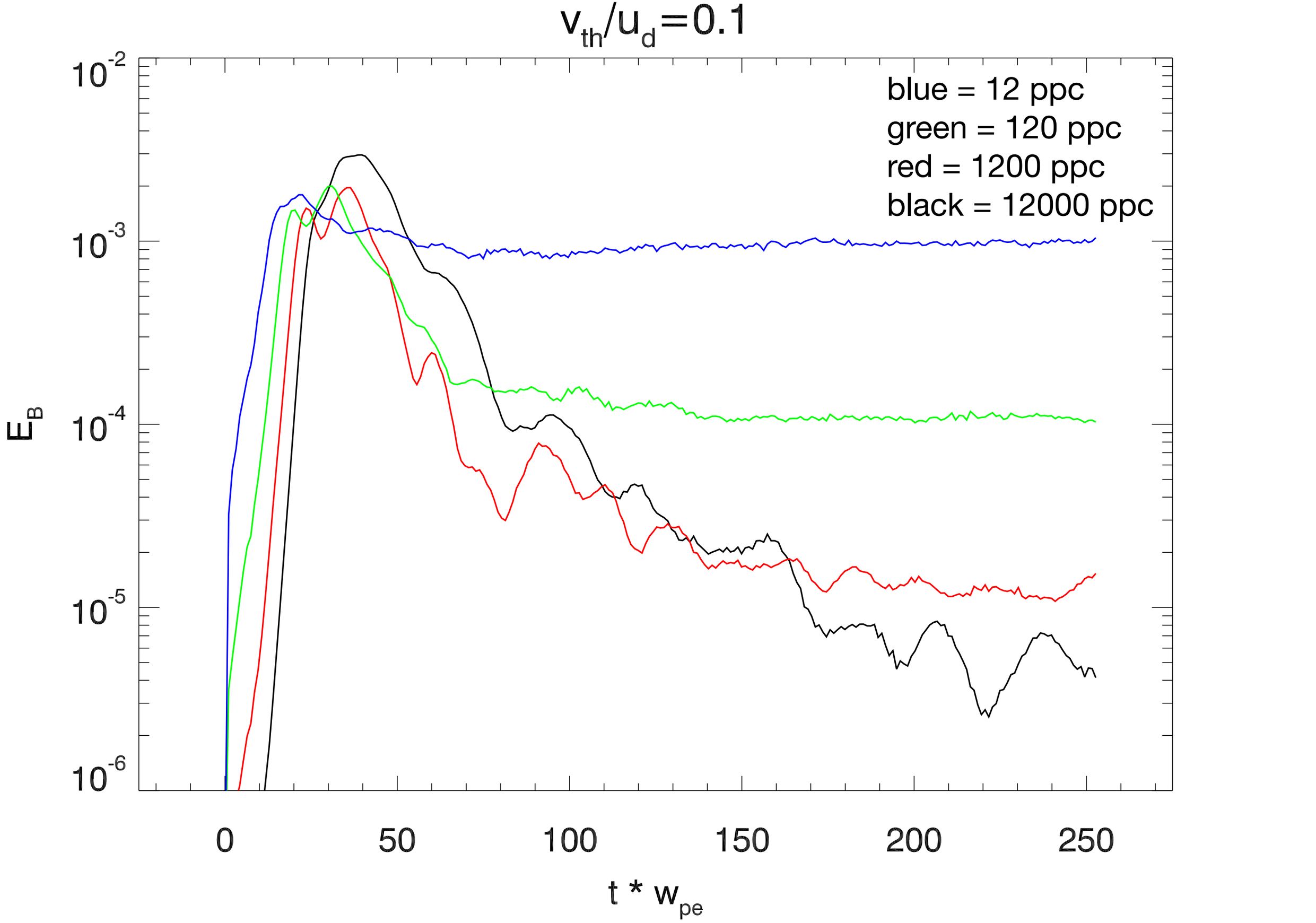

PIC “cold” data, 12000 particles per cell

$t = 35\omega_{pe}^{-1}$ $t = 250\omega_{pe}^{-1}$ $t = 35\omega_{pe}^{-1}$ $t = 250\omega_{pe}^{-1}$

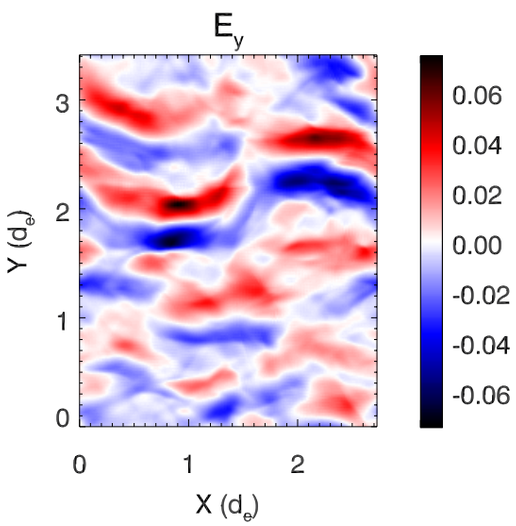

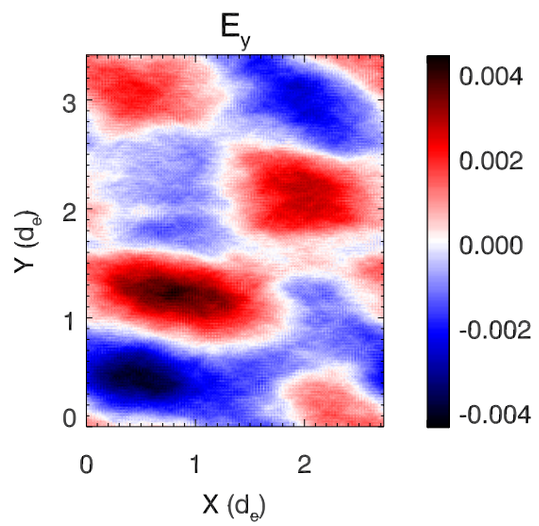

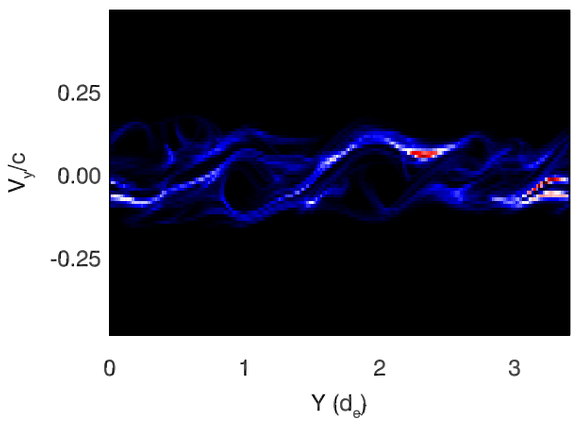

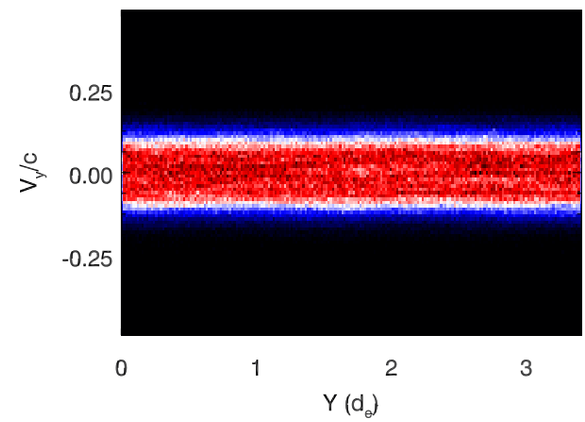

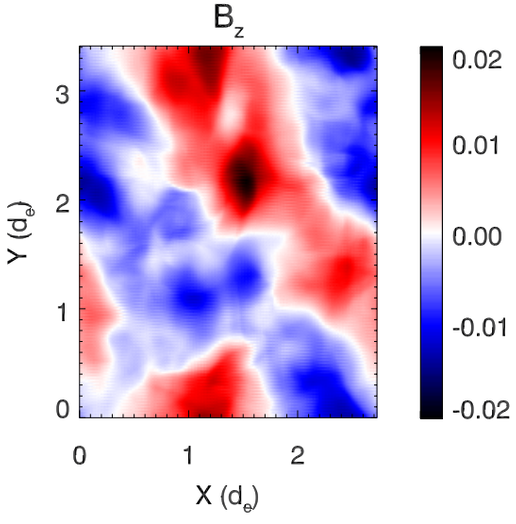

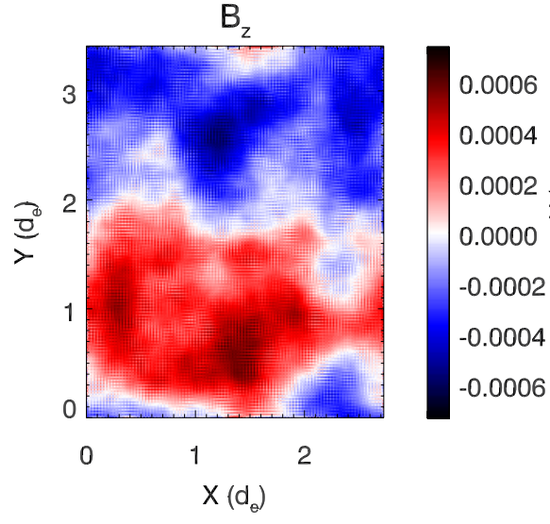

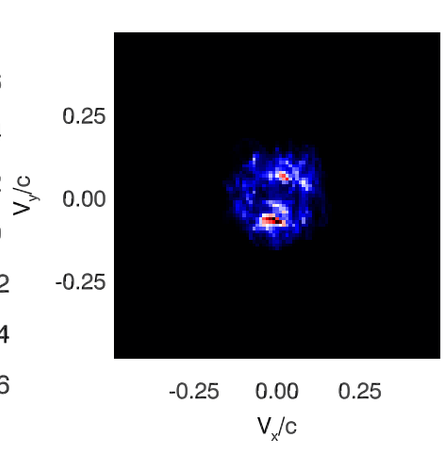

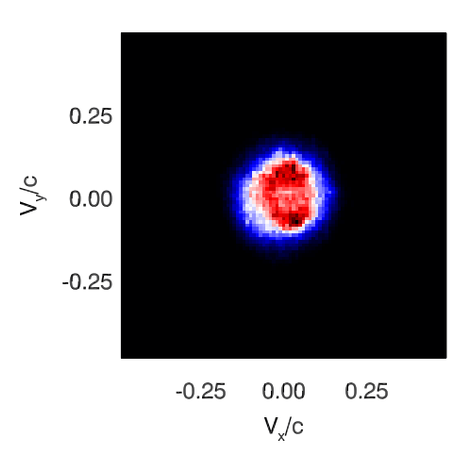

PIC “cold” data, 12 particles per cell

$t = 35\omega_{pe}^{-1}$ $t = 250\omega_{pe}^{-1}$ $t = 35\omega_{pe}^{-1}$ $t = 250\omega_{pe}^{-1}$

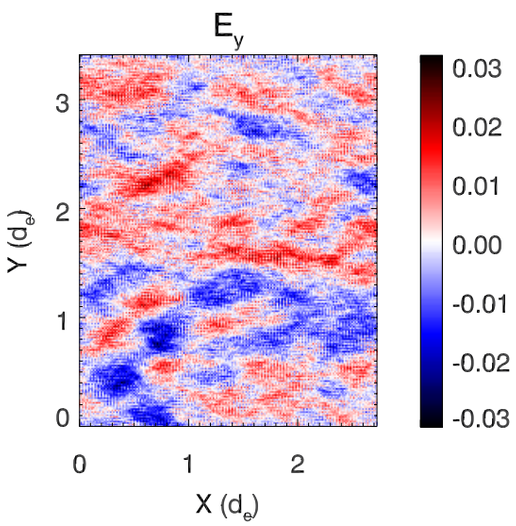

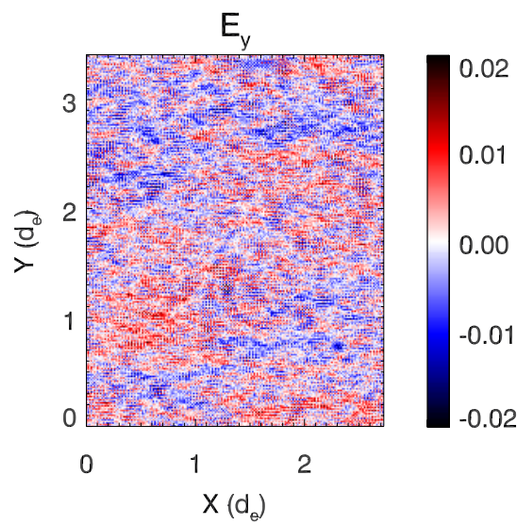

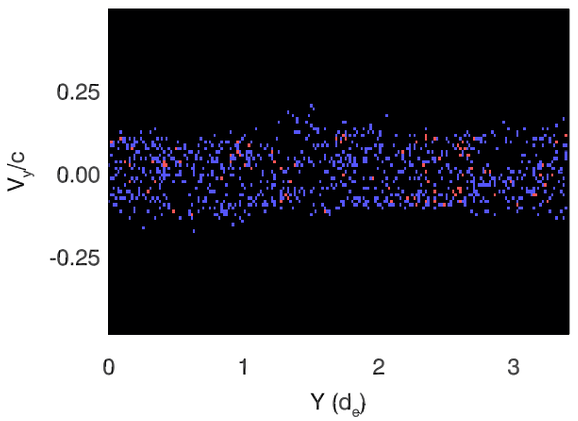

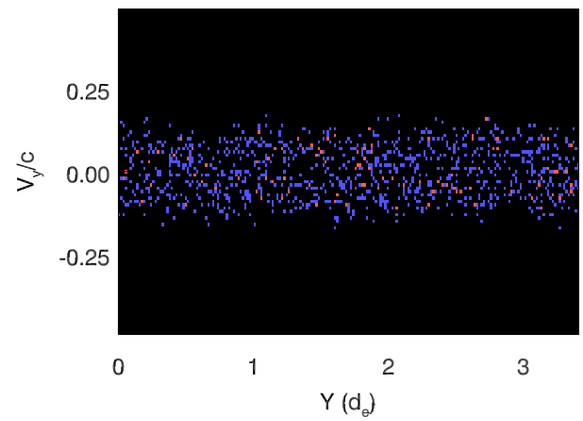

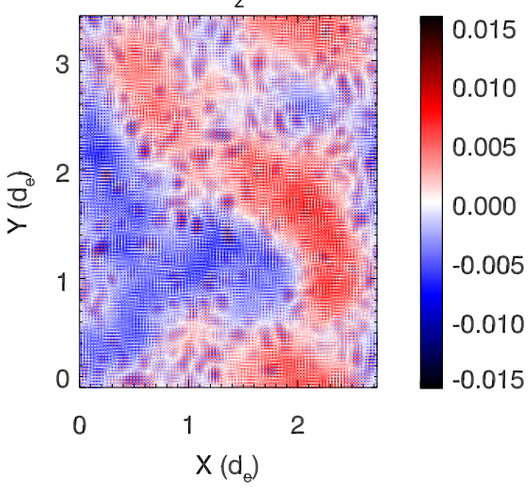

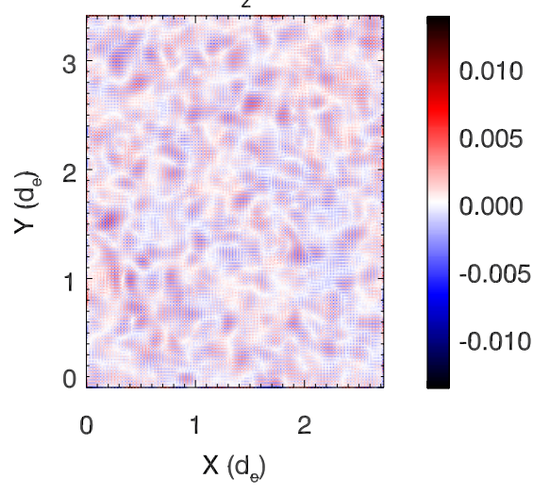

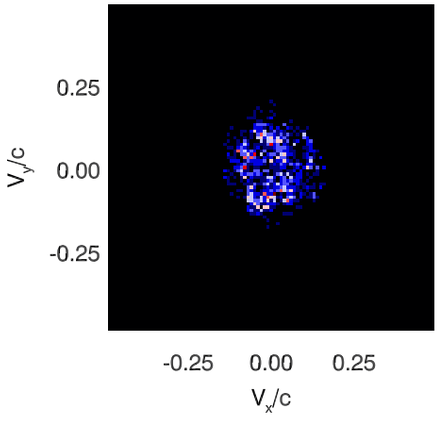

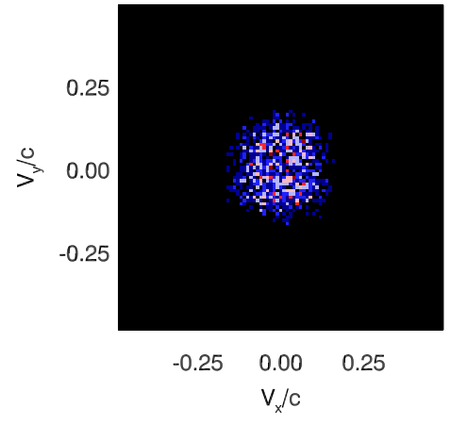

Summary and Future Outlook

- Some remaining numerical challenges (subdominant issues, but would be nice to fix)
  - Divergence errors — can be mitigated with better Riemann solver for Maxwell's equations? Some subtlety in the function space the current lives in
  - Realizability errors — distribution function can go negative, limiters on the Vlasov equation challenging because they might destroy implicit conservation relations
- Having access to a noise-free distribution function provides unparalleled access to the details of phase space dynamics
- **Gkeyll is a powerful and useful tool for the solution to kinetic equations**

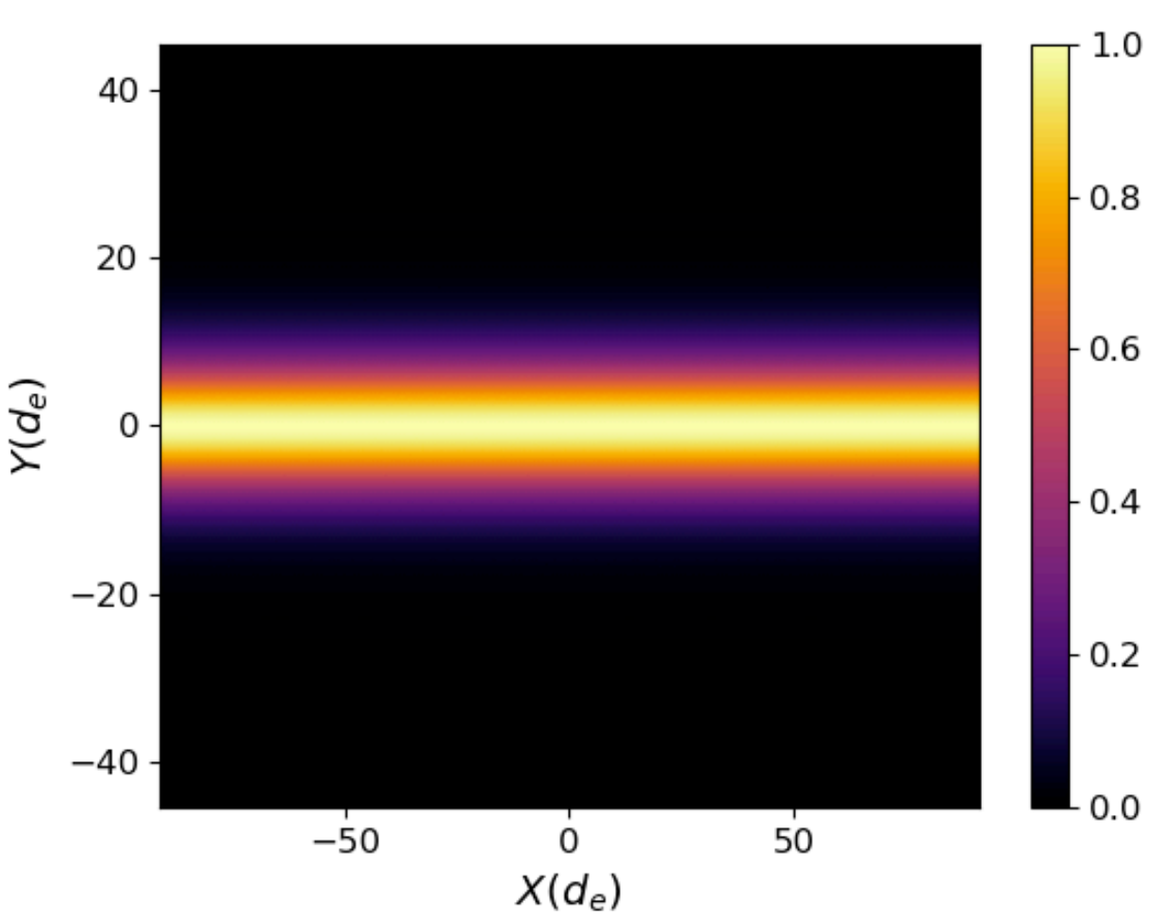

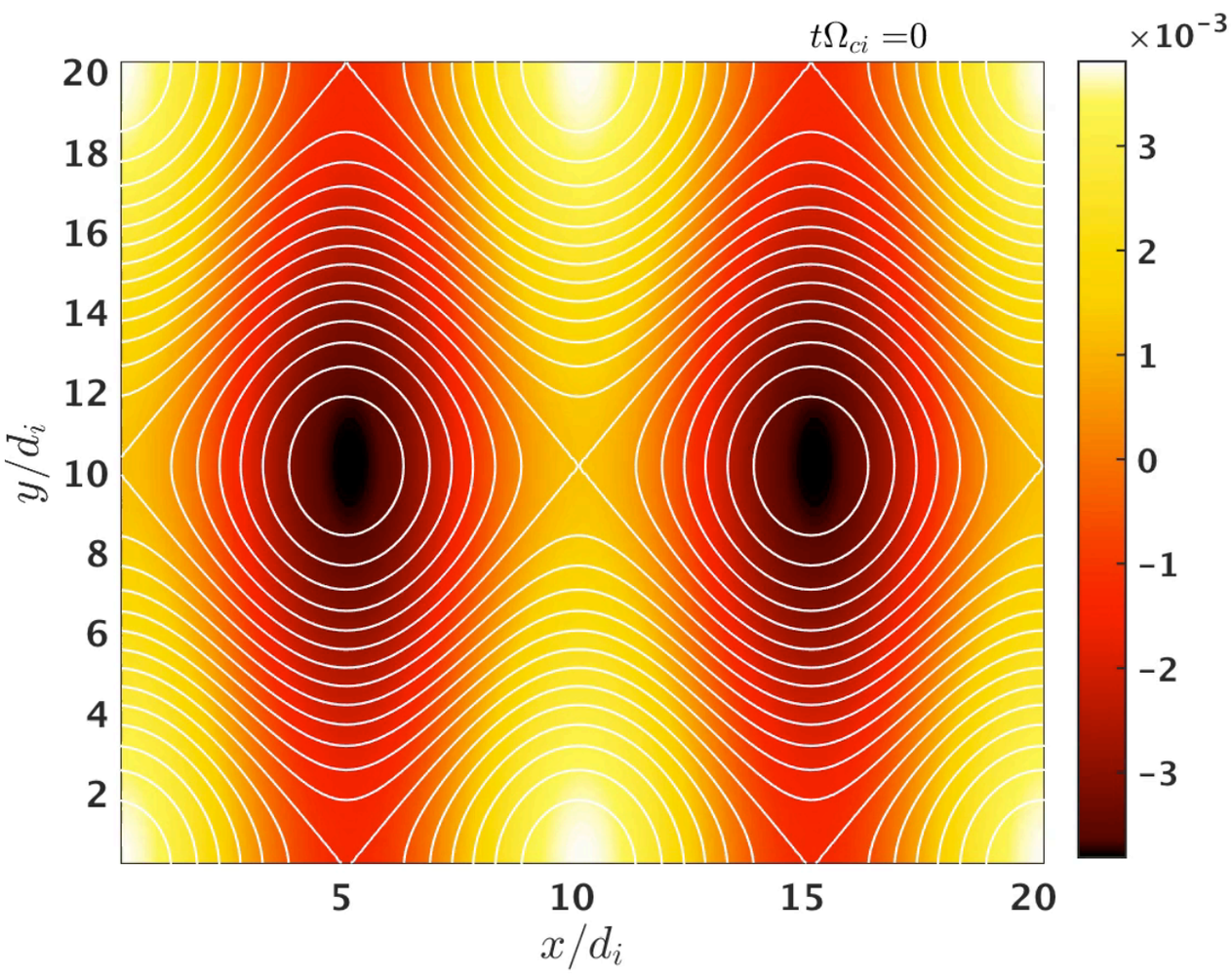

Supplemental Slides

Momentum Non-Conservation

$$\int_{K_j} w \frac{\partial f_h}{\partial t}\, d\mathbf{z} + \oint_{\partial K_j} w^- \mathbf{n} \cdot \hat{\mathbf{F}}\, dS - \int_{K_j} \nabla_z w \cdot \alpha_h f_h\, d\mathbf{z} = 0$$

$$\int_{K_j} m\mathbf{v} \frac{\partial f_h}{\partial t}\, d\mathbf{z} + \oint_{\partial K_j} m\mathbf{v}\mathbf{n} \cdot \hat{\mathbf{F}}\, dS - \int_{K_j} \nabla_z (m\mathbf{v}) \cdot \alpha_h f_h\, d\mathbf{z} = 0$$

$$\sum_j \sum_s \int_{K_j} m_s \mathbf{v} \frac{\partial f_h}{\partial t}\, d\mathbf{z} - \sum_j \int_{\Omega_j} \rho_{c_h} \mathbf{E}_h + \mathbf{J}_h \times \mathbf{B}_h\, d\mathbf{x} = 0$$

$$\sum_j \int_{\Omega_j} \frac{d}{dt} \left(\sum_s \langle m_s \mathbf{v} \rangle_s + \epsilon_0 \mathbf{E} \times \mathbf{B} \right) + \nabla \left(\frac{\epsilon_0}{2} |\mathbf{E}_h|^2 + \frac{1}{2\mu_0} |\mathbf{B}_h|^2 \right)$$
$$- \nabla \cdot \left(\epsilon_0 \mathbf{E}_h \mathbf{E}_h + \frac{1}{\mu_0} \mathbf{B}_h \mathbf{B}_h \right)\, d\mathbf{x} = 0$$

Choosing a basis set

- Key algorithm question: what sort of basis set should be chosen?
  - Common choice: tensor product basis
  - Other choices: reduced basis sets like the Serendipity Element space, or maximal order basis

$$N_{tensor} = (p+1)^d \qquad N_{serendipity} = \sum_{i=0}^{\min(d,p/2)} 2^{d-i} \binom{d}{i} \binom{p-i}{i} \qquad N_{max-order} = \frac{(p+d)!}{p!d!}$$

Lagrange Tensor	**Polynomial Order**	1	2	3	4	5	6	7
Dimension	$(p+1)^d$							
2		4	9	16	25	36	49	64
3		8	27	64	125	216	343	512
4		16	81	256	625	1296	2401	4096
5		32	243	1024	3125	7776	16807	32768
6		64	729	4096	15625	46656	117649	262144

Table 1: Number of degrees of freedom internal to a cell in the Lagrange Tensor polynomial space

Serendipity Element	**Polynomial Order**	1	2	3	4	5	6	7
Dimension	$\sum_{i=0}^{\min(d,p/2)} \binom{d}{i}\binom{p-i}{i}$							
2		4	8	12	17	23	30	38
3		8	20	32	50	74	105	144
4		16	48	80	136	216	328	480
5		32	112	192	352	592	952	1472
6		64	256	448	880	1552	2624	4256

Table 2: Number of degrees of freedom internal to a cell in the Serendipity polynomial space

Defining the basis set

- We've chosen a basis set, but monomials may not be the best basis function expansion in the cell
  - Monomials lead to a poorly conditioned mass matrix
  - Clever choice of polynomials may have favorable computational properties

- When constructing the basis function expansion within the cell, it is common in the DG community to employ a *nodal basis*, where nodes are specified on a reference cell and basis functions take the value of 1 at one node and zero at all other nodes

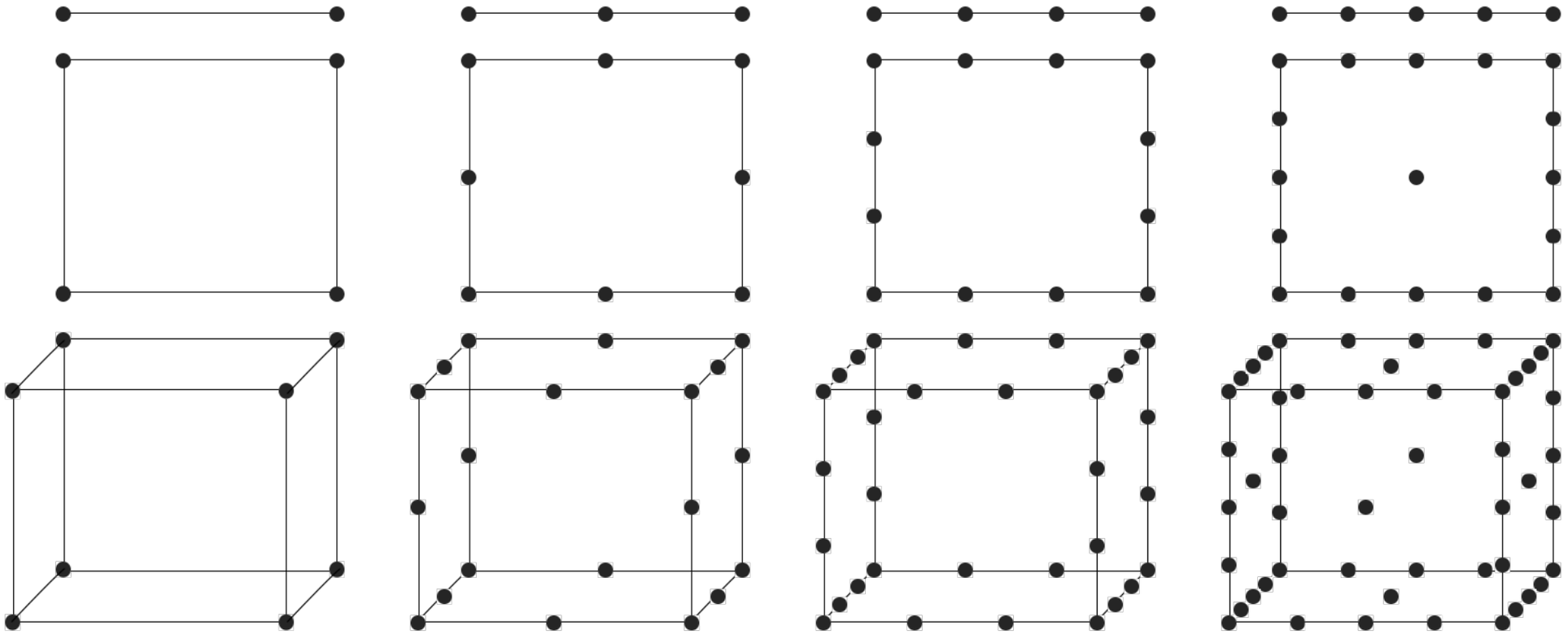

Scaling in parallel

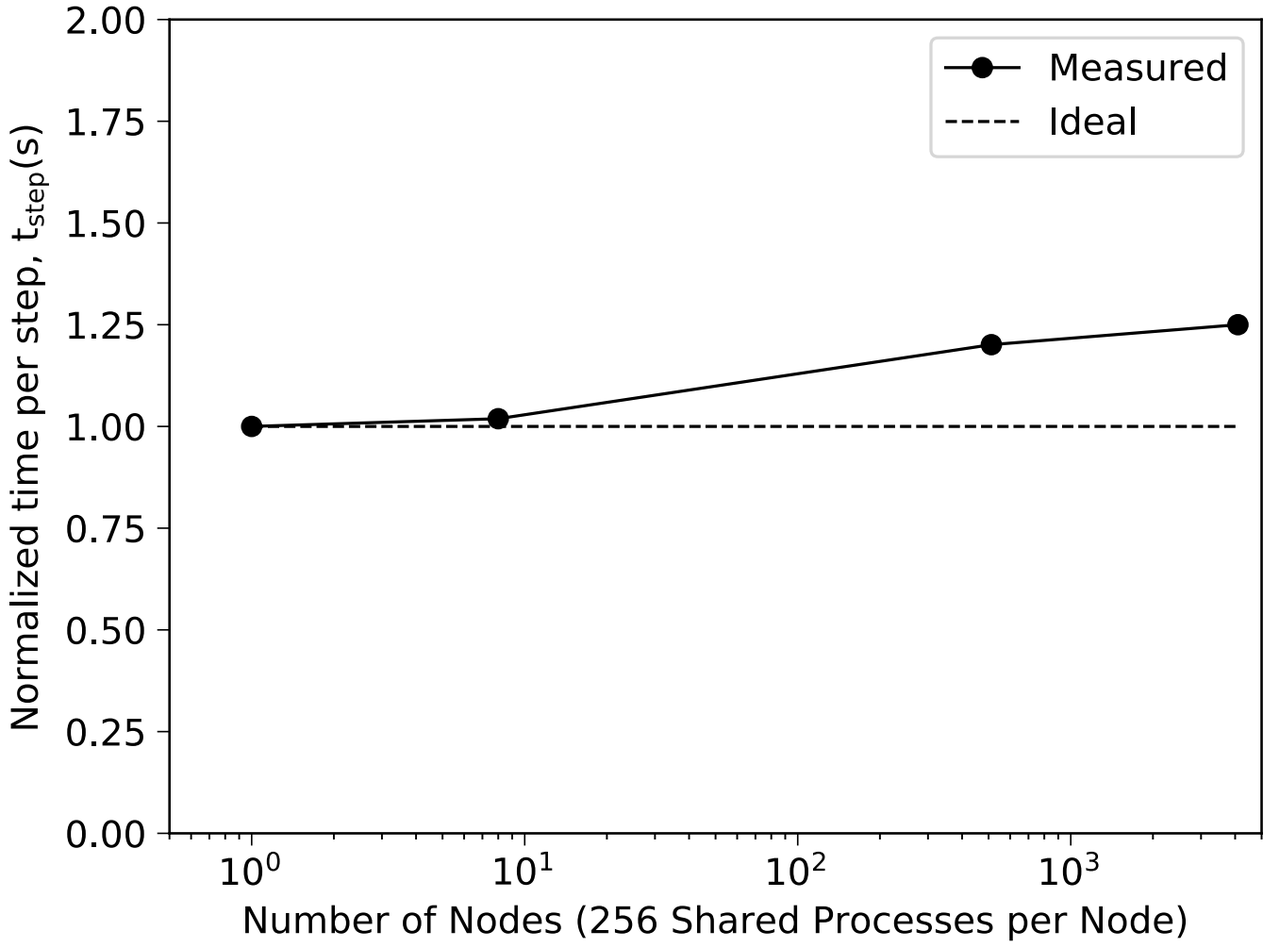

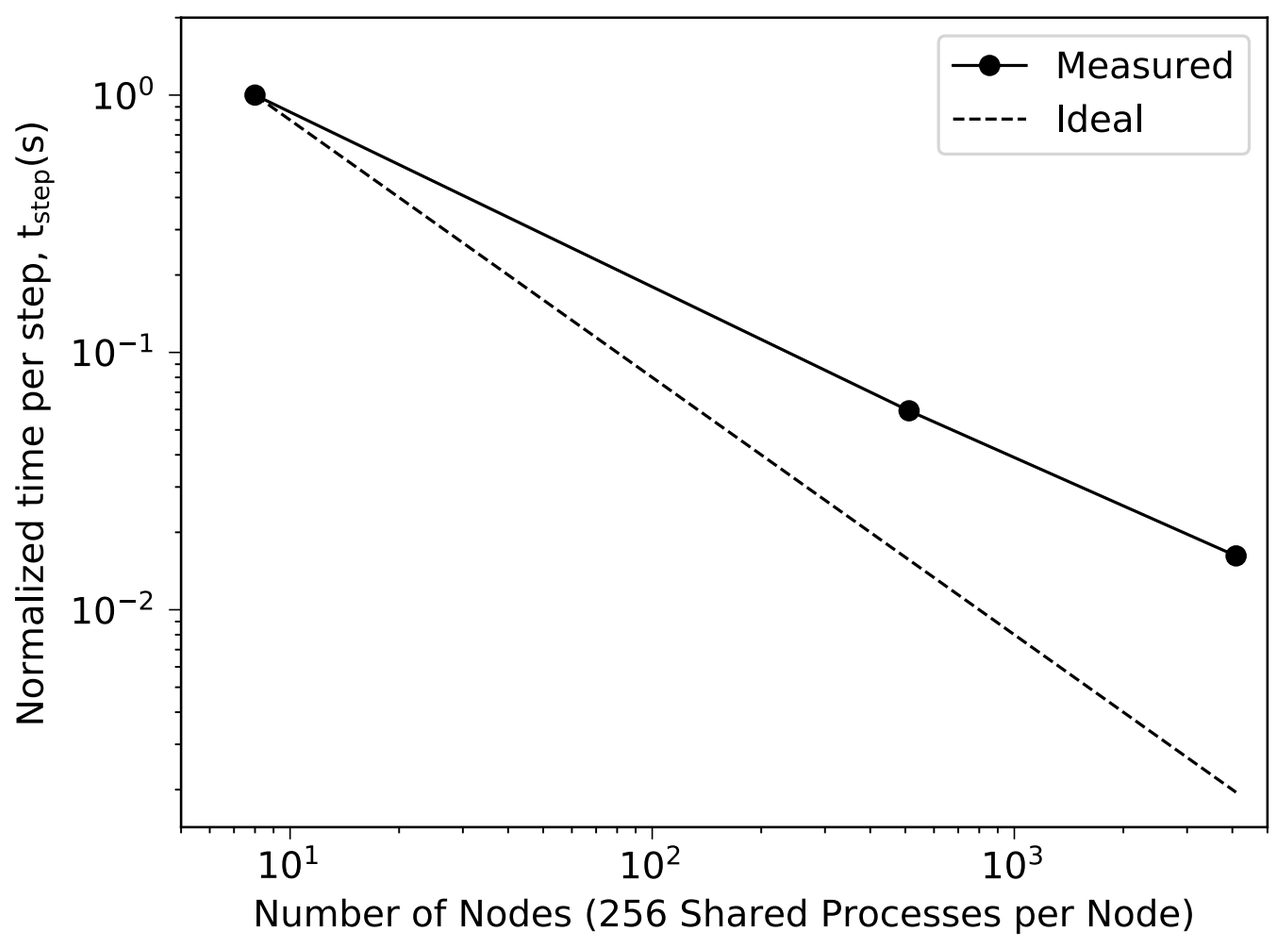

- The Vlasov solver leverages functionality in MPI-3 to attain better scaling on modern supercomputers
  - MPI-3 shared memory directives allow sharing of memory across compute nodes and can exploit hyper-threading, similar to MPI+OpenMP hybrid parallel models
  - Additional MPI-3 functionality such as MPI Datatypes, MPI Neighborhood Collectives, allows for an optimal synchronization algorithm

Numerical Demonstration of Conservation

- An initial density profile, coupled with a flow in both the protons and electrons, drives strong asymmetric flows

$$n(x, t = 0) = n_0(1 + \exp(-\beta_l(x - x_m)^2)) \qquad x < x_m,$$
$$= n_0(1 + \exp(-\beta_r(x - x_m)^2)) \qquad x > x_m,$$

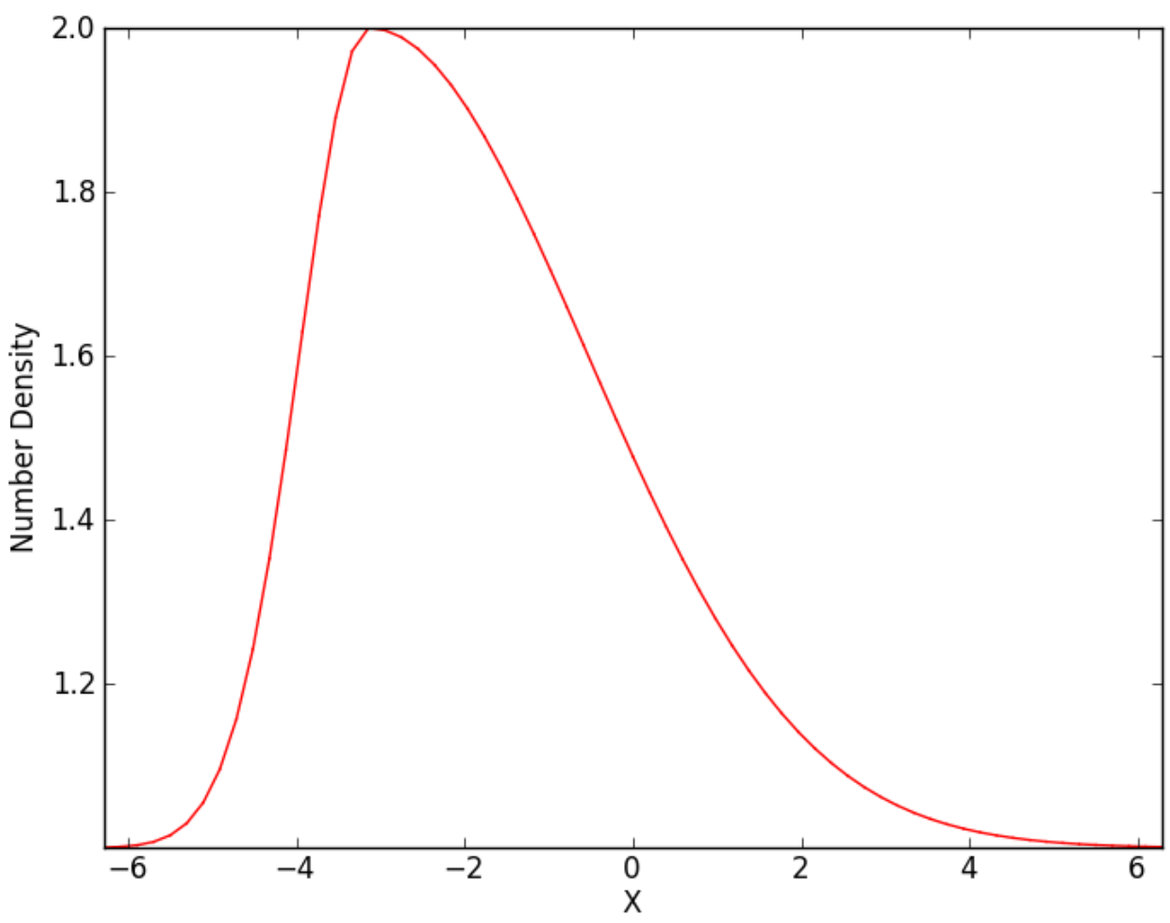

Energy conservation

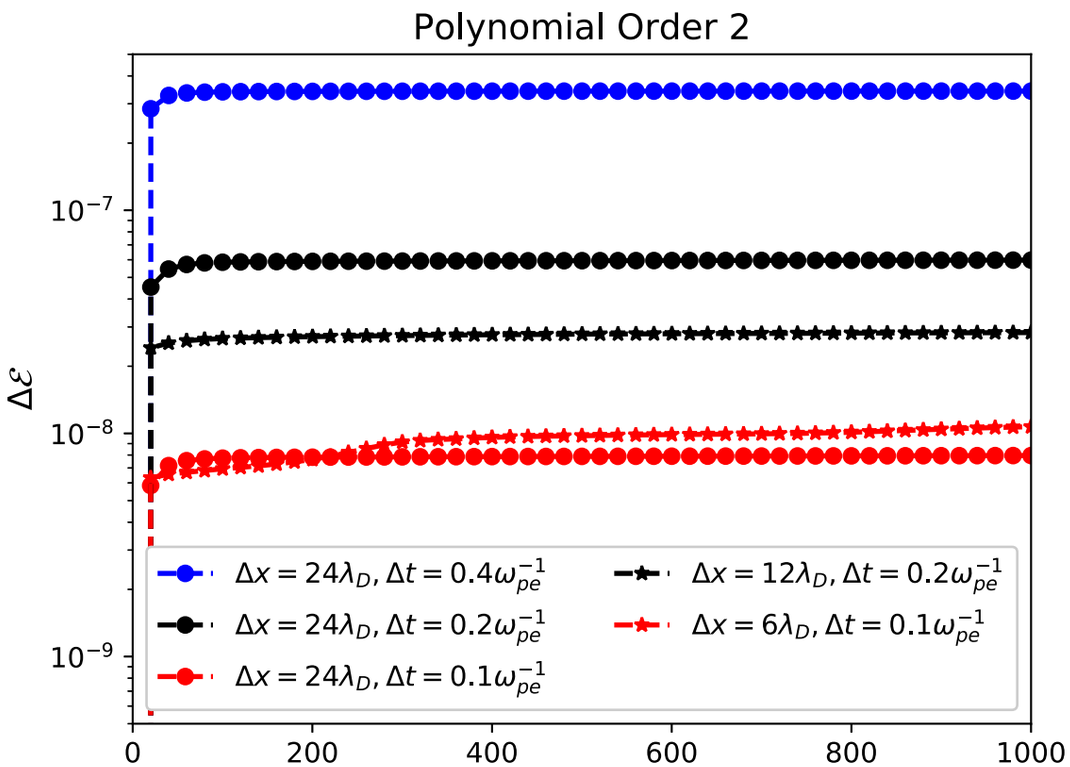

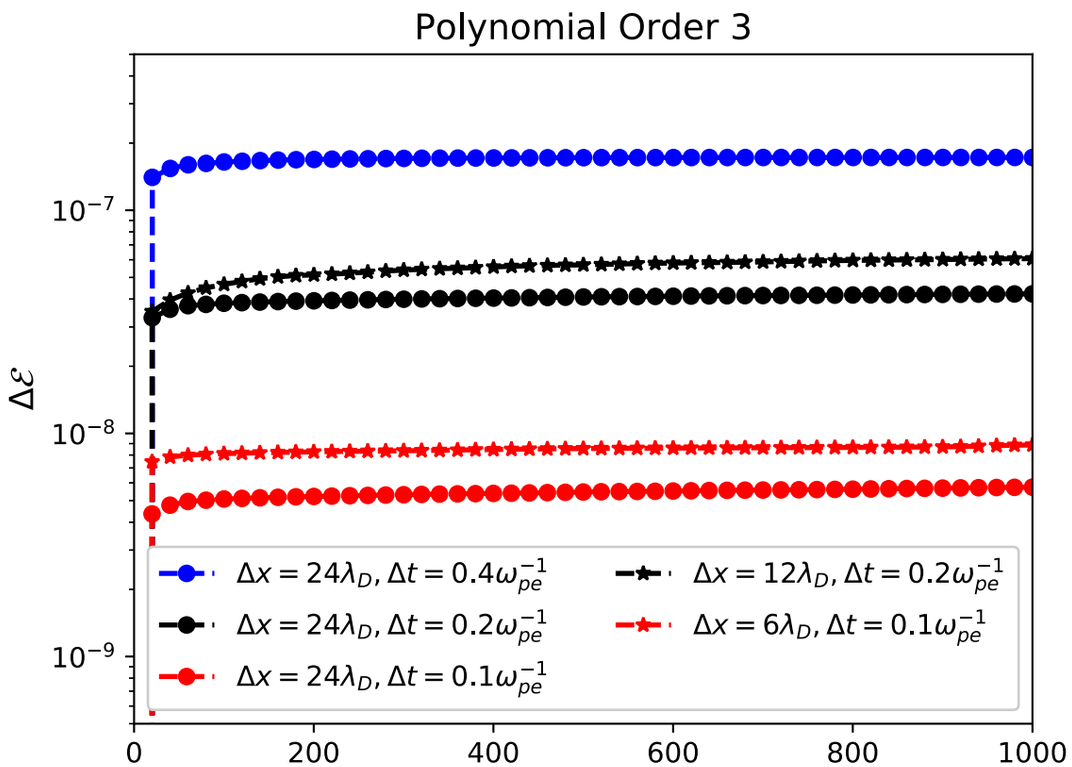

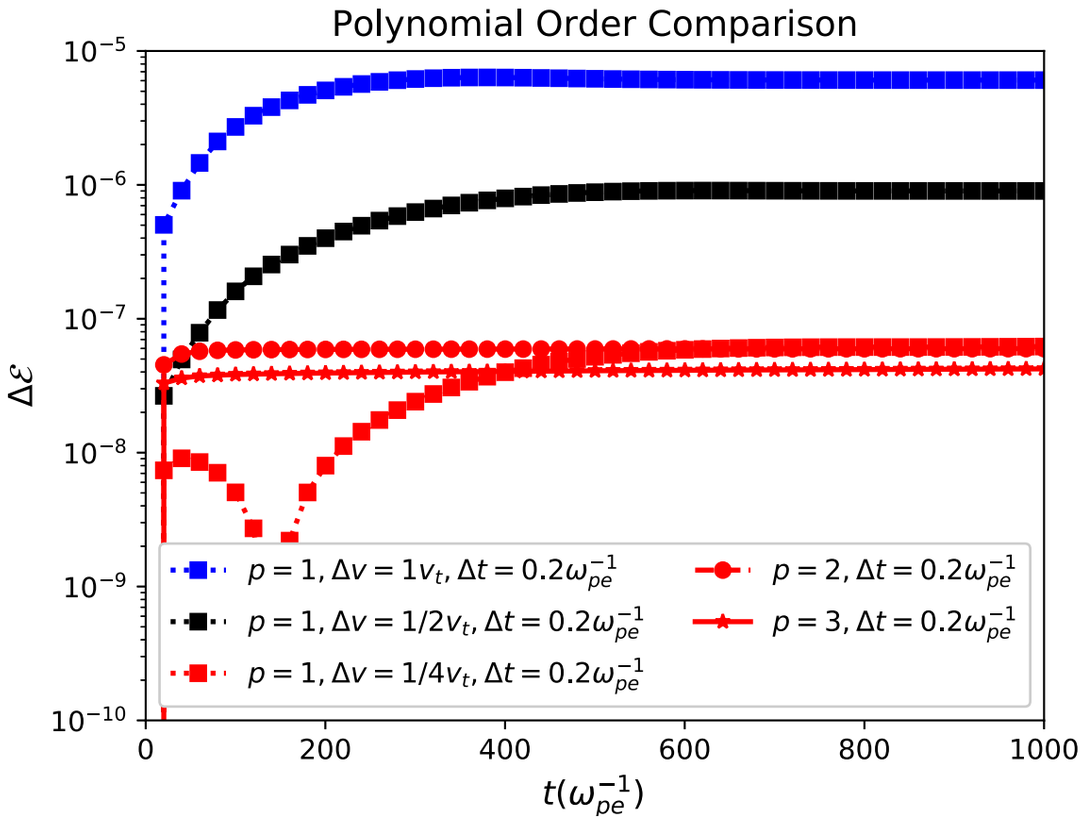

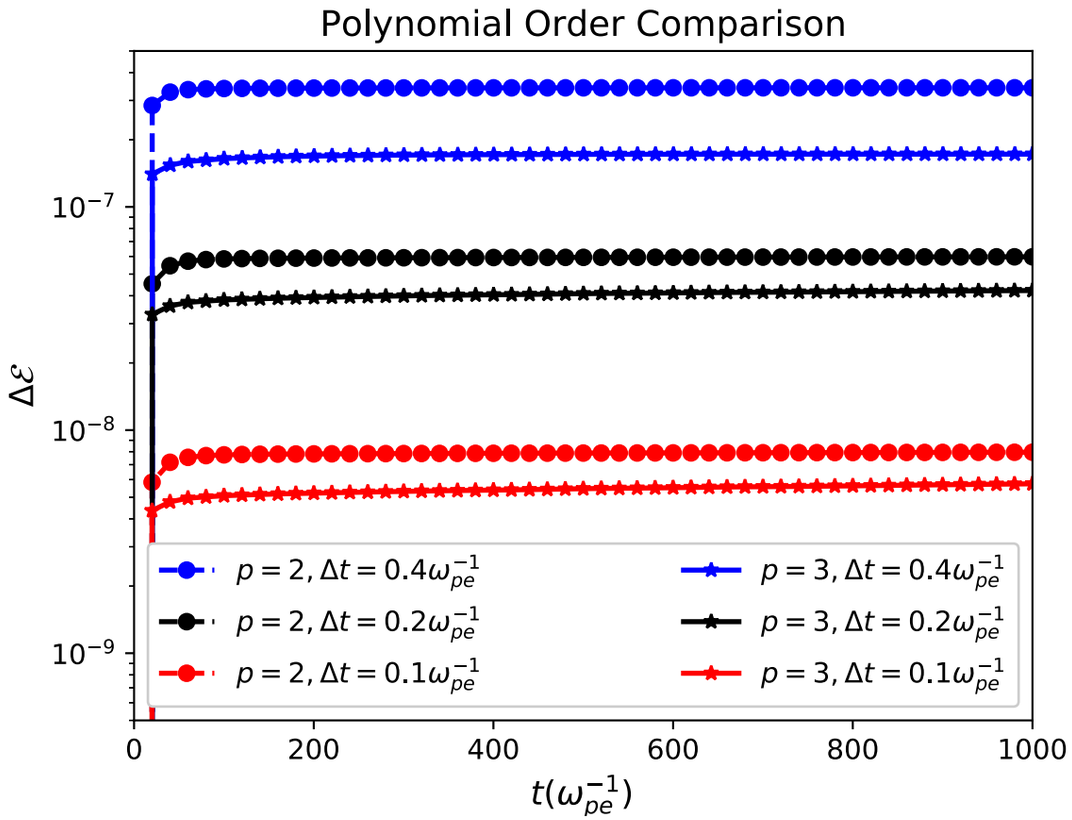

Momentum conservation

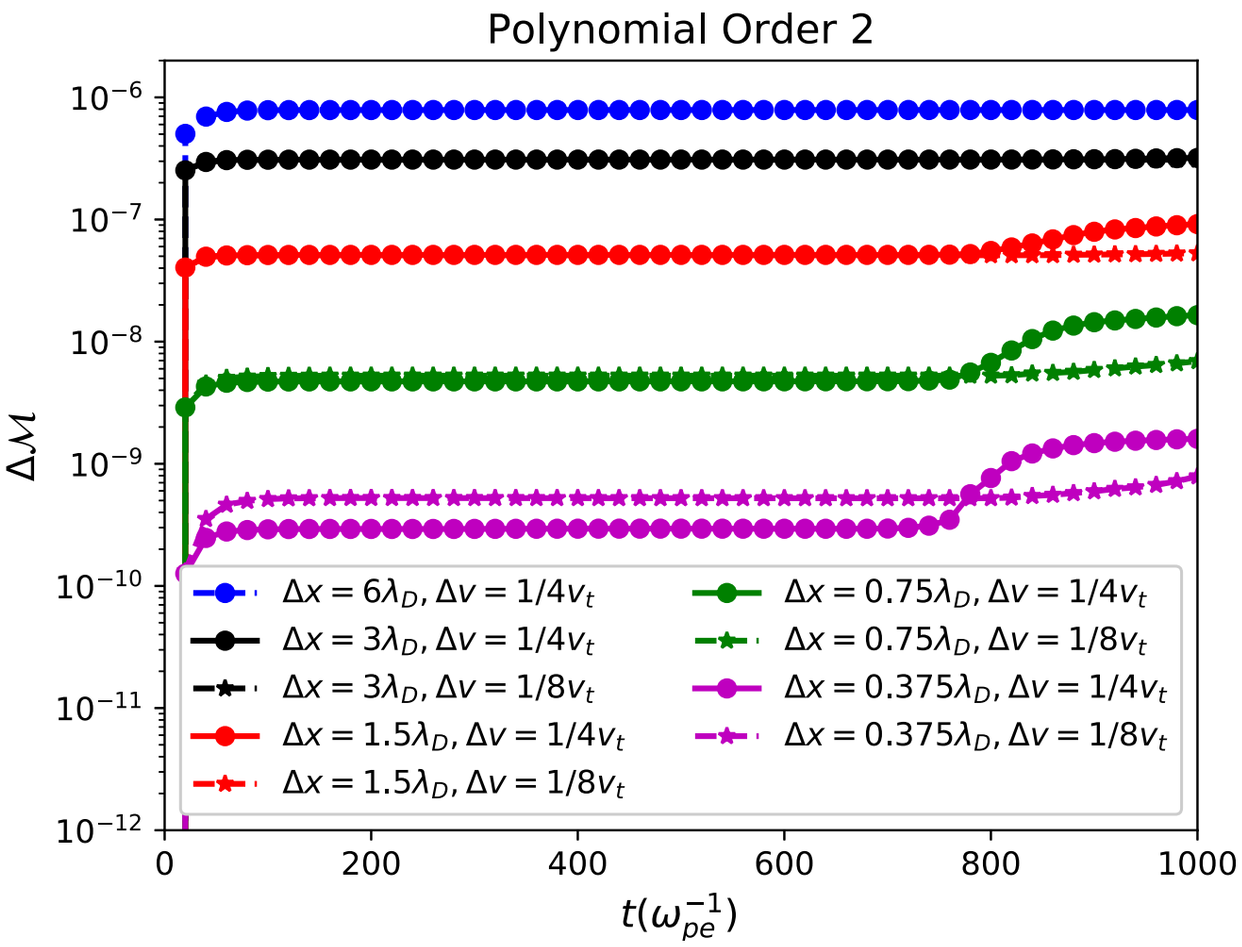

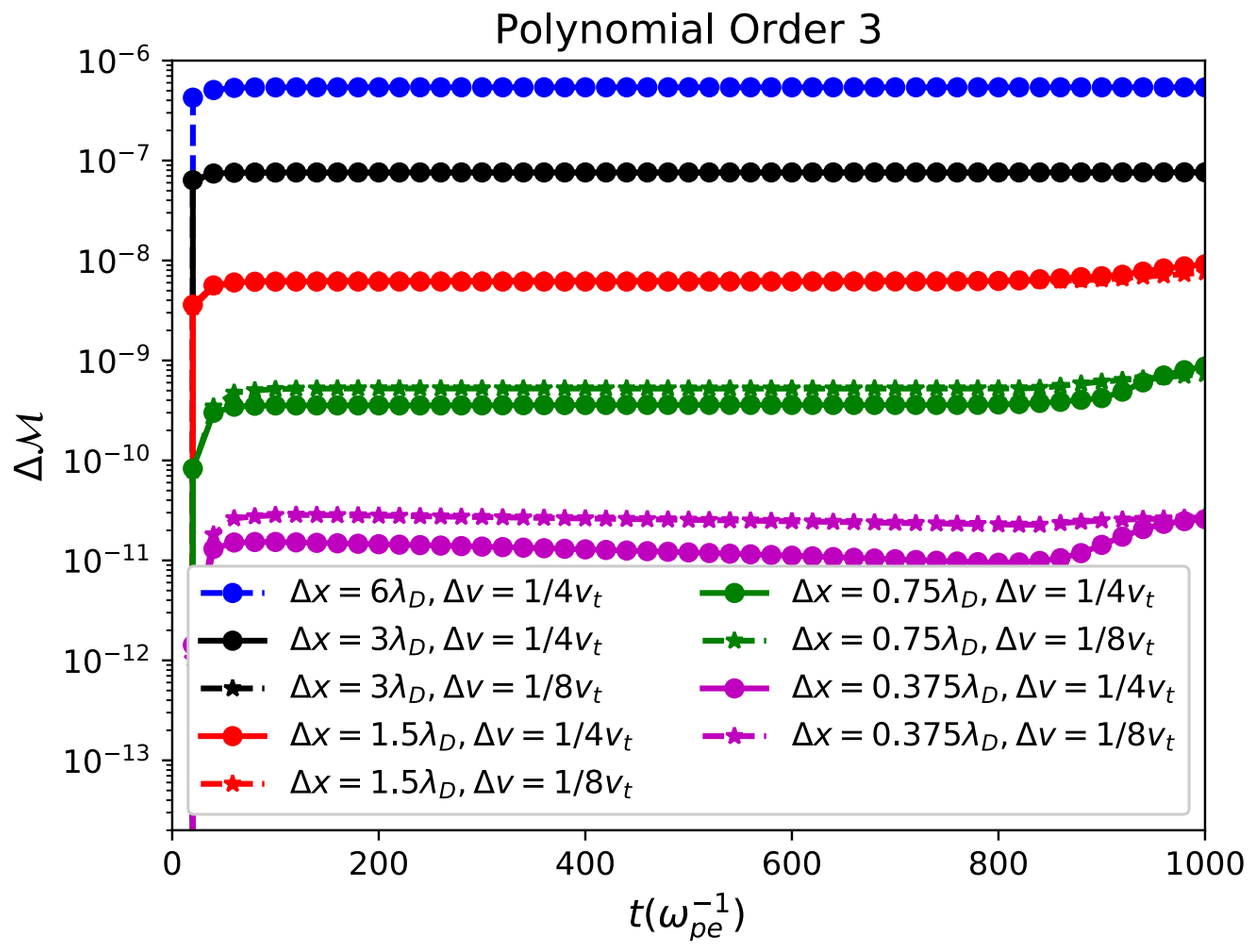

What about protons?

Proton dynamics

$$v_{th_e}/u_d = 0.1, \quad m_p/m_e = 64,$$

$$T_p = T_e, \quad u_{d_e} = u_{d_p} \quad \rightarrow \quad \mathcal{E}_p \gg \mathcal{E}_e$$

$$\Delta x \sim \pi\lambda_D, \quad \Delta v_e \sim v_{th_e}, \quad \Delta v_i \sim 2v_{th_i}, \quad p = 2$$

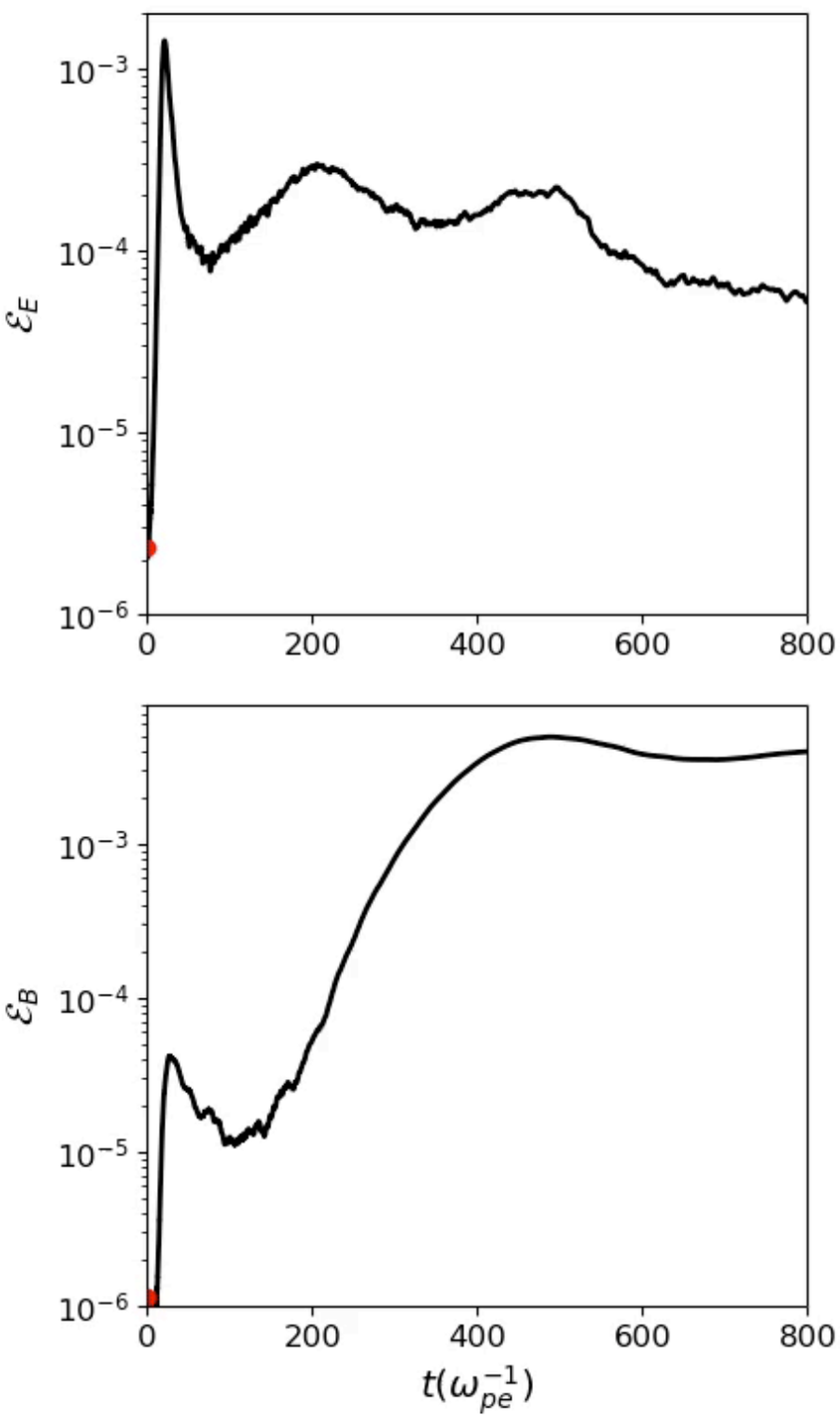

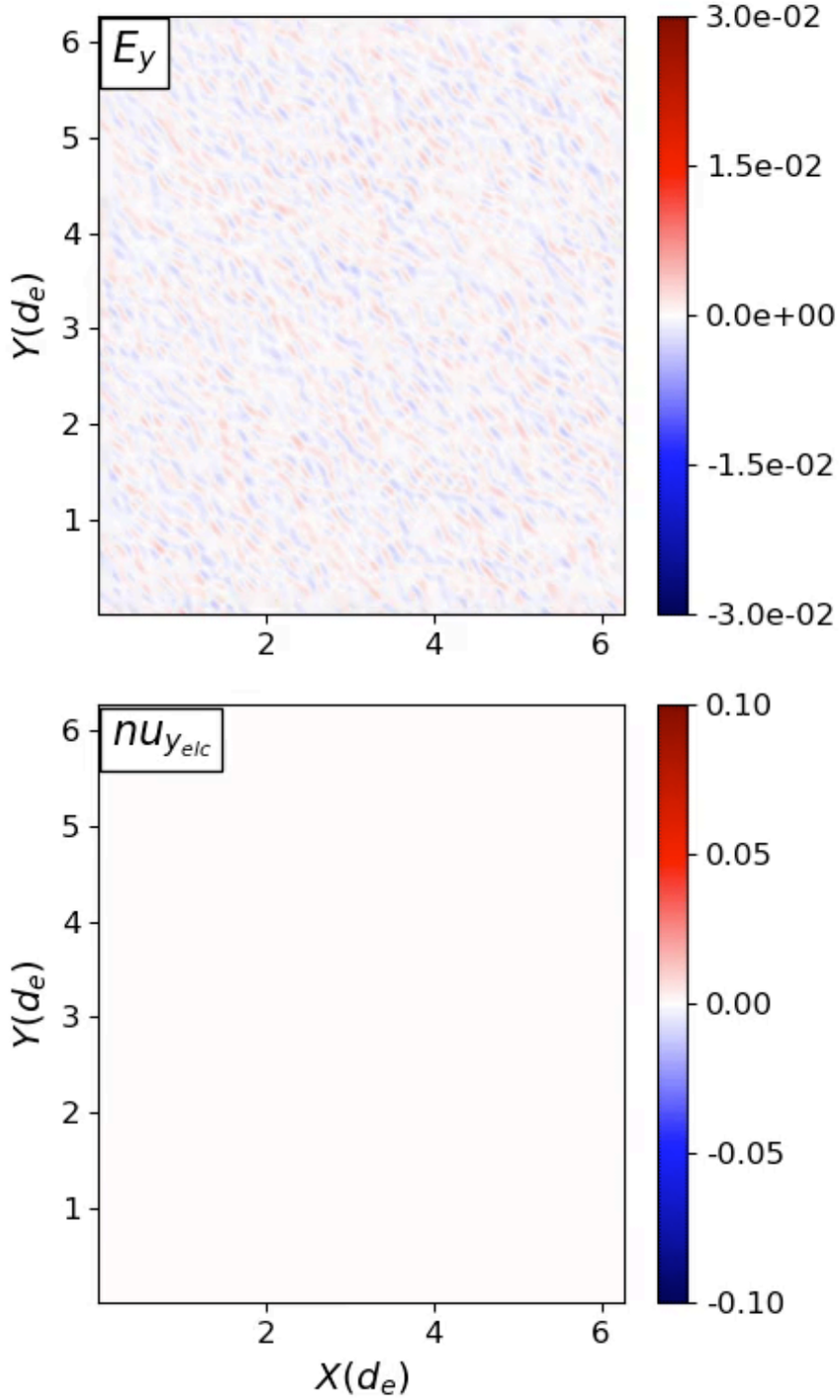

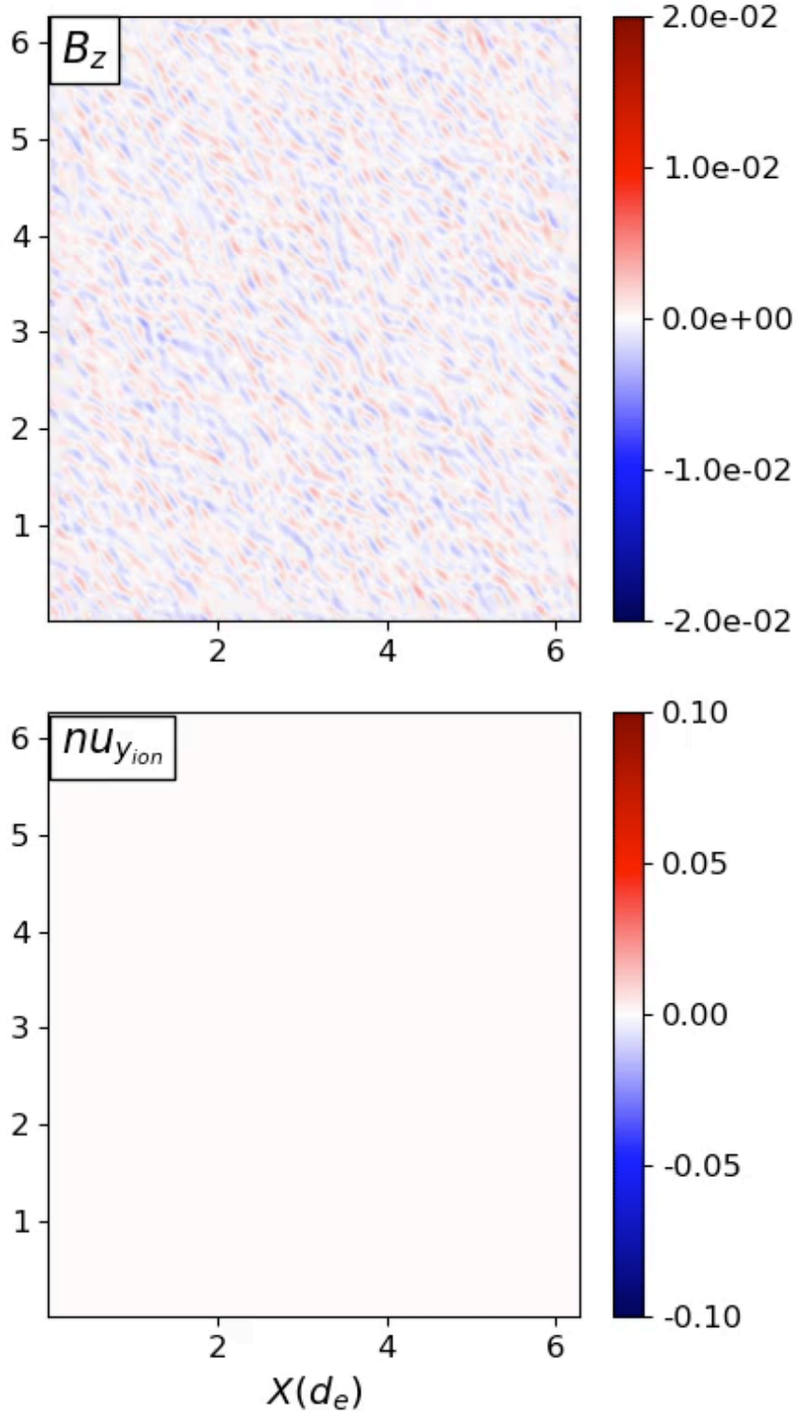

Proton dynamics

$$v_{th_e}/u_d = 0.1, \quad m_p/m_e = 64,$$
$$T_p = T_e, \quad u_{d_e} = u_{d_p} \quad \rightarrow \quad \mathcal{E}_p \gg \mathcal{E}_e$$

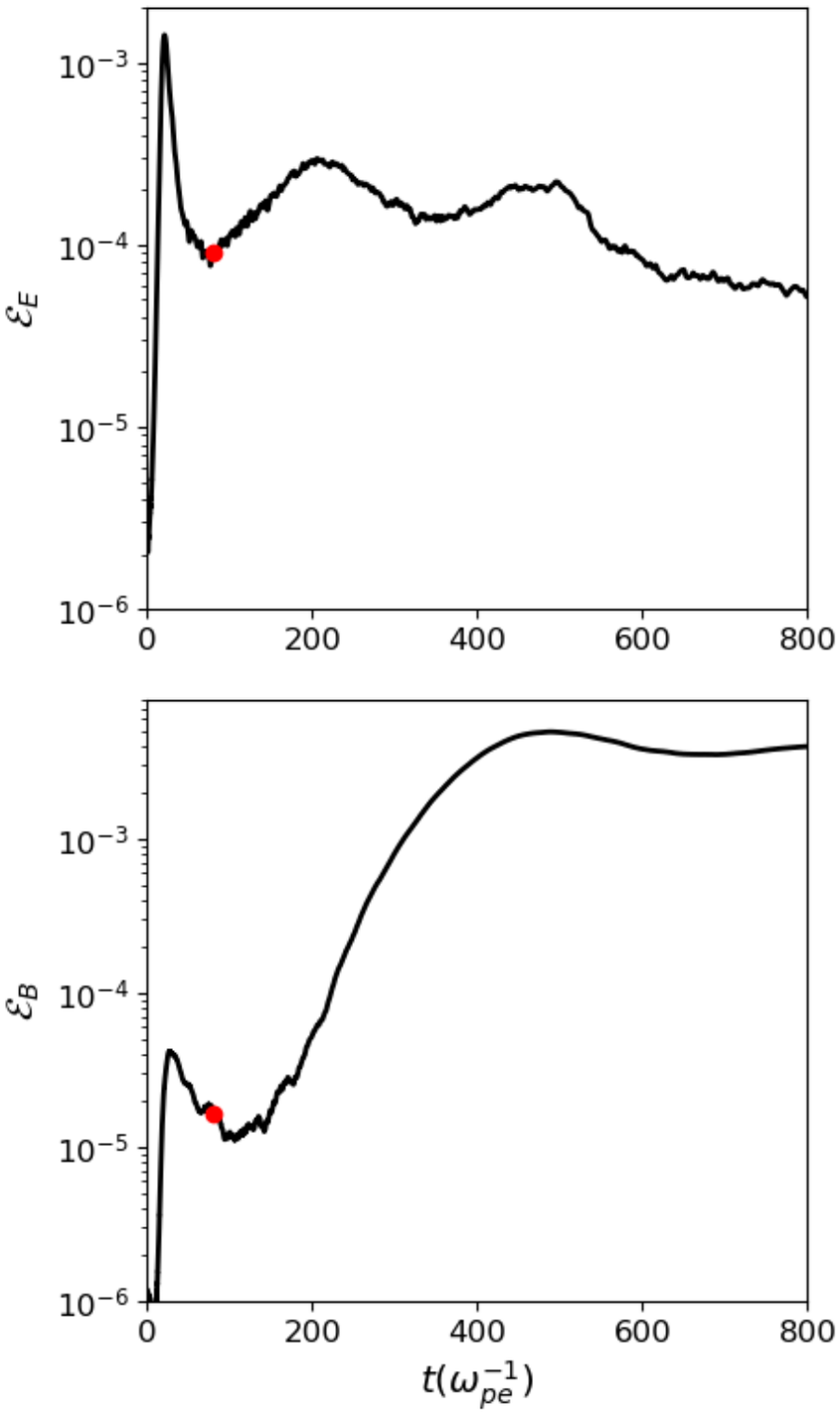

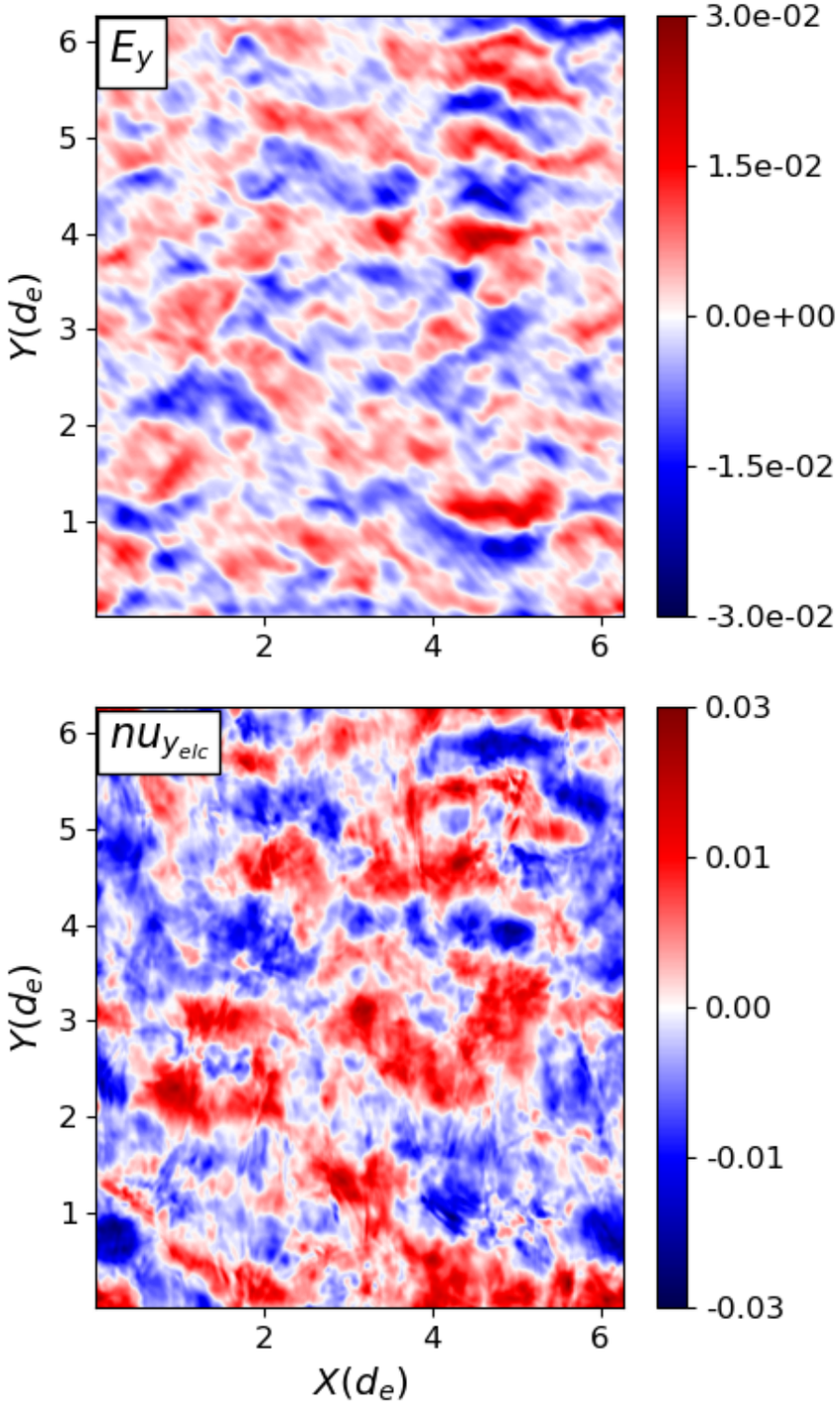

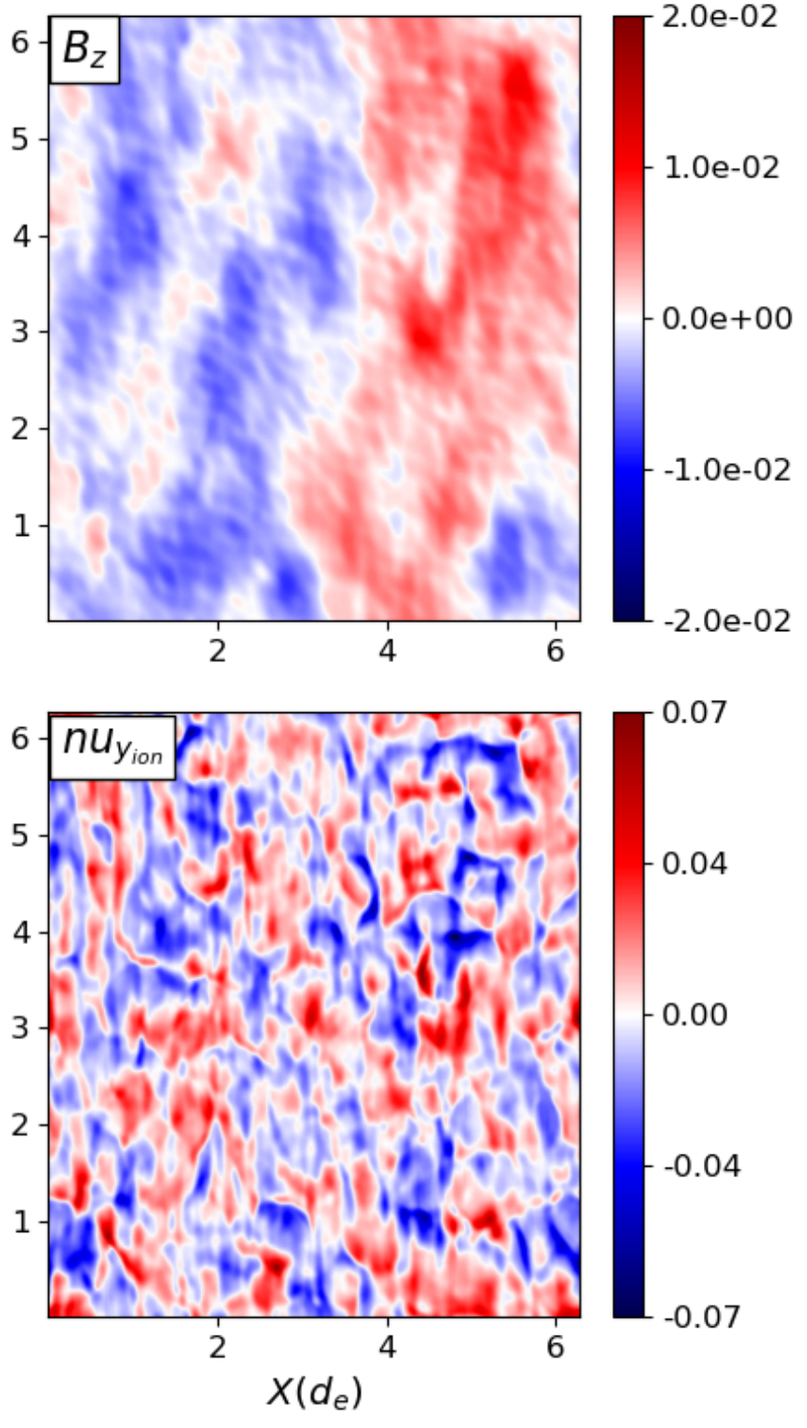

Proton dynamics

$$v_{th_e}/u_d = 0.1, \quad m_p/m_e = 64,$$
$$T_p = T_e, \quad u_{d_e} = u_{d_p} \quad \rightarrow \quad \mathcal{E}_p \gg \mathcal{E}_e$$

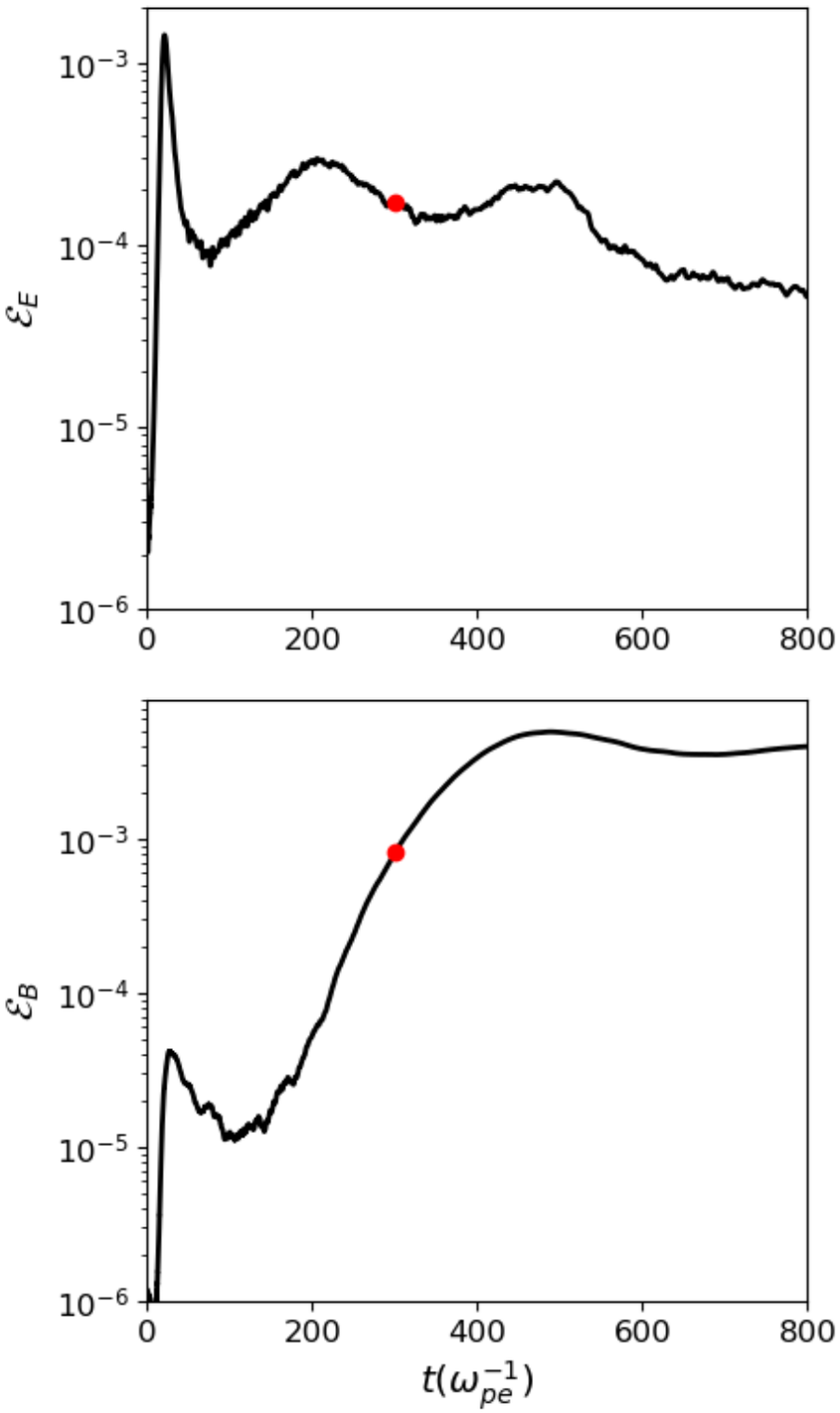

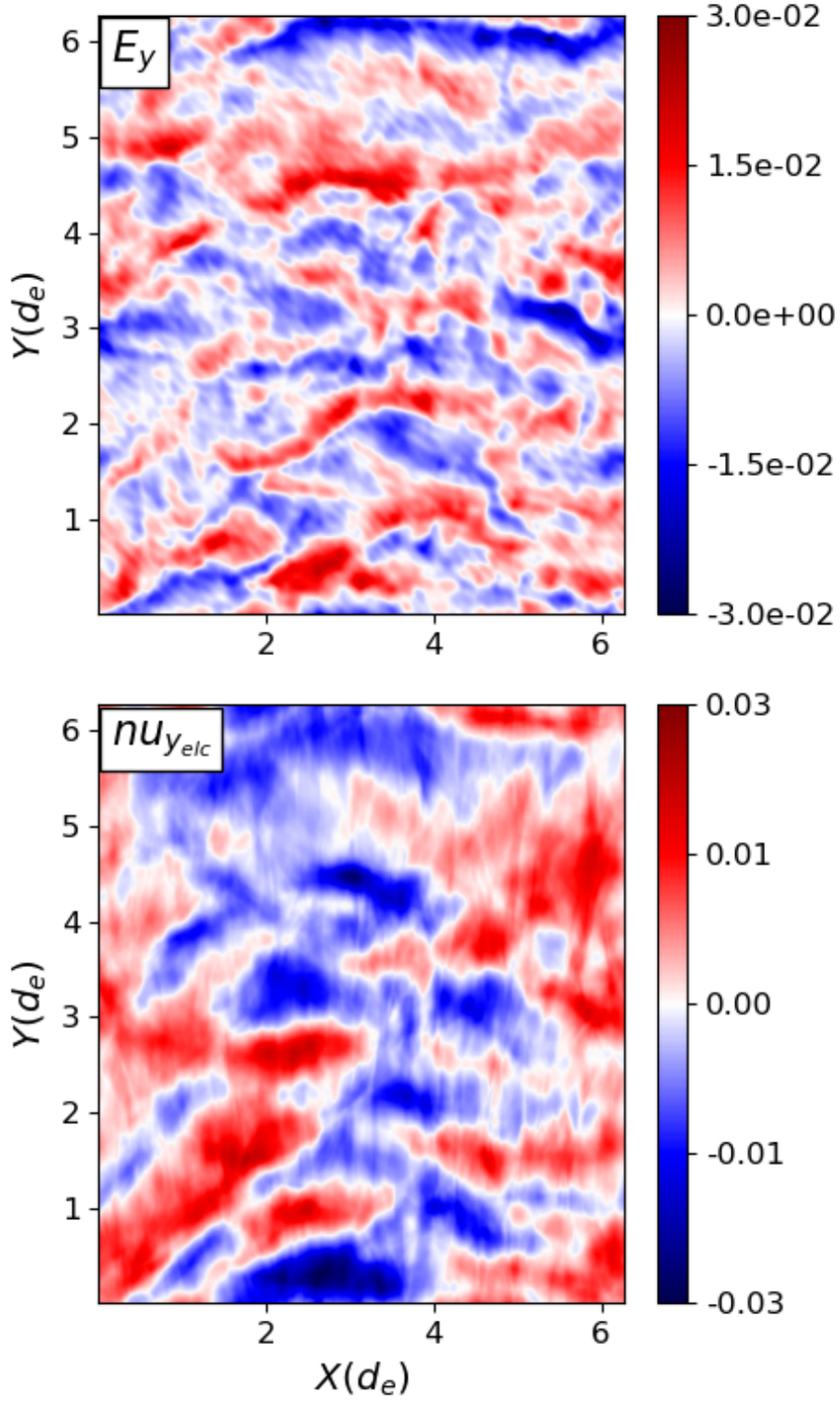

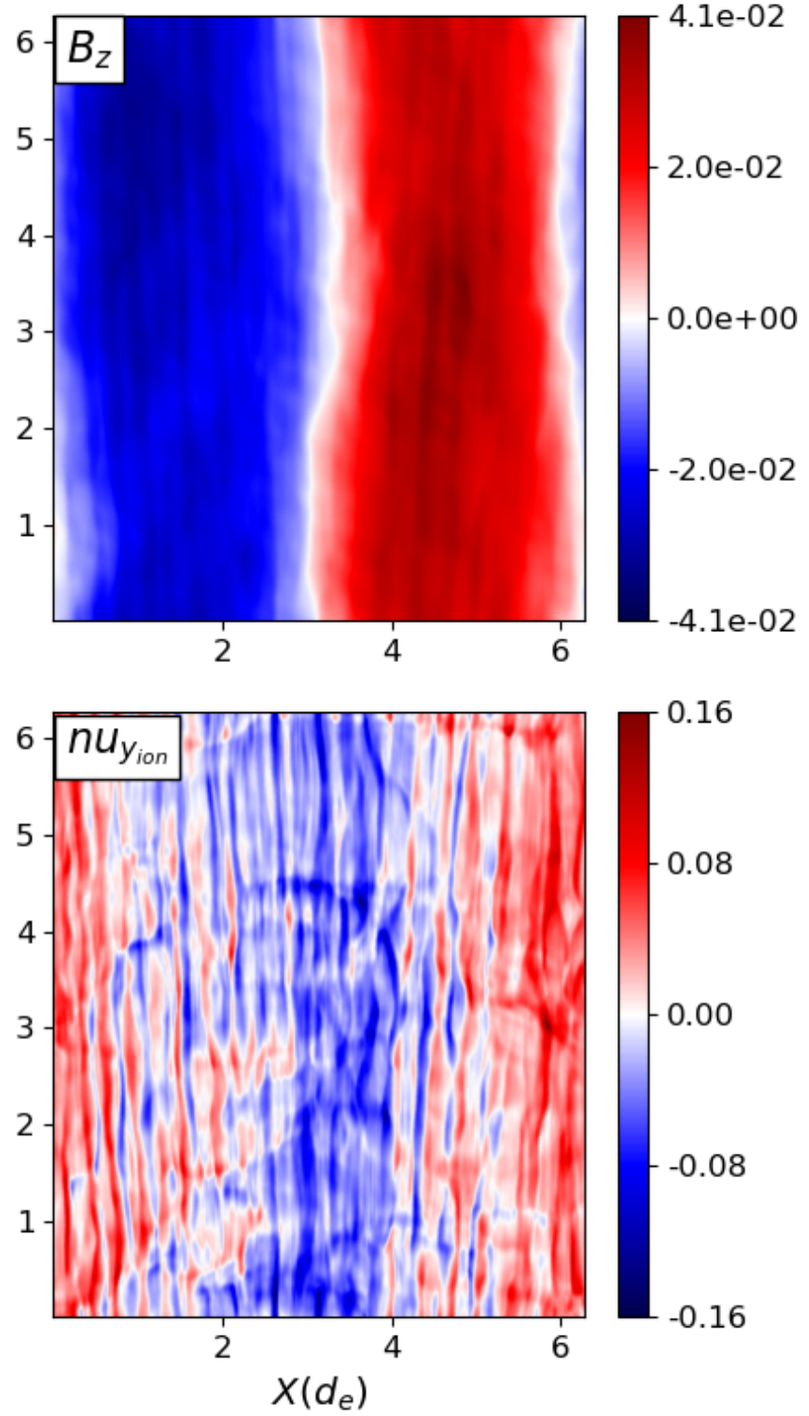

Proton dynamics

$$v_{th_e}/u_d = 0.1, \quad m_p/m_e = 64,$$
$$T_p = T_e, \quad u_{d_e} = u_{d_p} \quad \rightarrow \quad \mathcal{E}_p \gg \mathcal{E}_e$$